# ICSWRM 2021

Friday 10th September 2021

Committee on Global Environment

JSCE

# PROCEEDINGS OF THE INTERNATIONAL CONFERENCE ON SUSTAINABLE WATER RESOURCES MANAGEMENT (ICSWRM)

## Global Challenges & Opportunities

## Table of Content

# Message from the Organizing Committee

Dear Distinguished Delegates,

International Conference on Sustainable Water Resources Management is an international forum of excellent researchers and scholars engaged in scientific research dedicated to the enhancement of sustainable water resources, locally, regionally and globally. This academic research conference is at the aim of international scientific, engineering and technological progress to promoting excellence in water resources research.

This online conference, with the participation of world leading researchers in water resources research, a platform for them to present their state-of-the-art research outcome, demonstrating their excellent contribution to global challenges and opportunities. Hence, this conference plays an influential role in promoting developments in water resources research in a wide range of multidisciplinary applications as well as theoretical developments.

We wish that this conference will be a great prospect for researchers in the field of water resources, provide the opportunity for discussions and exchange ideas and contribute towards "sustainable water resources management".

Hope you will enjoy the event and contribute your knowledge to wider scientific community.

Best wishes from

Dr Ranjan Sarukkalige
Prof So Kazama
Prof Seiki Kawagoe

ICSWRM 2021 Organizing Committee.

10-Sep-2021

# Conference Program

**Friday 10th September 2021**

**9.00 – 9.15AM**

**OPENNING SESSION**

Introduction & Welcome address: *Dr Ranjan Sarukkalige*, Curtin University, Australia

Opening address: *Prof So Kazama*, Tohoku University, Japan

**9.15 – 11.00AM**

**SESSION 1: WATER RESOURCES ASSESSMENT: TOOLS & APPROACHES**

Session Chair: Dr Ranjan Sarukkalige

Application of flexible model structures to interpret dominant process controls on flow duration curves, *Chris Leong, Yoshiyuki Yokoo,* Fukushima University, Japan

Long-duration Maximum Precipitation Estimation for large basins dominated by Atmospheric Rivers using the WRF model, *Yusuke Hiraga, Yoshihiko Iseri, Michael D. Warner, Chris D. Frans, Angela M. Duren, John F. England, M. Levent Kavvas,* University of California, Davis, USA

Towards water security in the cities of La Paz and El Alto, Bolivia, *Pablo Fuchs, Javier Mendoza and Gustavo Ayal*a, Universidad Mayor de San Andrés, Bolivia

Performance of Machine learning algorithms for potential recharge areas mapping in high-altitude, Andean mountains, *Evelyn Aliaga and Freddy Soria,* Universidad Católica Boliviana, Bolivia

Evaluation of factors affecting the concentration of an emerging pharmaceutical pollutant (Sulfamethoxazole) in cities with absence of wastewater treatment systems by sensitivity analysis of a global fate transport model, *Andrea Agramont, Freddy Soria, Carolina Garvizu,* Universidad Católica Boliviana, Bolivia

Streamflow maps for small-sized basins of Japan, *Ryosuke Arai, Yasushi Toyoda, So Kazama*, Central Research Institute of Electric Power Industry, Japan

Integrated assessment of the flood and heat mitigation effect of vegetation in an urban residential area, *Qing Chang, So Kazama, Yoshiya Touge, Shunsuke Aita*, Wuhan University of Science & Tech, China

**12.00 – 2.30PM**

**SESSION 2: GROUNDWATER RESOURCES & CATCHMENT STUDIES**

Session Chair: A/Prof Chaiwat Ekkawatpanit

Boundary effect on pumping test estimations and ways of lowering groundwater level in Muscat Airport premises, *Luminda Gunawardhana, Ahmed Sana*, University of Moratuwa, Sri Lanka

Comparison drought index and observed agricultural drought in Indonesia, *Nurul Fajar Januriyadi, Bambang Heri, Idham Riyando Moe*, Pertamina University, Indonesia

Identifying the Spatiotemporal Variation in Qualitative and Quantitative Characteristics of Groundwater in Attanagalu Oya Basin, Sri Lanka, *Vinu I , Danushka U, Chaminda S.P, Dassanayake A.B.N,* University of Moratuwa, Sri Lanka

Spatiotemporal Variation of Groundwater Quality in Malwathu Oya Basin, Sri Lanka, *Madhushankha JML, Madhuwan ARB, Menan P, Chaminda SP,* University of Moratuwa, Sri Lanka

Identifying Flash Flood Potential Areas Using Morphometric Characterization of watershed, *Thapthai Chaithong*, Kasetsart University, Thailand

Employing satellite image derived water surface areas to estimate the small tank capacities in data-scarce regions, *S. M. A. D. R. M. Sammandapperuma, N. K. Gunasekara and C. Herath, General Sir John Kotelawala Defence* University, Sri Lanka

A comparison of the quality of spatial rainfall data products available over Attanagalu Oya catchment, Sri Lanka, *N. K. Gunasekara and T. D. S. Rashmika,* General Sir John Kotelawala Defence University, Sri Lanka

Flood Scenarios to facilitate emergency services resource planning, *Bandara Nawarathna,* Bureau of Meteorology, Australia

A comparison of the design peak-flow estimated using simulated and storm-hydrographs, *Faisal Al-Hinai, Luminda Gunawardhana*, Sultan Qaboos University, Oman.

Evaluation of the surface water-groundwater interaction in estimating water yield from an ephemeral river catchment in Western Australia, *Amila Basnayaka, Ranjan Sarukkalige*

**3.00-5.00PM**

**SESSION 3: IMPACTS OF CLIMATE CHANGE ON WATER RESOURCES**

Session Chair: Prof Seiki Kawagoe

Assessing the risk of river bank erosion under the context of climate change for Hochiminh City, Vietnam, *Ngoc Pham, Hoa Thi Pham, Angeli Doliente Cabaltica*, International University, Vietnam National University Ho Chi Minh City, Vietnam

Spatial changes of Urban Heat Island formation and its effect on the Ecology: A case study of Colombo City, Sri Lanka, *Kurugama KAKM, Dissanayake DMDOK, Chaminda SP*, University of Moratuwa, Sri Lanka

Local action on climate change: Opportunities and constraints in the Lower Yom and Nan River basin, Thailand, *Weerayuth Pratoomchai, and Naphol Yoobanpot,* King Mongkut's University of Technology North Bangkok, Thailand

Evaluation of altered flow regimes by dams and climate change in the Omaru river network using a distributed hydrological model, *Mineda H, Nukazawa K, Tanimura Y, Suzuki Y,* Miyazaki University, Japan.

Effects of Climate Change on Surface Water and Groundwater Recharge in the Yom and Nan River basin, Thailand, *Chanchai Petpongpan, Chaiwat Ekkawatpanit, Duangrudee Kositgittiwong*, King Mongkut's University of Technology Thonburi, Thailand

Estimation of current and future flooding using HEC RAS case study of Sedon catchment, LAO PDR, *Sengphrachanh Phrakonkham, Sisouvanh Kittavong*, National University of Laos, Laos.

Bias correction of WRF-ROMS for rainfall forecasting in the Upper Ping River Basin, Thailand, *Prem Rangsiwanichpong, Phakawat Lamchuan, Thienchart Suwawong,* Kasetsart University, Thailand

Assessment of Landslide Risk using Hydrological Model in the Upper Yom River basin, Thailand, *Chaiwat Ekkawatpanit, Chanchai Petpongpan,* King Mongkut's University of Technology Thonburi, Thailand

**5.00 – 5.15PM**

**CLOSING SESSION / VOTE OF THANKS**

**5.15PM Onwards**

**SOCIAL EVENT / NETWORKING, CATCHING-UP AND WRAPPING EVENT**

# Long-duration Maximum Precipitation Estimation for large basins dominated by Atmospheric Rivers using the WRF model

○Yusuke Hiraga[1*], Yoshihiko Iseri[1], Michael D. Warner[2], Chris D. Frans[2], Angela M. Duren[3], John F. England[4], M. Levent Kavvas[1]
[1]Department of Civil and Environmental Engineering, University of California, Davis, Davis, CA, United States
[2]Seattle District, U.S. Army Corps of Engineers, Seattle, WA, United States
[3]Northwest Division, U.S. Army Corps of Engineers, Portland, OR, United States
[4]Risk Management Center, U.S. Army Corps of Engineers, Lakewood, CO, United States

*E-mail: yhiraga@ucdavis.edu

## Abstract

The PMP estimation for long durations, such as seasonal scale durations on the order of several months is important for snowmelt-driven regions since extreme floods are often driven by both snow accumulation and snowmelt processes during winter and spring seasons rather than by a single rainstorm event. This study proposes a new framework using the Weather Research and Forecasting (WRF) model to estimate the long-duration Maximum Precipitation (MP). As a demonstrative case, we estimate the MP for the 6-month winter period (October to March) for the drainage areas of Bonneville Dam (621,600 km$^2$) and Libby Dam (23,270 km$^2$) in the Columbia River Basin dominated by atmospheric rivers (ARs). This study first examines the magnitude and duration of integrated water vapor transport over the CRB in order to identify historical AR events during the winter season in the target water years. Then, this study maximizes the precipitation depths during the identified AR events by simultaneously optimizing the AR position and its atmospheric moisture using the WRF Model. Finally, this study develops the long-duration MP sequences by substituting each historical AR event with the corresponding maximized AR event.

**Keywords:** Probable maximum precipitation (PMP), Integrated water vapor transport (IVT), Regional climate model (RCM), Pacific Northwest (PNW)

## 1. Introduction

The Probable Maximum Precipitation (PMP) concept has been widely used as a design basis to estimate the Probable Maximum Flood (PMF) (WMO, 2009). Although PMP with a single storm duration has been estimated by considerable number of approaches, such as the statistical approach (Hershfield, 1961; 1965), storm maximization approach (Hansen et al., 1994), and Numerical Weather Model (NWM)-based approach (Ohara et al., 2011), little attention has been given to the PMP estimation for long durations, such as seasonal scale durations on the order of several months. The PMP estimation for long durations is important especially for snowmelt-driven regions since extreme floods are often driven by both snow accumulation and snowmelt processes during winter and spring seasons rather than by a single rainstorm event. As a way of estimating the PMP for long durations, WMO (2009) suggests the "similar process substitution method". This method, however, is only applicable to a limited number of watersheds where sufficient observation data are available, and highly depends on the subjective judgment of hydro-meteorologists. Therefore, this study proposes a new framework using the Weather Research and Forecasting (WRF) model to estimate the physically-based PMP for long durations.

## 2. Study area

This study estimates the Maximum Precipitation (MP) for the 6-month winter period (October-March) for the drainage areas of Bonneville Dam and Libby Dam in the Columbia River Basin (CRB). The CRB is located in the Pacific Northwest, extending over seven U.S. states and southern British Columbia, Canada. The total drainage areas above Bonneville Dam and Libby Dam are about 621,600 km$^2$ and 23,270 km$^2$ respectively. Along the Pacific Northwest region, ARs, defined as long and narrow corridors of strong Integrated Water Vapor Transport (IVT) (Eqn 1), play a critical role in transporting massive amounts of water vapor from the eastern Pacific Ocean, contributing to the majority of wintertime extreme precipitation (Neiman et al., 2008; Warner et al., 2012).

$$IVT = \frac{1}{g}\int_{1000}^{300} q\bar{U}dp$$

where $g$ is the gravitational acceleration (m s$^{-2}$), $q$ is the specific humidity (kg kg$^{-1}$), $\bar{U}$ is the horizontal wind speed (m s$^{-1}$), and $p$ is the pressure (hPa).

## 3. Methodology

### 3.1 Model and data

This study uses the Advanced Research version of WRF, version 3.9.1, for conducting numerical experiments to estimate the long-duration MP. The model configuration

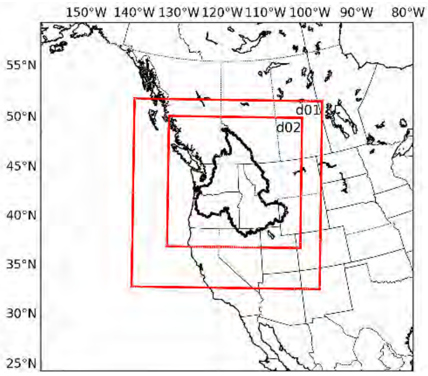


**Figure 1 Domain configuration for the WRF simulations (red) and Columbia River Basin (black)**

consists of two nested domains with horizontal grid resolutions of 36 km and 12 km. Figure 1 shows the geographic coverage of the domains. For the initial conditions (ICs) and boundary conditions (BCs) in the WRF model, this study uses the National Centers for Environmental Prediction's (NCEP) Climate Forecast System Reanalysis (CFSR; Saha et al., 2010) and the National Oceanic and Atmospheric Administration (NOAA) Twentieth Century Reanalysis version 2c (20CRv2c; Compo et al., 2011). The physical parameterization schemes used in the model is described in Hiraga et al. (2021).

### 3.2 Proposed framework

In this study, a new framework is proposed to estimate the long-duration MP during the winter season in AR dominant regions as follows:

- Step 1: Select target water years based on the historical precipitation depth and average temperature over a specified basin;
- Step 2: Identify historical AR events over a specified basin during the winter season in the target water years based on the AR category scale developed by Ralph et al. (2019);
- Step 3: Maximize the cumulative precipitation depths over the target drainage areas within a specified basin during the identified AR events by simultaneously optimizing the AR position and atmospheric moisture. This study optimizes the atmospheric moisture by relative humidity perturbation (RHP) method which proportionally increases RH at ICs and BCs of the modeling domain where IVT values are higher than 250 kg $m^{-1}$ $s^{-1}$ (RHP-IVT method; Hiraga et al., 2021);
- Step 4: Substitute each historical AR event with the corresponding maximized AR event to form the sequence of maximized precipitation events (design precipitation sequence) during the winter season;
- Step 5: Develop the long-duration MP estimation during the winter season over the target drainage areas by accumulating the design precipitation sequence formed in the above step 4.

## 4. Results and discussion

Figure 2 depicts the AR-induced precipitation maximization results obtained by step 3 in Section 3.2. Figure 2 shows time-averaged IVT fields and spatial distributions of the

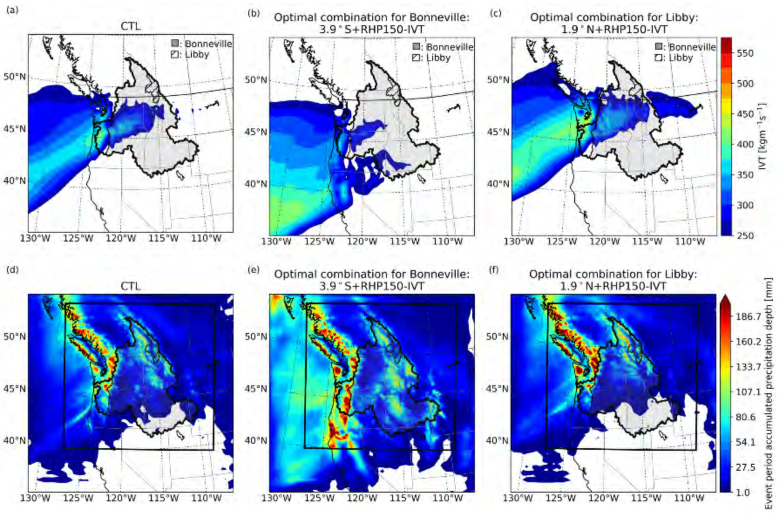


**Figure 2 The spatial distribution of the time-averaged Integrated water vapor transport (IVT; kg $m^{-1}$ $s^{-1}$) (a-c) and accumulated precipitation depths (d-f) during the atmospheric river event 22-a in the 2017 water year (1800 UTC 11 Mar to 1800 UTC 16 Mar 2017)**

accumulated precipitation depths obtained by the control simulation (Fig. 2a and d) and the simulation with the optimal AR position and its atmospheric moisture for the drainage areas of Bonneville Dam (Fig. 2b and e) and Libby Dam (Fig. 2c and f) during the identified AR event in the 2017 water year. In the case of the optimization for Bonneville Dam's drainage area: 3.9◦ south shifting and RHP150-IVT (Fig. 2b and e), the region with strong IVT is transposed to further south and becomes wider compared to the control simulation's result. Accordingly, the precipitation depths over the CRB increased especially in the southern part of the domain.

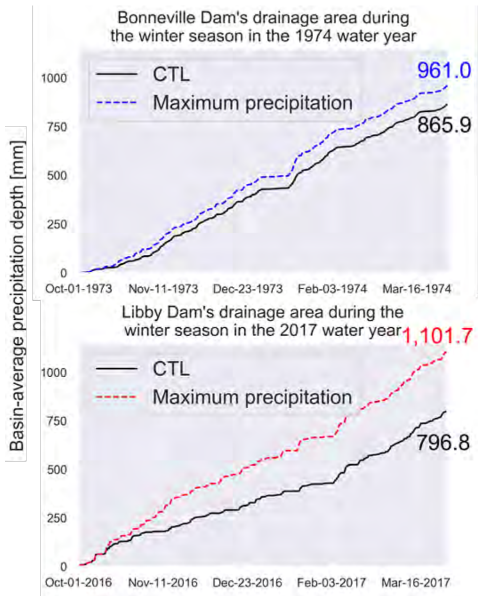


**Figure 3 Long-duration maximum precipitation for drainage areas of Bonneville Dam and Libby Dam**

Figure 3 shows the developed long-duration maximum precipitation sequences by step 4 and step 5 in Section 3.2. We can see that the cumulative design precipitation depths increase with time while maintaining an increasing trend over the control simulation's results.

## Acknowledgements

This study was supported by U.S. Army Corps of Engineers (USACE) Grant 3-20B35-Department of Army Engi-W912HZ-17-2-0001. The CFSR dataset (ds093.0, doi: 10.5065/ D69K487J for 1979 to 2010, ds094.0, doi: 10.5065/D61C1TXF for 2011 to present), and the 20CRv2c dataset (ds131.2, doi: 10.5065/ D6N877TW) were obtained through the NCAR/UCAR Research Data Archive. The PRISM dataset is obtained from the PRISM Climate Group (http://www.prism.oregonstate.edu/).

## References

1) Hershfield, D.M., 1961. Estimating the probable maximum precipitation. J. Hydraul. Div. 87 (5), 99–116.
2) Hershfield, D.M., 1965. Method for estimating probable maximum rainfall. J. Am. Water Works Assoc. 57 (8), 965–972. https://doi.org/10.1002/j.1551-8833.1965.tb01486. x.
3) Hansen, E.M., Fenn, D.D., Corrigan, P., Vogel, J.L., Schreiner, L.C., Stodt, R.W., 1994. Probable maximum precipitation -Pacific Northwest states: Columbia River (including portions of Canada), Snake River and Pacific coastal drainages. NWS Hydrometeorological Rep. 57, 353. https://www.nws.noaa.gov/oh/hdsc/PMP_documents/HMR57.pdf.
4) Ohara, N., Kavvas, M.L., Kure, S., Chen, Z.Q., Jang, S., Tan, E., 2011. Physically based estimation of maximum precipitation over American River Watershed. California. J. Hydrol. Eng. 16 (4), 351–361. https://doi.org/10.1061/(ASCE)HE.1943-5584.0000324.
5) World Meteorological Organization (WMO), 2009. Manual on estimation of Probable Maximum Precipitation (PMP), WMO-No. 1045, https://library.wmo.int/doc_num.php?explnum_id57706.
6) Warner, M.D., Mass, C.F., Salathe´e, E.P., 2012. Wintertime extreme precipitation events along the Pacific Northwest Coast: climatology and synoptic evolution. Mon. Weather Rev. 140, 2021–2043. https://doi.org/10.1175/MWR-D-11-00197.1.
7) Neiman, P.J., Ralph, F.M., Wick, G.A., Lundquist, J.D., Dettinger, M.D., 2008. Meteorological characteristics and overland precipitation impacts of atmospheric rivers affecting the West coast of North America based on eight years of SSM/I satellite observations. J. Hydrometeorol. 9, 22–47. https://doi.org/10.1175/ 2007JHM855.1.
8) Saha, S., Moorthi, S., Pan, H.-L., Wu, X., Wang, J., Nadiga, S., Tripp, P., Kistler, R., Woollen, J., Behringer, D., Liu, H., Stokes, D., Grumbine, R., Gayno, G., Wang, J., Hou, Y.-T., Chuang, H.-ya., Juang, H.-M., Sela, J., Iredell, M., Treadon, R., Kleist, D., Van Delst, P., Keyser, D., Derber, J., Ek, M., Meng, J., Wei, H., Yang, R., Lord, S., van den Dool, H., Kumar, A., Wang, W., Long, C., Chelliah, M., Xue, Y., Huang, B., Schemm, J.-K., Ebisuzaki, W., Lin, R., Xie, P., Chen, M., Zhou, S., Higgins, W., Zou, C.-Z., Liu, Q., Chen, Y., Han, Y., Cucurull, L., Reynolds, R.W., Rutledge, G., Goldberg, M., 2010. The NCEP climate forecast system reanalysis. Bull. Am. Meteorol. Soc. 91 (8), 1015–1058. https://doi.org/10.1175/2010BAMS3001.1.
9) Compo, G.P., Whitaker, J.S., Sardeshmukh, P.D., Matsui, N., Allan, R.J., Yin, X., Gleason, B.E., Vose, R.S., Rutledge, G., Bessemoulin, P., Br¨onnimann, S., Brunet, M., Crouthamel, R.I., Grant, A.N., Groisman, P.Y., Jones, P.D., Kruk, M.C., Kruger, A.C., Marshall, G.J., Maugeri, M., Mok, H.Y., Nordli, Ø., Ross, T.F., Trigo, R.M., Wang, X. L., Woodruff, S.D., Worley, S.J., 2011. The twentieth century reanalysis project. Q. J. R. Meteorol. Soc. 137 (654), 1–28. https://doi.org/10.1002/qj.776.
10) Yusuke Hiraga, Yoshihiko Iseri, Michael D. Warner, Chris D. Frans, Angela M. Duren, John F. England, M. Levent Kavvas. 2021. Estimation of Long-duration Maximum Precipitation during a winter season for large basins dominated by Atmospheric Rivers using a Numerical Weather Model, Journal of Hydrology, 598, 126224. https://doi.org/10.1016/j.jhydrol.2021.126224.

# Application of flexible model structures to interpret dominant process controls on flow duration curves

○Chris Leong[1*], Yoshiyuki Yokoo [1]
[1]Faculty of Symbiotic Systems Science, Fukushima University, 960-1296, 1 Kanayagawa, Fukushima-city, Japan

*E-mail: leongchris@sss.fukushima-u.ac.jp

**Abstract**

There has been significant progress made towards understanding the process controls that impact the shape of the flow duration curve (FDC). However, the transferability of such knowledge over large spatial scales is still lacking, partly due to the model structural approaches. In this study: (1) we propose a simple framework to transform hydrological models from fixed to flexible structures to better represent the unobserved underground layer, (2) with the flexible model structure, provide an interpretation of the dominant processes in the underground layer that impact the shape of the FDC. The framework captures characteristic event timescales from identical recessions and groups them as dominant processes which are then used to construct the flexible model. The results main results are, (1) wet catchments have more complex model structures than arid catchments. However, it also suggests that the relationship between the internal components of model structures in arid catchments are more complex than wet catchments. (2) Highly arid catchments can have no underground structure, due to dominant surface processes and lesser occurring underground processes. (3) The FDC shape was controlled by how climate affected the role of dominant processes in the intermediate layers. In humid catchments, the intermediate layers had less impact on the storage and release processes from the deepest layers. Therefore, these catchments were able to generate and maintain flows, thus displayed flat tailed FDCs. However, in dry catchments, the dominant processes were more active towards the surface, thus the intermediate layers were more effective. This affected the ability for the deepest layers to generate flows, therefore, displaying FDC tail dips. The dips became more pronounced as the processes were dominantly activated at the surface due to intense differences in aridity and precipitation. Lastly, not only is a catchments' ability to generate flows important for developing flexible model structures but also the ability to maintain flow magnitudes is equally important.

**Keywords:** Flow duration curve; Flexible model structures; Dominant processes; Process-based

# Towards water security in the cities of La Paz and El Alto, Bolivia

○ Pablo FUCHS [1*], Javier MENDOZA[1], Gustavo AYALA [2]
[1]Institute of Hydraulics and Hydrology, Universidad Mayor de San Andrés, La Paz, Bolivia
[2]Inter-American Development Bank (IDB)/Ministry of Environment and Water, La Paz, Bolivia

*E-mail: jfuchs@umsa.edu.bo

**Abstract**

Water security is broadly defined by UN-Water as "the capacity of a population to safeguard sustainable access to adequate quantities of acceptable quality water for sustaining livelihoods, human well-being, and socio-economic development, for ensuring protection against water-borne pollution and water-related disasters, and for preserving ecosystems in a climate for peace and political stability". In order to achieve water security in two major and neighboring cities of western Bolivia, La Paz and El Alto cities, several studies were carried out in the last decade. Here, we summarize and describe the state of the art of water resources research in this region based on monitoring and modeling techniques, which were developed based on data from an ongoing network of Automatic Weather and hydrometric stations installed at high altitudes (i.e. greater than 4400 m a.s.l.) and that are working since 2011. As this region partly depends on water resources resulting from the melting of a large number of glaciers located at headwater catchments, the quantification of glacier melt and mass balance is of primary interest. Therefore, we also show the results obtained during fieldwork at some glaciers where the following variables are measured at monthly and annual timescales: glacier mass balance, equilibrium line altitude, and glacier retreat. Finally, we discuss the direction of our future work, which will focus on the integration of the results obtained so far into a water management model that will consider water supply and demand analyses to further derive water management policies to effectively address future water availability and scarcity under different climatic and socioeconomic scenarios.

**Keywords:** Water security, water resources, high-altitude mountain catchments, glacier retreat, Bolivia

# Performance of machine learning algorithms for potential recharge areas mapping in high-altitude Andean mountains

○Evelyn Aliaga[1,2], Freddy Soria [1*]
[1]Centro de Investigación en Agua, Energía y Sostenibilidad, Universidad Católica Boliviana "San Pablo"
[2]Civil Engineering Department, Universidad Católica Boliviana "San Pablo"

*E-mail: fsoria@ucb.edu.bo

**Abstract**
High Andean wetlands of the Bolivian Altiplano have an important role in the hydrological cycle. Factors such as climate change constitute a threat to their existence, because of which its study and mapping is relevant to promote its conservation. Here we evaluate the performance of the Random Forest RF, Support Vector Machine SVM and Multivariate Adaptative Regression Splines MARS machine learning algorithms, to map potential recharge areas. The results show that the RF algorithm had the best performance compared to the SVM algorithm and the MARS algorithm as evaluated by the Receiver Operating Characteristic ROC algorithm.

**Keywords:** machine learning, algorithm, high-altitude, maps of potential recharge areas

## 1. Introduction

High Andean wetlands of the Bolivian Altiplano play a multiple role in the hydrological cycle. Located in a semiarid mountainous region, they allocate important groundwater recharge zones given their sponge-like dynamics storing surface water from rain and glacier water melt, providing as well forage for camelids and endemic local species, and recourses for locals. Access to natural water sources is currently influenced by climatic and anthropic factors. Andean wetlands face multiple threats, from climate change to anthropogenic intervention, which is why their monitoring constitute a relevant resource for their conservation.

Among the approaches for wetland mapping, remote sensing mapping, e.g., using satellite imagery, provide several advantages, among which economy would the most important one. In this article we aim to exploit the capabilities of using remote sensing information together with base maps analyzed with Geographic Information Systems (GIS), with machine learning algorithms to map groundwater recharge areas in mountainous areas, as an alternative to traditional database treatment and analysis. Thus, we extend the proposal of Pourghasemi et al. (2020), who applied machine learning algorithm on 16 effective factors to map potential groundwater recharge in a zone with mild topography. In our case, we apply the Random Forest Regressor (RFR), Support Vector Regressor (SVR) and Multivariate Adaptative Regression Splines (MARS) algorithms in a scarped topographic area, for potential recharge area mapping.

## 2. Study area

The high Andean area of the Cordillera Real the Northern Puna ecoregion in Bolivia, covers an area of 3647 $km^2$, along and altitudinal range of 4448 masl (Chillieco Peak) and the Mururata Peak at 5868 masl (Fig.1). The average temperature during the day is 4.5 ° C and -5 ° C at night (Beck et al., 2000). The high Andean wetlands in the Cordillera Real de La Paz are located on plains and slopes within an altitudinal range of 2858 to 6466 masl. The dominant land use type is used as fresh and nutritious forage throughout the year, mainly due to the surface water regulation and storage properties of wetlands. The water table reaches its highest at the end of the rainy season in March, when it stores the rain, surface water as well as glacier melt, to promote life during the dry, clear-sky winters, characterized by high evapotranspiration, and intense solar radiation.

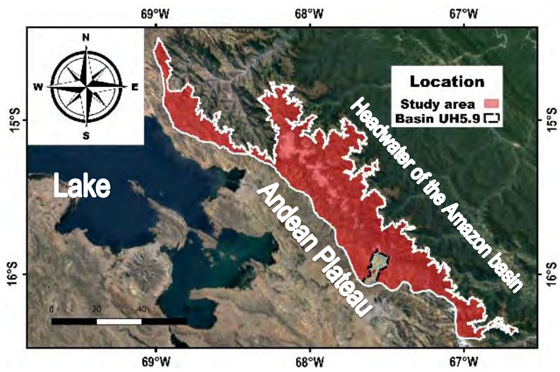


Fig.1 Location of study area.

## 3. Methodology

This study adapt the methods suggested by (Pourghasemi et al., 2020) to the wetlands of the scarped high-Andean areas of the Bolivian Altiplano. Background information as well as conservation and sustainability data were obtained from the

BIOTHAW project (Dangles et al., 2014) and other public source data.

The first step consists on applying the algorithm Least Absolute Shrinkage and Selection Operator (LASSO) for the sensitivity analysis of recharge parameters. Then, there were compared three supervised machine learning algorithms: the RFR, SVR and MARS to predict maps based on Soil Conservation Service (SCS) curve numbers (CN). The performance of the algorithm was quantitatively assessed by the Receiver Operating Characteristic (ROC) algorithm, and qualitatively assessed by visual adjustment superimposed maps on Google Earth satellite imagery. The ROC judges the performance of an algorithm based on the Area Under the Receiver Operating Characteristic Curve (AUROC); when AUROC is close to 1, the performance of the algorithm is good, whereas, if the AUROC is close to 0, the algorithm performance is low.

## 4. Results and discussion

As an example, the results shown correspond to the basin UH 5.9. The application of the LASSO algorithm (Fig. 2) pointed to the parameter annual maximum temperature as the most sensitive one, in areas with mixed topographic composition in watersheds with highland hydrological characteristics. Likewise, the visual adjustment of the map predicted by the RF algorithm (Fig.3) adequately fits recharge areas over CN of 99; CN equal to 62 over flat areas.

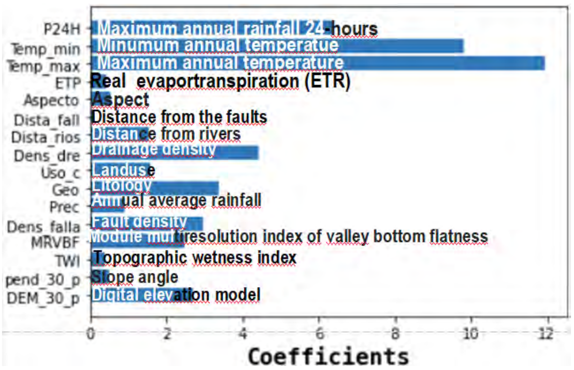


Fig. 2. Sensitivity analysis performed by LASSO for the UH 5.9

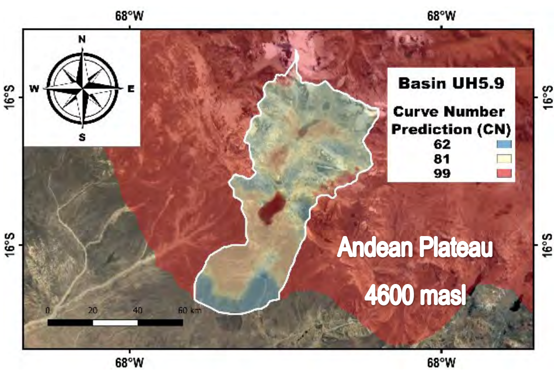


Fig. 3. Visual adjustment of the map

Regarding algorithm AUROC performance, the results shown in (Fig. 4) indicate that the RF algorithm had the best performance among all. RFR's AUROC is in a range of 0.936 to 0.997, followed by the SVM's AUROC (0.907 to 0.991) and the MARS's AUROC (0.859 to 0.984).

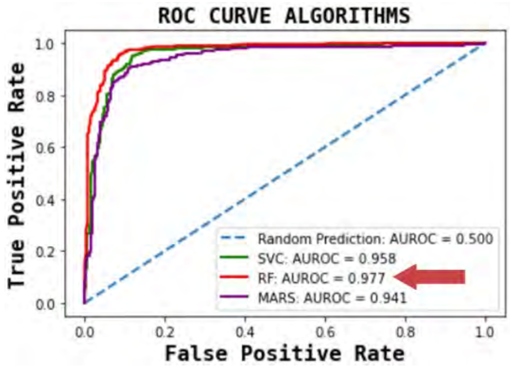


Fig. 4 Performance of the algorithms by ROC for the UH 5.9

## 5. Conclusions

The RF algorithm slightly surpasses the SVM and MARS algorithms, after its AUROC value above 0.950. The visual comparison of the maps generated showed that the performance vary according the topographic characteristics of the area. The application of the RFR algorithm showed good results for areas with slopes of 0 - 32 degrees; the SVR algorithm showed good performance for areas with slopes of 44 - 76 degrees, while for areas with slopes of 0 - 12 degrees its performance was inaccurate. The application of the MARS algorithm showed the worst performance; it performed well for certain areas, whereas for areas with slopes of 0 - 12 degrees and 44 - 77 degrees, recharge zones were erroneously flagged.

## References

1) Beck, S., Sarmiento, J., Paniagua, N., Miranda, C., & Ribera, M. O. (2000). Humedales de Bolivia, una aproximación a su conocimiento actual. 119–150.
2) Dangles, O., Meneses, R. I., & Anthelme, F. (2014). BIOTHAW: Un proyecto multidisciplinario que propone un marco metodológico para el estudio de los bofedales altoandinos en un contexto de cambio climático. Ecología en Bolivia, 49(3), 6–13.
3) Pourghasemi, H. R., Sarhadi, N., Yousefi, S., Tavangar, S., Ghaffari Nazarlou, H., & Santosh, M. (2020). Using machine learning algorithms to map the groundwater recharge potential zones. Journal of Environmental Management, 265, 110525. https://doi.org/10.1016/j.jenvman.2020.110525

# Evaluation of factors affecting the concentration of an emerging pharmaceutical pollutant (Sulfamethoxazole) in cities with absence of wastewater treatment systems by sensitivity analysis of a global fate transport model

○Andrea Agramont[1*], Freddy Soria[1], Carolina Garvizu [1]
[1]Centro de Investigación en Agua, Energía y Sostenibilidad, Universidad Católica Boliviana "San Pablo", La Paz, Bolivia

*E-mail: andy.agramontc31@gmail.com

**Abstract**
In La Paz Bolivia, the Choqueyapu River is part of one of the main water systems of the municipality of La Paz-Bolivia, being the main collector of domestic and industrial waste, without any previous treatment, which constitutes an important source of emerging pollutants, representing a potential risk to public health. The dispersion of Sulfamethoxazole, which is the drug with the greatest presence in Latin America, was modeled in the trajectory of the Tributary Basin of the Choqueyapu River, with the GIS and Global-FATE tools. First, different input data has been mapped, such as pending, flow direction and accumulation, population consumption of sulfamethoxazole, total population, among others. The next stage includes the calibration of the model and its sensitivity analysis to assess the performance of the model and understand the incidence of the factors in the dispersion of the pollutant. Finally, an interpretation is made of the results obtained with respect to the concentration of the studied drug.
**Keywords:** Sulfamethoxazole, model, water resources, Choqueyapu, GIS

## 1. Introduction

At present, Emerging Contaminants or EC in the environment has been recognized as a worldwide concern, mainly due to the widespread dissemination and accumulation of pharmaceutical compounds and their implication in antimicrobial resistance (AMR) or their presence in drinking water (PNUMA, 2017). ECs are defined as a substance of different origin and chemical nature that are found in the environment in minimal concentrations and can represent a risk (potential, observed or real) for public-health and the environment (Janet Gil *et al.*, 2012a).

The problem with EC comes from the resistance it generates to microorganisms against the effects of an antimicrobial agent and has the ability to multiply in its presence, there are 3 the main categories, which may vary according to jurisprudence and regulations of the country in which it is applied, where those of pharmaceutical origin will be highlighted (Janet Gil *et al.*, 2012b).

The environmental presence of antibiotics represents 3 important threats, the first is the development of resistant pathogenic bacterial strains due to the constant contact between them, hindering their effectiveness in the use of these antibiotics for the treatment of people and even animals, second, in the difficulty for its removal in conventional treatment plants focused on municipal wastewater, and finally on its bioaccumulation in plants, algae and living beings.

As the spread of resistance is associated with excessive consumption, population increase and misuse of medicines and antibiotics among humans, animals and within various agricultural practices, united with poor sanitation, the risks associated with this pollutant will only increase over the years, and according to (OMS, 2020; O'Neill Commission, 2014) projects indicates that antimicrobial resistant infections may become the leading cause for death at a worldwide level by 2050.

Sulfamethoxazole is a bactericidal antibiotic, indicated as a treatment for infections of various kinds this antibiotic is termed low-cost and over-the-counter, frequently found in high concentrations in rivers and lakes of low-income countries, and is ranked in the high-priority list of pharmaceuticals relevant to the water cycle by the Global Water Research Coalition (de Voogt *et al.*, 2009).

In 2005, studies carried out by the Latin American Federation of the Pharmaceutical Industry showed that from a list of the 20 best-selling drugs in Latin America, sulfamethoxazole was the second most sold, only surpassed by aspirin. (Gonzales, 2005).

On the other hand, a recent evaluation carried out by the German Enviroment Agency, of more than 1000 international publications, detected emerging contaminants in more than 70 countries around the world, of which sulfamethoxazole has been the antibiotic most found in the aquatic environment, being reported in 47 countries, the same situation is repeated in the area of the larger cities of the municipality of La Paz, where investigations have been carried out in the Choqueyapu river and the common denominator in aquatic ecosystems has been Sulfamethoxazole (eg, Salazar *et al.*, 2020; Medina *et al.*, 2021), which could be due to the low absorption in the receptor organism that antibiotics have, for which it ends up being eliminated, via the urinary route, although it is mostly excreted via the fecal route, between 25 and 75% of its metabolites and is also excreted in breastmilk (Frank-Andreas Weber *et al.*, 2014).

Although, to date, different actions have been carried out to maintain the water quality in the basins that cross the municipality of La Paz, the task to control emerging pollutants is complex, due to the limited availability of information in this field among many other reasons. It is still far from being able to understand the magnitude of the problem that the EC would entail, especially in a developing country such as Bolivia, which is highly vulnerable to different crises, putting a lot of pressure on resource management water in the preventive phase (Álvarez, 2018)

## 2. Study area

La Paz is one of the municipalities that make up the city that bears the same name, through which the Choqueyapu River passes, belonging to the Beni River, it is born in the Chacaltaya mountains with an approximate length of 44 km and a height of 5500 m s. n. m.


Fig.1 Study area image of the tributary basin of the Choqueyapu River represented with a red line

The climate of La Paz has been described as a "high mountain tropical climate", with a dry winter, no rain, or little recurrent rains, which causes the humidity during the months of May to October to be lower.

In the basin, the Choqueyapu River covers a length of 10 km, it presents slopes up to approximately 55%, decreasing to 0%. in the middle and lower parts of its route covering the entire area with an urban presence. (Carpio, 2017).

Despite having carried out different studies and analyzes, such as those carried out by the Contraloria General del Estado (2013), having denoted the existence of a very high contamination, coming from anthropogenic activities such as the paint, textile, food, pharmaceutical industry , domestic wastewater, among others, which is why the concern for its water quality has alarmed different government entities and researchers in general (eg, Comptroller General of the State, 2013; Ballivián, 2012; Oscar, 2019). They have carried out studies on ECs because the regulations do not contemplate them.

## 3. Methodology

Obtaining and preparing the information was based on the requirements of the GLOBAL-FATE model so that it can develop the simulation correctly and obtain the expected results.

### *3.1 Obtaining secondary information*

For the study and determination of the data of: flow, connection to wastewater treatment, accumulation flow, flow direction model and slopes, the topography of the study area was required. The maps generated for these analyzes are prepared at scales from 1: 20,000 to 1: 50,000, depending on the objectives, availability, collection and review of available information regarding the geographical-physical characteristics of the basin.

To carry out the work, a series of bibliographic and cartographic information has been gathered. Additionally, to carry it out, the study area was defined, with the delimitation of the basins of interest; In order to gather relevant and accurate information, the following institutions were used:

a) Gobierno Autónomo Municipal de la ciudad de La Paz GAMLP. - It has a base cartography of the different basins of the city of La Paz and its water courses, as well as orthorectified aerial photographs of the place.

b) EPSAS. - The database has a cartography of the sewerage networks of the entire city of La Paz, updated to 2018.

c) SIGED. - The Statistical Geographic Information System for Development (SIGED) of the National Institute of Statistics (INE), is a system of cartographic and statistical information with a graphical interface, it contemplates a socio-economic information data of the census population for the date 2012, allowing consult the information at different levels.

d) GeoBolivia maps portal. - Geographic information platform produced by state institutions for all of Bolivia, it is a free and public access repository.

### *3.2. Information preparation*

3.2.1 Vector Data

To obtain the vector data, various ARCGIS tools were used, starting from the preliminary design obtained through the spatial analysis of the Digital Elevation Model, using the Spatial Analysis tool incorporated into the ArcGis program. Corrections were made for pixels with absence of numerical data, using the nearest neighbor method by default.

We started from the digital elevation model (DEM) to obtain:

Flow direction, Flow Accumulation, Slope.

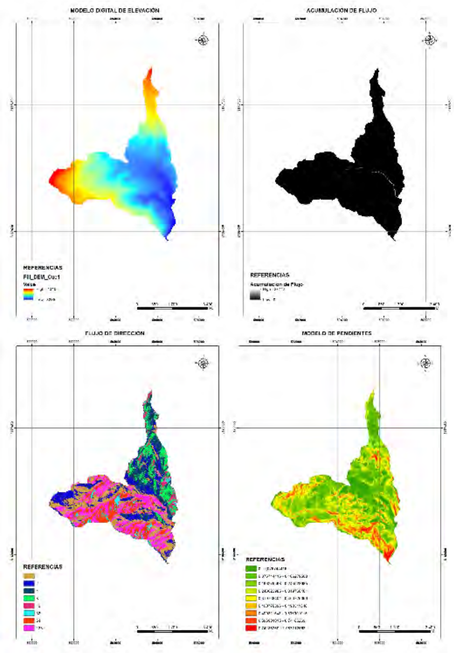


Fig.2 From left to right, above: DEM and Flow Accumulation Bottom: Flow direction and Slope.

To obtain the population, only the people that comprise the study area were taken into account, a population projection was made for the year 2020 because the last census carried out, throughout the country, was carried out for the last time in 2012:

$$P_{2020} = P_t(1+r)^n$$

where:

$P_{2020}$: Projected population

$P_t$: Actual population

$r$ : Intercensal growth rate = 0,96%

$n$: Subtraction between the year for which data are available, and the year to be projected = 8

The map of the sewerage system was obtained from the GeoBolivia repository, which shows the distribution of drinking water and basic sanitation projects in the local territory of the city of La Paz, updated until March 2018

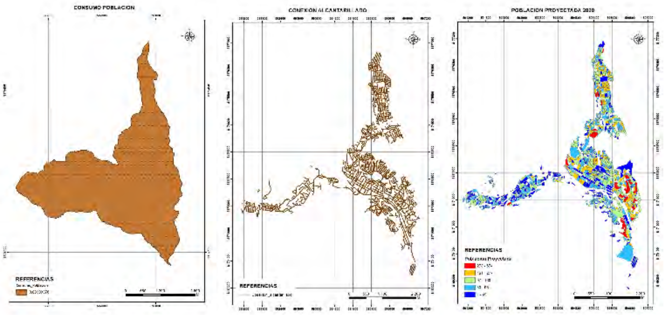


Fig.3 From left to right, Antibiotic consumption, Sewage system, Population of the area.

*3.2.2. Charged Parameters*

For the model, 12% was taken for the elimination of the sulfamethoxazole, according to the bibliographic reference, the lowest percentage was chosen since it was the lowest in a range that oscillates between 12 and 69% obtained from Zhang *et al.*, (2015) and Ternes (1998).

The decay rate for sulfamethoxazole was established by Pistocchi *et al.*, 2012, where indicates the first-order linear kinetics in samples of water bodies, with factors that vary from 0.0069 for a DT50 of 1 day, to 0.003 for which it is assumed that there is no decay of the pollutant in the water body, consequently, for the final result, the data of 0.0069 was used, since this value is the one that is closest to the half-life time obtained by studies by Guerrero (2019).

*3.3. Calibration.*

For the calibration of the model, the maximum and minimum values of table 1 were used. The values are grouped by type of zone and by concentration in [ng / m3] to estimate a possible range of calculations of computationally modeled concentrations in the Choqueyapu River basin.

| Zone | Concentration | Mean | Minimun | Maximum | Population | Author |
|---|---|---|---|---|---|---|
| Alemania | | - | - | 4700 | - | Hirsch et al. (1999) |
| EEUU | | 220 | - | 0 | - | Lindsey et al. (2001) |
| Sena River (Francia) | | 190 | - | 0 | 12.341.418 | Tamtam et al. (2008a) |
| Francia | | 63 | 20 | 5440 | - | Tamtam et al. (2008b) |
| Po River (Italia) | | 2,1 | 1,83 | 23,9 | PTAR descargas | Zuccato et al. (2010) |
| Arno River (Italia) | | 5,3 | 1,7 | 114 | - | |
| Ebro River (España) | | 89 | - | - | - | |
| Delta Mekong River ( U Vietnam) | | 111 | 125 | 3130 | 171.000 | Shimizu et al. (2013) |
| Delta Mekong River( R Vietnam) | | 26 | 7 | 560 | - | |
| Delta Pearl River (China) | | - | 28,7 | 1245 | 1.237.000 | Peng et al. (2014) |
| Ghana | | 2102 | 5 | 9640 | - | Segura et al. (2015) |
| Kenya | | 13,36 | 1 | 49,56 | - | |
| Mozambique | | 11420 | 511 | 53828 | - | |
| South Africa | | 2090 | 3 | 10568 | - | |
| Cuenca Katari U | | 130 | 15 | 2180 | 1.280.000 | Archundia (2017) |
| Cuenca Katari K | | 24,2 | 18 | 310 | - | |
| Cuenca Afluente del Río Choqueyapu | | 0,3489 | 51,113 | 187,8 | 89.630 | This Study |

Table 1. Comparison of the observed concentrations of sulfamethoxazole (ng / m3) in surface waters with data from the literature.

3.4. Sensitivity Analysis

The method of "parameter disturbance" was used, which is the variation of one parameter of the model while the rest remains constant, so that the variations suffered in the state variables reflect the sensitivity of the solution to the modified parameter ((Aguilar, 2017)).

The chosen inputs were: DT50, Time or flow, Population, Consumption-Excretion of the drug and percentage of removal of the contaminant according to the type of WWTP. The sensitivity analysis addressed the change in DT50 values according to those exhibited in Pistocchi *et al.*, (2012)Regarding the time of year, the inter-monthly variations of the flow were taken as data, to verify how these affected the Maximum output concentration results. The product of the multiannual monthly water balance of the Choqueyapu River basin are presented for the rainy season of 2018, where a bimodal climatological regime is appreciated with rainy seasons between the months of November to May, being reduced between the months of March to October.

Population density was varied based on the results of the population registered by the INE, in 2012, and then the corresponding projection was made for the next 10 years. The variation of the consumption data was made from the data obtained in the Results section, where it was multiplied by a constant factor of increase. And finally, the variation in the removal effectiveness of the different WWTPs was made by choosing to use the removal percentage that was presented in the document by García *et al.*, (2011)entitled Emerging contaminants: effects and removal treatments, where a review of the different types of treatments and their percentage of effectiveness against pharmaceutical CE.

All data was converted to percentages of change, for a better management of the information in a graph that agglomerates all the information, and to be able to analyze it as a whole.

## 4. Results and discussion

After converting the maps to ASCII format, they were introduced to the GLOBAL-FATE model, obtaining the following results:

4.1 Application of the Model

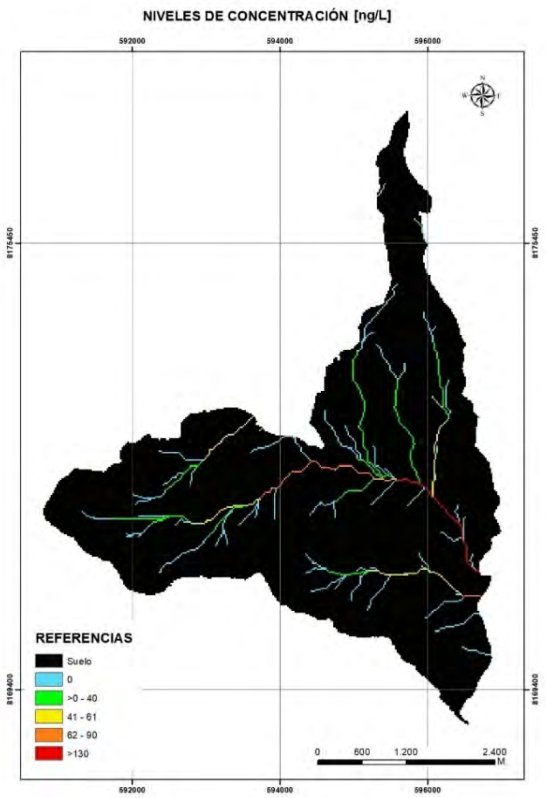


Fig.3 Map resulting from the application of the model

Regarding the specific results of the modeling carried out, the concentration of sulfamethoxazole found in the sewerage network that flows into the Choqueyapu River shows the main sector where all the effluents are collected, as the main source potentially contaminated with Sulfamethoxazole, reaching concentrations above 130 [ηg / L]. This data is interesting since the half-life kinetics of the drug is less than 24 hours. The Water Framework Directive for Emerging Contaminants and the predicted no effect concentrations (PNECs) specify 590 [ηg / L] as the maximum acceptable limit, which means that the results obtained are much lower (Grill *et al.*, 2016)Even so, on-site studies by Salazar *et al.*, 2020; Medina *et al.*, 2021 showed profiles of high resistance percentages in samples of total resistant coliforms for sulfamethoxazole-trimethoprim, with values 39% and 73% respectively, which indicates a potential threat even for the concentration levels simulated by the model.

The results suggest that the model has limitations to operate at a reduced local scale (micro-basin), since the results are very specific, firstly, because it is a canalized river and also because of the complexity of the interactions between the sewerage system and the receiving body, in addition to the specific information gap, such as drug consumption data at the municipal, local and / or district level. Those differences translate into a limitation when interpreting the results of the model, in aspects such as, the greater or lesser dilution of the substance.

The model shows an interesting capacity so that it can be used to test the effectiveness of management strategies related to the control of the consumption of pharmaceutical products and the implementation and improvement of wastewater treatment in order to offer evaluations of impacts from the consumption of pharmaceutical products and the health of the river network ecosystem. Assessments in relation to climate change could also have significant potential through the application of this model.

4.2. Calibration


Fig.4 Figure result of Table 1

Fig.5 Data from African countries are excluded, due to high concentrations that make it difficult to visualize

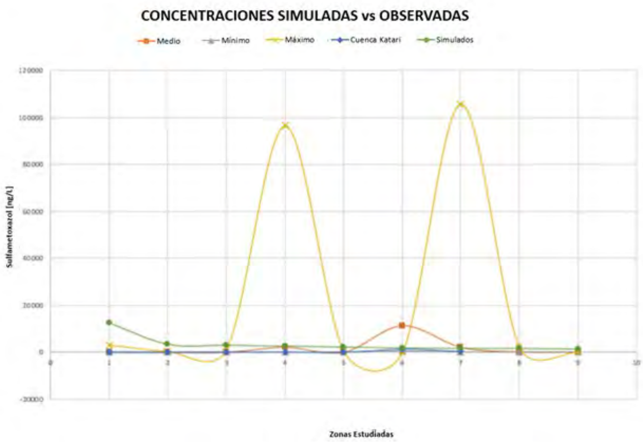


differences with other countries.

For the data found in the model, a partial comparison was made with the data collected, it should be noted that these could not be compared one by one in a respective area, to verify their correlation. If not, the data found throughout the entire water body was compared. This causes that there is no information on sulfamethoxazole concentration data sampled in the modeled basin, so the values were compared in relation to the maximum and minimum ranges, when possible, of international and local data, the latter being carried out with the ranks found in the Katari Basin.

As a result of the calibration, the data found in the model are within the ranges obtained according to the field observation, so they are considered acceptable; however, the ideal is to have data from the basin to be modeled, which was not possible. due to the long period of monitoring that this requires and because the objective of the project was to demonstrate the applicability of the model. The values found can be related to the data of the concentrations found in the basins of the different countries, compiled in external bibliography, so it is considered that the model fulfills its function of modeling the concentration of sulfamethoxazole along the Tributary Basin of the Choqueyapu River.

4.3 Sensitivity Analysis

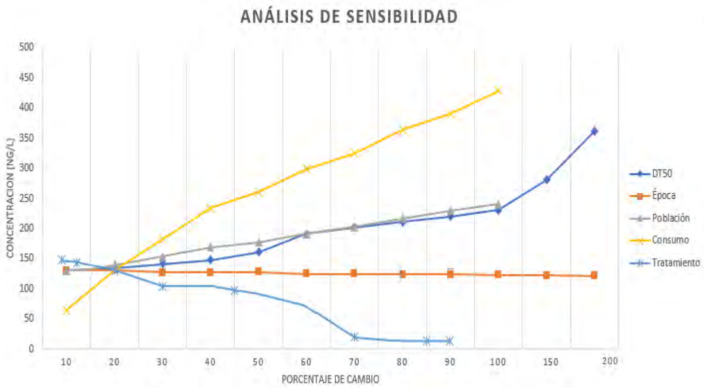


For the sensitivity analysis, variations were made in 5 input parameters: DT50, month-to-month flow, population quantity, population consumption, and percentage of removal from wastewater treatment plants.

a) DT50: Since its variability depends on two important factors which are: i) the amount of solar radiation to which the substance is exposed and ii) the stability of the substance when it is in contact with water or other substances, which can lead to other compounds more or less dangerous than the original. Although it is not possible to know the incidence of these two aspects in the variability of DT50 due to not having historical data measured in the field and/or laboratory, the fact that it is possible that any alteration in the course of the river, such as a vaulting that blocks solar radiation, as well as the interaction of sulfamethoxazole with other substances coming from the sewers, whether of industrial or domestic origin with which it can react, can alter its dispersion and permanence capacity.
b) Time of year and month-to-month flow. Analyzing the sensitivity of the model according to the time of year and its relationship with the variability of the flows in the rivers during the dry season or the rainy season, did not express a greater influence on the concentration of sulfamethoxazole obtained in the simulation results. That seems to have no reason and could be explained due to the complexity of the interactions at the high resolution of the basin where the proposal was worked on. The resolution of the available flow input data affected the development of the model, since, according to the author (Font *et al.*, 2019), the model does not behave more reliably when the flow is less than 100 [m3/ year]. This was evidenced when the sensitivity analysis was replicated, varying the flow data below 90 [m3 / year], where the concentration data remained constant.
c) Population Density. The population increase defines a linear growth of the trend line, assuming variations in percentage ranges from 10 to 10, until the percentage of change is doubled. As a result, in the graph of the sensitivity analysis, the resulting concentrations of sulfamethoxazole are observed, which increase as the population increases, although not greatly, this due to the low growth rates that exist for the municipality of La Paz, to obtain representative variations of the population, projections for 60 years had to be used.
d) Population consumption of sulfamethoxazole. It was the most important variable at the time of conducting the sensitivity analysis. It is the variable that most affects the sensitivity of the model. This shows that, with an increase in the consumption of this drug by 100%, there would be concentrations of up to 450 [ηg / L].
e) Treatment. For the case of wastewater treatment, the drug concentration values were significantly reduced as the performance of the WWTP was higher. The model is very accurate when calculating to reduce the amount of pollutant based on pollutant removal.

Physical variables such as slope, flow direction, flow accumulation, among others, were not taken into account in the sensitivity analysis, because although these may change over time due to urbanization processes, this is not the case. for a vaulted river and a highly urbanized basin. However, it is possible that, for other types of studies, a sensitivity analysis on geomorphometric parameters could be interesting to assess the effect of the configuration of sewage and drainage networks on the concentration and presence of emerging pollutants in water bodies, in cities with similar conditions to those of La Paz, mainly in cities with significant deficiencies in sanitation.

## 5. Conclusions

Choqueyapu River is the main collector of waste in the city, as well as Sulfamethoxazole, reaching concentrations above 130 [ηg / L]. Although it is within the acceptable limits proposed by PNECs (590 [ηg / L]), even so, on-site studies conducted by Medina et al., 2021; Salazar et al., 2020 showed high resistance percentage profiles in samples of total resistant coliforms for sulfamethoxazole.

As a result of the calibration, the data found in the model are within the ranges obtained according to the field observation, so they are considered acceptable, however the correct path is to have data from the basin to be modeled, but there is a gap in this type of studies in Bolivia

Although the model has had limitations, currently these are the only tools that allow us to predict and represent the behavior of certain phenomena, variables, as in the case of this paper, analyzing the dispersion of sulfamethoxazole. Even so, this is a field that has not been explored much in Bolivia, therefore, it is appropriate and important to practice in the use of these systems in order to generate results that fill the information gaps in the different environmental fields and help us to better understand the situation to be studied.

A model must be fed and updated, the important thing is to have calibrated the diverse amount of information used as input data, however, these data can and must be updated to bring the model closer to reality, and in many cases the information had to be approximated or projected, it is necessary to carry out research to gather important details so that the projection of the results is even more accurate. It should be emphasized that the results of a model depend on the quality of the input data. In this specific case, all available and official information was used, based on which the calibration and data preparation necessary for the model to work correctly was carried out, so the results obtained are very close to the current real conditions, even considering the problems of the model at small scales.

A cumulative effect of the concentration of this antibiotic, its metabolites and other products from the metabolism and side reactions of sulfonamides can also have negative effects and influence the final toxicity. One of the few research papers that focused on the ecotoxicity of sulfamide metabolites suggested that the inhibitory effects were increased when sulfamethoxazole metabolites were mixed with trimethoprim, a drug that is regularly prescribed together with sulfamethoxazole to increase its antibiotic efficiency (Eguchi *et al.*, 2004). There is ambiguity and little information on the effects of sulfamethoxazole when exposed to vegetables and plants for human consumption through irrigation with water contaminated with this drug, but this does not imply that there is no risk in cities such as La Paz, where the incidence could be high.

The results suggest the importance of increasing attention to the generation of information in the field, so that the modeling of transport and fate of a greater number of pharmaceuticals promotes better water management and decision making in the Choqueyapu River. Actions should not only consider the most important problems that afflict this important body of water, but also initiate preventive and mitigating actions that encompass emerging contaminants, which will undoubtedly be a major future problem if something is not done.

Since the kinetics of pollutant degradation, or its transformation to other more or less hazardous substances, depends on temperature and solar incidence, it is recommended that laboratory or computational modeling studies be carried out that can take into account these two aspects that GLOBAL-FATE does not consider for pollutant dispersion.

The calibration of the model enhances the need to study the behavior of the antibiotic in different aquatic environments, it should be noted in this case that although the body of interest is the tributary basin of the Choqueyapu River, most of the transport of this antibiotic to the river is done through pipes, which prevents its interaction with the sun, so its degradation is not known in limited or restricted bodies of sun, so the results of the values obtained should be higher than those found. This field also opens the analysis to the impact of the construction of the embankment in the entire course of the Choqueyapu River, which would not only imply an affectation to the natural biodegradation processes, but also to the photochemical degradation of the pharmaceuticals present in the river.

## References


1) Aguilar CPMJ. 2017. Analisis de sensibilidad en la dinamica de herbicidas en las Cuencas de Olivar Available at: https://abe.ufl.edu/faculty/carpena/files/pdf/zona_no_saturada/estudios_de_la_zona_v7/c337-343.pdf [Accessed 13 August 2021]
2) Álvarez VSA. 2018. América Latina pone su atención en la seguridad hídrica Available at: https://blogs.worldbank.org/es/latinamerica/america-latina-pone-su-atencion-en-la-seguridad-hidrica [Accessed 7 March 2021]
3) Carpio JM. 2017. Hydraulic Study of the upper La Paz River. (September 1998) DOI: 10.13140/RG.2.2.12418.07364
4) Contraloria General del Estado. 2013. Contaminación ambiental en la cuenca del río la paz Available at: www.contraloria.gob.bo
5) Eguchi K, Nagase H, Ozawa M, Endoh YS, Goto K, Hirata K, Miyamoto K, Yoshimura H. 2004. Evaluation of antimicrobial agents for veterinary use in the ecotoxicity test using microalgae DOI: 10.1016/j.chemosphere.2004.07.017
6) Font C, Bregoli F, Acuña V, Sabater S, Marcé R. 2019. GLOBAL-FATE: A GIS-based model for assessing contaminants fate in the global river network. *Geoscientific Model Development Discussions*: 1–30 DOI: 10.5194/gmd-2019-8
7) Frank-Andreas Weber A, aus der Beek T, Bergmann A, Carius Gregor Grüttner adelphi A, Silke Hickmann A, Ebert I, Hein A, Küster A, Rose J, Koch-Jugl J, et al. 2014. Fármacos en el medio ambiente – la perspectiva global Available at: www.umweltbundesamt.de/umweltbundesamt.de/umweltbundesamt [Accessed 12 June 2021]
8) García C, Gortáres P, Drogui P. 2011. Emerging contaminants: effects and removal treatments. *Revista QuímicaViva* (2): 96–105
9) Grill G, Khan U, Lehner B, Nicell J, Ariwi J. 2016. Corrigendum to 'Risk assessment of down-the-drain chemicals at large spatial scales: Model development and application to contaminants originating from urban areas in the Saint Lawrence River Basin' [Sci. Total Environ. Vol 541, (2016) 825-838] doi 10.1016/j.scitotenv.2015.09.100. *Science of the Total Environment* **551–552**: 753–754
10) Guerrero ARJ. 2019. DETERMINACIÓN DE LA CINÉTICA DE DEGRADACIÓN DEL SULFAMETOXAZOL. *Tesis*
11) Janet Gil M, María Soto A, Iván Usma J, Darío Gutiérrez O. 2012a. Emerging contaminants in waters: effects and possible treatments Contaminantes emergentes em águas, efeitos e

possíveis tratamentos
12) Janet Gil M, María Soto A, Iván Usma J, Darío Gutiérrez O. 2012b. Emerging contaminants in waters: effects and possible treatments Contaminantes emergentes em águas, efeitos e possíveis tratamentos. **7** (2): 52–73 Available at: http://www.scielo.org.co/pdf/pml/v7n2/v7n2a05.pdf
13) Medina C, Ginn O, Brown J, Soria F, Garvizu C, Salazar Á, Tancara A, Herrera J. 2021. Detection and assessment of the antibiotic resistance of Enterobacteriaceae recovered from bioaerosols in the Choqueyapu River area, La Paz – Bolivia. *Science of the Total Environment* **760** DOI: 10.1016/j.scitotenv.2020.143340
14) OMS. 2020. Resistencia a los antimicrobianos Available at: https://www.who.int/es/news-room/fact-sheets/detail/antimicrobial-resistance [Accessed 28 August 2021]
15) Pistocchi A, Marinov D, Pontes S, Gawlik BM. 2012a. Continental scale inverse modeling of common organic water contaminants in European rivers. *Environmental Pollution* **162**: 159–167 DOI: 10.1016/J.ENVPOL.2011.10.031
16) Pistocchi A, Marinov D, Pontes S, Gawlik BM. 2012b. Continental scale inverse modeling of common organic water contaminants in European rivers. *Environmental Pollution* **162**: 159–167
17) PNUMA. 2017. *PNUMA, 2017*.
18) Salazar D, Ginn O, Brown J, Soria F, Garvizu C. 2020. Assessment of antibiotic resistant coliforms from bioaerosol samples collected above a sewage-polluted river in La Paz, Bolivia. *International Journal of Hygiene and Environmental Health* **228** DOI: 10.1016/j.ijheh.2020.113494
19) Ternes TA. 1998. Occurrence of drugs in German sewage treatment plants and rivers. *Water Research* **32** (11): 3245–3260 DOI: 10.1016/S0043-1354(98)00099-2
20) de Voogt P, Janex-Habibi M-L, Sacher F, Puijker L, Mons M. 2009. Development of a common priority list of pharmaceuticals relevant for the water cycle. *Water Science and Technology* **59** (1): 39–46 DOI: 10.2166/WST.2009.764
21) Zhang L, Cao Y, Hao X, Zhang Y, Liu J. 2015. Application of the GREAT-ER model for environmental risk assessment of nonylphenol and nonylphenol ethoxylates in China. *Environmental Science and Pollution Research* **22** (23): 18531–18540 DOI: 10.1007/s11356-015-5352-3

# Streamflow maps for small-sized basins of Japan

○Ryosuke Arai[1,2*], Yasushi Toyoda [1], So Kazama[2]
[1]Central Research Institute of Electric Power Industry, Abiko 1646, Abiko-shi, Chiba 270-1194, Japan
[2]Graduate School of Engineering, Tohoku University, Sendai 980-8579, Japan

*E-mail: arai@criepi.denken.or.jp

**Abstract**
We generated streamflow maps for small-sized basins (~10 km$^2$) throughout Japan using artificial neural networks (ANNs). Modeled output streamflow characteristics relied upon the input of 176 basin characteristics and consisted of mean annual and daily streamflow percentiles. Although mean annual and high streamflow characteristics performed well, low streamflow characteristics were inadequate. Nevertheless, the ANNs for Japan proposed herein significantly outperformed those of a previous study exhibiting excellent global-scale ability.

**Keywords:** Artificial neural network; Run-of-river hydropower; Basin characteristic

## 1. Introduction

Artificial neural networks (ANNs), which are a subset of machine learning algorithms, can be used to model complex nonlinear relationships between inputs and outputs. Recently, ANNs, capable of estimating streamflow characteristics using basin characteristics as input, achieved extremely high accuracy at a global scale[1)]. Beck et al. (2015)[1)] and Barbarossa et al. (2018)[2)] trained ANNs using observed discharge data from thousands of basins worldwide, achieving coefficient of determination ($R^2$) values of 0.88 and 0.92 for their mean streamflow indices, respectively. Ultimately, Beck et al. (2015)[1)] concluded that the ANNs outperformed four macroscale hydrological models used globally. However, there are significant challenges to maintaining this level of accuracy in small-sized basins of Japan.

In this study, target basins with negligible anthropogenic disturbances were selected for the development of the ANNs. For input, 176 basin characteristics were used for mapping the streamflow characteristics in small-sized basins throughout Japan. The basin size was set as ~10 km$^2$ to map the streamflow characteristics.

## 2. Data

### 2.1 Target basins

Since the present study aimed to map the streamflow characteristics in ungauged basins, anthropogenic influences on discharge data in the target basins were sought to be eliminated. Thus, referencing the Dam Yearbook and map of Geospatial Information Authority of Japan (https://maps.gsi.go.jp/), only those basins without upstream dams or hydropower stations, and a minimum of five years of available discharge data, were extracted. Ultimately, 419 target basins were identified throughout Japan.

### 2.2 Streamflow and basin characteristics

Streamflow and basin characteristics correspond to output and input data for the ANNs, respectively.

We employed mean annual ($Q_{MEAN}$) and daily streamflow percentiles ($Q_{Percentile}$) as the streamflow characteristics over the observation period. The units of $Q_{MEAN}$ and $Q_{Percentile}$ were expressed by runoff height, mm·y$^{-1}$ and mm·d$^{-1}$, respectively. Nine indices of $Q_{Percentile}$ were used: $Q_1$, $Q_5$, $Q_{10}$, $Q_{20}$, $Q_{50}$, $Q_{80}$, $Q_{90}$, $Q_{95}$, and $Q_{99}$, where the values correspond to the exceedance probability of daily streamflow.

In this study, 176 basin characteristics were selected pertaining to climate, land use, geology, soil, and topography. Geographic information system data were integrated in ESRI ArcGIS (v.10.6), and basin characteristics were extracted from the corresponding coverage areas. Resolutions were adjusted by nearest neighbor interpolation to ensure equal treatment of characteristics.

## 3. Methodology

### 3.1 ANN Development

We developed feed-forward ANNs to estimate streamflow characteristics by inputting 176 variables of basin characteristics (Fig. 1). The generalization performance of the ANNs was evaluated with a leave-one-out cross validation procedure, commonly employed for the assessment of streamflow estimation in ungauged basins[3)].

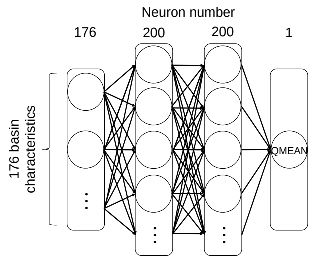


Fig.1 ANN structures.

### 3.2 Mapping streamflow characteristics

To extract small-sized basin, basins with areas ~10 $km^2$ were identified throughout Japan using 90 m resolution DEM data[4]. As a result, 8,901 basins were identified, and their corresponding basin characteristics were extracted. Finally, streamflow was estimated for all identified basins through inputting the extracted basin characteristics into the trained ANNs.

## 4. Results and discussion

Figure 2 shows the results of the leave-one-out cross validations for the ANNs. Good generalization performances were observed for $Q_{MEAN}$, $Q_{10}$, and $Q_{20}$ ($R^2 \geq 0.70$). The performances across $Q_{Percentile}$ varied significantly ($R^2 = 0.21$–0.79), decreasing from $Q_{10}$ (0.79) to Q99 (0.21). Nevertheless, at the national-level, the performance of the ANNs derived in this study greatly outperformed that of Beck et al. (2015) [1] with excellent global-scale performance (Fig. 2).

Streamflow maps in small-sized basins (~10 $km^2$) are shown for $Q_{MEAN}$ (Fig. 3(a)) and Q1 (Fig. 3(b)), as the results for all other values of $Q_{Percentile}$ displayed similar features to $Q_{MEAN}$. The highest values of $Q_{MEAN}$ were distributed in the heavy snowfall areas of Tohoku and Hokuriku, facing the Japan Sea. Comparatively, the highest values for $Q_1$ were distributed in the typhoon-prone areas of Kyushu, Shikoku, and Kinki, facing the Pacific Ocean. $Q_{MEAN}$ also displayed high values in these heavy rainfall areas.

## 5. Conclusions

The present study generated maps of streamflow in small-sized basins (~10 $km^2$) throughout Japan using ANNs. The generalization performance for $Q_{MEAN}$ and high streamflow characteristics were good, although decreased performances were recorded for low streamflow characteristics. Nevertheless, at the national-level, the performance of the ANNs derived in this study greatly outperformed that of a previous study with excellent global-scale performance.

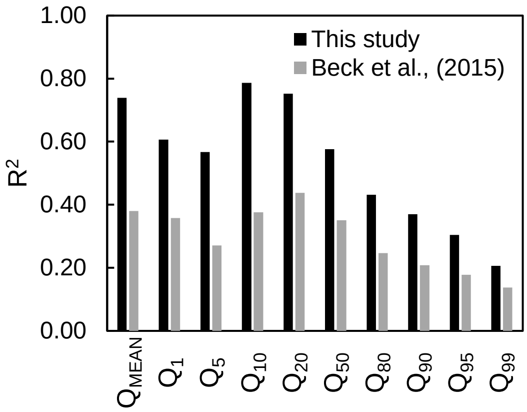


Fig. 2 Generalization performance of ANNs.

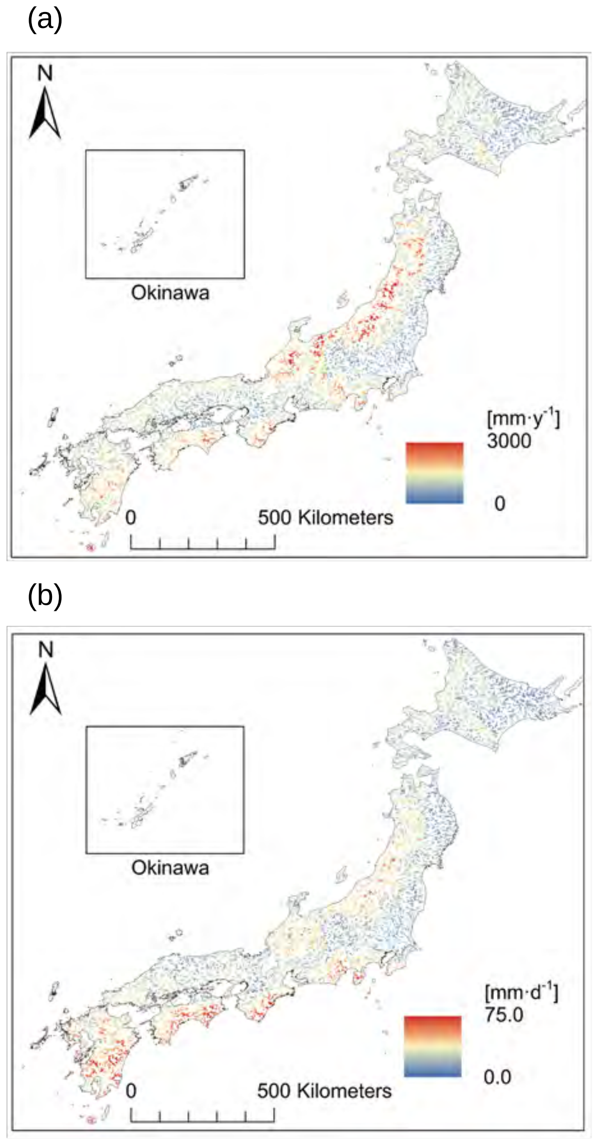


Fig. 3 Streamflow of small-sized basins (~10 $km^2$) for (a) $Q_{MEAN}$, and (b) $Q_1$.

## References

1) Beck, H. E., de Roo, A., van Dijk, A. I. J. M. 2015. Global maps of streamflow characteristics based on observations from several thousand catchments. J. Hydrometeorol. 16(4), 1478–1501.
2) Barbarossa, V., Huijbregts, M. A. J., Beusen, A. H. W., Beck, H. E., King, H., Schipper, A. M. 2018. Erratum: FLO1K, global maps of mean, maximum and minimum annual streamflow at 1 km resolution from 1960 through 2015. Sci. Data. 5, 180078.
3) Razavi, T., Coulibaly, P. 2013. Streamflow prediction in ungauged basins: Review of regionalization methods. J. Hydrol. Eng. 18(8), 958–975.
4) Lehner, B., Verdin, K., Jarvis, A. 2008. New global hydrography derived from spaceborne elevation data. EOS. 89(10), 93–104.

# Integrated assessment of the flood and heat mitigation effect of vegetation in an urban residential area

○Qing Chang[1,2*], So Kazama[1] , Yoshiya Touge [1] , Shunsuke Aita[1]
[1]Graduate School of Engineering, Tohoku University, Sendai 980-8579, Japan
[2]School of Urban construction, Wuhan University of Science and Technology, Wuhan, Hubei, 430072, China

*E-mail: qing.chang.q3@gmail.com

**Abstract**
This study attempted to explore the effect of urban vegetation on mitigating urban heat island and runoff. A small urban catchment in Japan was used as the study site. Remotely sensed data were obtained and used for a distributed representation of vegetation growth information by converting to canopy storage abilities as well as comparison with simulated results. The effects of the vegetation amount (changing of LAI values) were considered. The SWMM model, the Rutter model and energy balance model are coupled to simulate the urban vegetation interception process and the energy flux process. The results showed that the coupled model had a satisfied performance with different process modeling. When LAI increased to 1.4 times the original value, total runoff decreased by 10%, and the average surface temperature in summer decreased by 2.5 degrees Celsius. When the LAI decreased to 80%, the total runoff increased by 6%, and the average surface temperature in summer decreased by 1.5 degrees Celsius.

**Keywords:** urban vegetation; urban heat island; runoff mitigation; coupled model.

## 1. Introduction

With the expansion of cities and the formation of larger cities, the temperature of those urbanized areas will become higher compared with the surrounding suburbs, creating a heat island effect. The heat island effect affects the climate of the surrounding areas, and at the same time, temperature differences cause air movement, increasing the scope of air pollution. The formation of the heat island effect has been shown to be closely related to urbanization (Solecki et al., 2005).

There have been numerous studies on vegetation in urban areas, including aspects of both hydrological and energy flux. The major research methods to evaluate the effect of urban vegetation mainly include numerical modeling and direct measurement. Since the hydrological model is relatively well developed, there have been many modeling and measuring studies about the process of vegetation interception or the effect of runoff mitigation. In addition, in recent years, energy balance monitoring and modeling technology has improved, so modeling research has increased.

An integrated evaluation was conducted the study based on hydrological and energy balance processes simulations. The coupled model used include the Storm Water Management Model (SWMM), the Rutter interception model (Rutter et al. 1977) and a single-layer energy budget model. The main purpose is to evaluate the effectiveness of urban green infrastructures on mitigating urban flood runoff and heat island by conducting integrated model simulations and thus the results could be used as reference for decision makers of future city construction in Japan. The specific targets include: (i) simulating the effects of urban vegetation on flood and heat mitigations and (ii) trying to find reasonable green infrastructure methods and strategies which could be implemented in future period planning.

## 2. Study area

We chose the Kunimigaoka area (KA) in Sendai city, Japan, for the case study. KA is a predominantly residential area located in the northwestern part of Sendai (Fig. 1). This catchment covers approximately 46 ha with a moderately sloping topography. The construction processes in the KA mainly occurred during the 1990s. Currently, the degree of urbanization is rather complete, and the land use changed little after 2005. The surface runoff is first collected by gutters built on both sides of the roads and then drains into stormwater sewer conduits. At the outlet of the sewer system, there is a regulation pond. The stormwater first drains to this regulating pond and then to a downstream river.

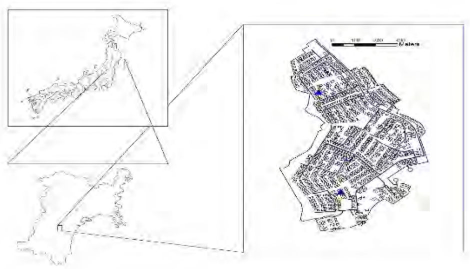

Fig.1 . Location of the study catchment.

## 3. Methodology

### 3.1 Data preparation

The DEM data of the studied area was obtained from the Ministry of Land, Infrastructure, Transport and Tourism of Japan (MLIT, https://www.mlit.go.jp/). The detailed storm pipeline data were provided by Sewer Administration Office of Sendai City. The study area has around totally 400 conduits and manholes. Rainfall was collected by two tipping-bucket rain gauges within the catchment from February 26, 2018, to July 29, 2018, and included 23 individual events with a record resolution of 0.5 mm. These 23 rainfall events were used for model calibration and validation. The normalized difference vegetation index (NDVI) was selected as the indicator for the vegetation amount in the study area.

### 3.2 The coupling of models

The SWMM was selected for the hydrological modeling part of this study. This model was developed by the US-EPA and is widely used for rainfall-runoff and water quality modeling in urban catchments. SWMM is a concept-based spatially distributed model. In the model, spatial heterogeneity was realized by dividing the target catchment into several sub-catchments, which were considered the basic hydrological response units. Each sub-catchment was treated as a nonlinear reservoir that received inflow from rainfall and upstream sub-catchments. Then, within the sub-catchments, the inflow was partitioned into different components, such as depression storage, evaporation, infiltration and runoff. The governing equation of the sub-catchments was a combination of the continuity equation and Manning equation. The runoff generated by sub-catchments was usually drained to the sewer pipe system. Where the 1-d Saint-Venant principle was applied.

## 4. Results and discussion

Figure 2 summarizes changes in urban vegetation (changes in the LAI) for variations in the surface temperature and reductions in total runoff. With the increase in urban vegetation, the surface temperature and total runoff decreased, indicating that urban vegetation has the ability to reduce runoff and the urban heat island effect.

Figure 3 shows the trend of surface temperature changes under different land use and different LAI scenarios over a period of one month. It can be seen that both the maximum temperature and the average temperature basically followed the same general trend. The impact of rainfall events on temperature is obvious. Rainfall usually results in significant reductions in temperature. This is because the input solar energy flux during rainy days is reduced. On the other hand, vegetation traps a part of the rainwater. The evaporation of this part of rainwater requires heat consumption, which leads to an increase in latent heat. The role of the LAI is that an increase in the LAI decreases the average and maximum temperature values.

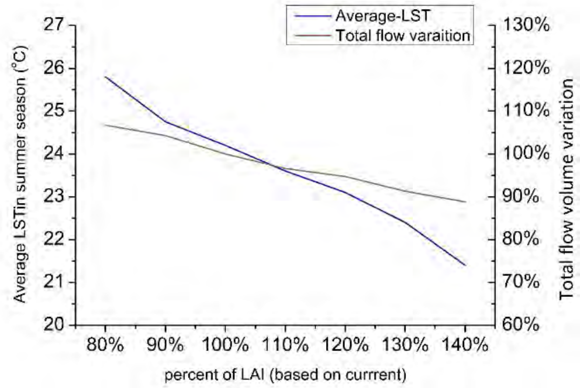


Fig. 2 The relationships of different LAI values with catchment-averaged LSTs (degrees Celsius) and the total flow volume (percentage).

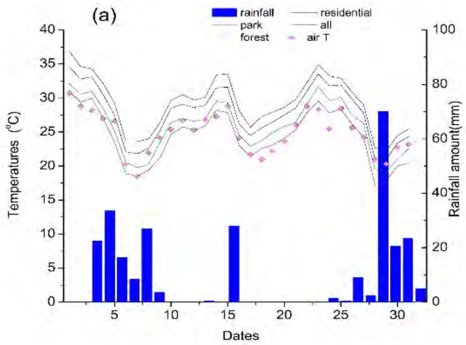


Fig. 3 Average daily surface temperature values in August 2018 when LAI= current value

## 5. Conclusions

Urban vegetation plays an important role in the urban hydrological cycle and heat cycle. In this study, the value of the LAI was used to represent the amount of urban vegetation. The results showed that when LAI increased to 1.4 times the original value, total runoff decreased by 10%, and the average surface temperature in summer decreased by 2.5 °C. When the LAI decreased to 80%, the total runoff increased by 6%, and the average surface temperature in summer decreased by 1.5 °C. These results will provide a valuable reference for future urban green infrastructure planning.

## References

1) Rutter, A. J., & Morton, A. J. (1977). A predictive model of rainfall interception in forests. III. Sensitivity of the model to stand parameters and meteorological variables. Journal of Applied Ecology, 567-588.
2) Solecki, William D.; Rosenzweig, Cynthia; Parshall, Lily; Pope, Greg; Clark, Maria; Cox, Jennifer; Wiencke, Mary (2005). "Mitigation of the heat island effect in urban New Jersey". Global Environmental Change Part B: Environmental Hazards. 6 (1): 39–49.

# Boundary effect on pumping test estimations and ways of lowering groundwater level in Muscat Airport premises

○Luminda Gunawardhana[1*], Ahemd Sana[2]
[1]Department of Civil Engineering, University of Moratuwa, Katubedda, Sri Lanka

[2]Department of Civil and Architectural Engineering, Sultan Qaboos University, Al-Khoud 123, Oman

*E-mail: gunawardhanaluminda@gmail.com

**Abstract**
Pumping tests and analytical models are commonly used in estimating aquifer properties. Numerous assumptions used in deriving these analytical models generate uncertainties in final estimations. This study used data collected in a pumping well and two monitoring wells during a constant rate pumping test conducted in Muscat International Airport premises. The pumping well is located near to a stream, which violates the assumption of aquifer with aerially extensive. Moreover, significant hydraulic gradient towards the sea did not satisfy the assumption of horizontal potentiometric surface. Accordingly, a three-dimensional numerical model was developed using MODFLOW to simulate transient groundwater flow during the pumping test. To compare the differences in estimations, Neuman (1974) analytical solution was also used with and without considering the stream boundary effect. Results showed that the estimated aquifer properties with and without the boundary effect can be differ by 12%, 23% and 54% for transmissivity, anisotropy and specific yield, respectively. Numerical simulation conducted by considering a horizontal potentiometric surface as in the analytical model produced an averaged root-mean-squared-error (RMSE) of 0.055 m, which is approximately 57% higher than the RMSE value estimated with the effect of the hydraulic gradient. Four pumping scenarios were considered for lowering the average groundwater level by 0.5m around the runaway. It was estimated that altogether 24 pumping wells with the pumping rates vary from 222 to 1564 $m^3$/day, are required to achieve the expected reduction.

**Keywords:** Constant-rate pumping test, Unconfined aquifer, Stream boundary, Muscat Airport

## 1. Introduction

Muscat airport, which is located in the heart of the Muscat city in Sultanate of Oman, experienced groundwater level rises over 1.5m in most of its observation wells since 2010. This effect is likely a result of the groundwater recharge from extreme rainfall events occured in 2007 (Cyclone Gonu) and 2010 (Cyclone Phet), decline in agricultural activities in the area due to increase urbanization and water lecage from sewer lines and septic tanks. It was decided to manage the aticipated issues with rising groundwater level by pumping adequate amount of water from the shallow aquifer. accordingly, a series of pumping tests were conducted by drilling 8 pumping wells and 16 monitoring wells.

When analyzing pumping test data, it is primly important to conceptualize the surrounding boundary conditions appropriately. Impervious underground structures limit the groundwater flow in the down-gradient side from the structure, thereby limiting the effective aquifer contribution during the pumping test. Therefore, a greater drawdown is expected at a particular point compared to that without the barrier effect. In contrast, water bodies (rivers, wetlands, reservoirs etc.) locate within the radius of influence of the pumping well add more water to the aquifer thereby reducing drawdown effect (Todd and Mays 2004).

In this study, drawdown data collected in a pumping well (PW-7 in Fig. 1) and two monitoring wells (MW-17 and MW-18) were analyzed by considering the effect of a stream locates near to the pumping well. Neuman (1974) analytical solution, which accounts the effects of the partial penetration wells and the aquifer anisotropy, was used with the modified boundary condition to address the assumption of infinite aquifer extent. To account the effect of natural hydraulic gradient along with the other site conditions addressed in analytical solution, a numerical simulation was carried out using MODFLOW groundwater flow simulation model (Harbaugh et al. 2000). In the second stage, numerical model was expanded to cover the entire airport area including all pumping wells and monitoring wells. Accordingly, a series of pumping scenarios were tested for lowering the groundwater level by 0.5 m around the runaway area.

## 2. Study area

Muscat is the capital city of Oman located at the southeast tip of the Arabian Peninsula. It is a coastal city where the Muscat International Airport is located in the vicinity of the coast. Upstream side of the catchment area consists of a series of rugged mountains and Ophiolite hills run parallel to the coastline. Fig. 1 shows the locations of the pumping wells drilled for conducting the pumping tests.


Fig.1 Pumping wells used for estimating aquifer properties

## 3. Methodology

The pumping well is 25 m deep and consists of an 11.8 m effective well screen. Each pumping well consists of two monitoring wells, which are identical in their configurations and they were placed 15 m and 50 m away from the pumping well. The monitoring wells are 15 m deep and have an effective well screen of 6 m in each. A constant-rate pumping test was conducted for 24 hours and a recovery test was performed for 12 hours. Pumping rate was measured using a flow meter and it was maintained at a constant level throughout the pumping test. Additionally, the constant rate of pumping was assured by sending the discharge water through a weir tank with a V-notch gauge. A piezometer attached to the discharge pipe between the flow meter and the weir tank was also used to ascertain a constant flow rate. Groundwater levels were monitored simultaneously using hand-held water-level monitoring devices in all wells with 15-second intervals at the beginning of each tests. The observation interval was gradually increased up to 1-hour as the drawdown change decreases. Two soil samples were collected at 3 m and 19 m below the ground surface. Sieve analysis classified the soil samples as medium grain with almost similar soil properties. Lithological data from three boreholes in the airport premises classified the unconfined aquifer as alluvium with a clay layer below 70 m depth.

## 4. Results and discussion

Fig. 2a and b show the drawdown data matched with Neuman (1974) analytical solution with and without the boundary effect. Results showed that the estimated aquifer properties with and without the boundary effect can be differ by 12%, 23% and 54% for transmissivity, anisotropy and specific yield, respectively. It was also estimated that about 0.41 m of drawdown difference near to the stream can be attributed to the boundary effect. For the MODFLOW numerical model, 24 pumping wells with 1500 $m^3$/day rate in each continued for two-week pumping and one week recovery session were considered. Fig. 2c shows the groundwater levels after 4 such sessions. It was estimated that altogether 24 pumping wells with the pumping rates vary from 222 to 1564 $m^3$/day, are required lowering the average groundwater level by 0.5m around the runaway.

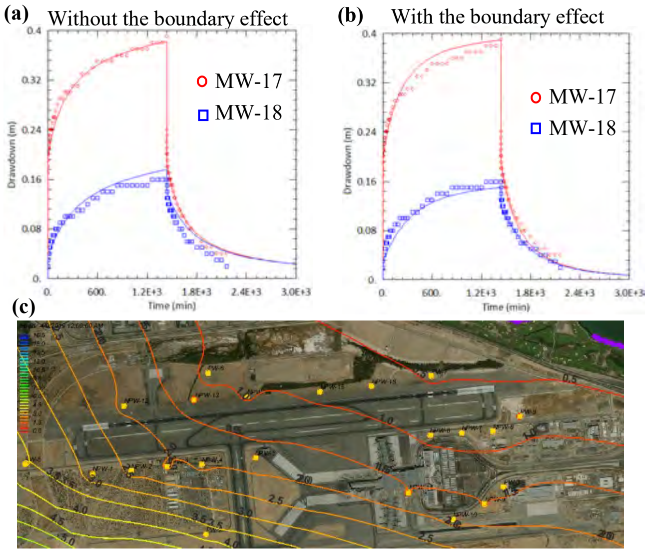


Fig. 2a and 2b shows Neuman (1974) curves matching with the drawdown records in monitoring wells and Fig 2c shows groundwater level simulated by MODFLOW model.

## 5. Conclusions

When compared with the analytical models, the numerical groundwater flow model would better perform in simulating drawdown records and therefore more reliable in estimating aquifer properties in areas with complex site conditions. Proposed pumping scenario indicated the possibility of achieving the required water level reduction. However, further studies with actual field testing pumping sessions are required to understand the long-term pumping effects on reducing the groundwater levels.

## References


1) Harbaugh AW, Banta ER, Hill MC, McDonald MG: MODFLOW-2000, The U.S. Geological Survey Modular Ground-Water Model – User guide to modularization concepts and the ground water flow process. U.S. Geological Survey, Open-File Report 00-92, 2000.
2) Neuman SP: Effect of partial penetration on flow in unconfined aquifers considering delayed gravity response. Water Resources Reserches 15, 899–908, 1974.
3) Todd DK, Mays LW: Groundwater Hydrology, 3rd edition New York: John Wiely and Sons, 656p, 2004.

# Comparison drought index and observed agricultural drought in Indonesia

〇Nurul Fajar Januriyadi[1*], Bambang Heri[2], Idham Riyando Moe[2]
[1]Department of Civil Engineering, Pertamina University, Indonesia
[2]Ministry of public work and housing of Indonesia, Indonesia

*E-mail: Nurul.fj@universitaspertamina.ac.id

**Abstract**
The study aims to compare the SPI values to the drought of agriculture to find the suitable period and threshold of the Drought index. Corrected satellite rainfall data recorded from 1979 to 2020 used to generate the different periods of Standardized precipitation index (SPI). Based on the results shows the crop failure area of some regions corresponds to the SPI value. However, more observation data with higher resolution could give a better estimation of the threshold value of SPI.

**Keywords:** Drought index, SPI, Post-fire observations, Kamaishi

## 1. Introduction

Indonesia is the largest archipelago country in the world with a total islands number of more than 17 thousand. It is a vast equatorial archipelago extending 5,150 kilometers east to west with a total area of more than 5 million km2. The large area has an impact on the spatial distribution of different climates. This difference has an impact on the types of water-related disasters that occur, some areas in Indonesia experience drought. Spatial identification is very important to provide an overview of the condition of Indonesia's drought disaster.

Furthermore, one of the major factors of drought disasters is the availability of rainfall during a period. Standardized precipitation index (SPI) is a popular method to identify the availability of rainfall within a certain period [1,2]. SPI could estimate the probability of the water shortage in certain periods, lower SPI values associate with the severity of drought. However, different periods produce different SPI values. This study aims to compare the SPI values to the drought of agriculture to find the suitable period and threshold of SPI.

## 3. Methodology

### 3.1 Standardized Precipitation Index

McKee [3] introduce SPI to evaluate the surplus and deficit of precipitation during a given period. It calculated using a continuous long precipitation data, ideally at least 30 years. A set of average values of certain period can be selected to determine a set of time scales of periods which is from 1 month to 12 months. These represent arbitrary but typical time scales for precipitation deficits to affect water sources.

## 4. Results and discussion

To compare the correlation between drought index and drought observation. We collected the area of crop failure. Figure 1 shows the example of comparison spatial SPI value and crop failure based on provinces in August 2014. The figure indicates the west region of Sumatra Island has higher SPI compare to the other regions. It corresponds to the higher area of crop failure in the region. During period of august 2014, some provinces located in west part of Sumatra Island (i.e., Aceh, North Sumatera and West Sumatra) recorded the area of crop failure of more than 100 ha. However, some regions show opposite correlation between SPI value and crop failure area. It caused the scale of crop failure area is province level, which has high uncertainty. It also caused by the characteristic of the region, which could have different threshold value of SPI.

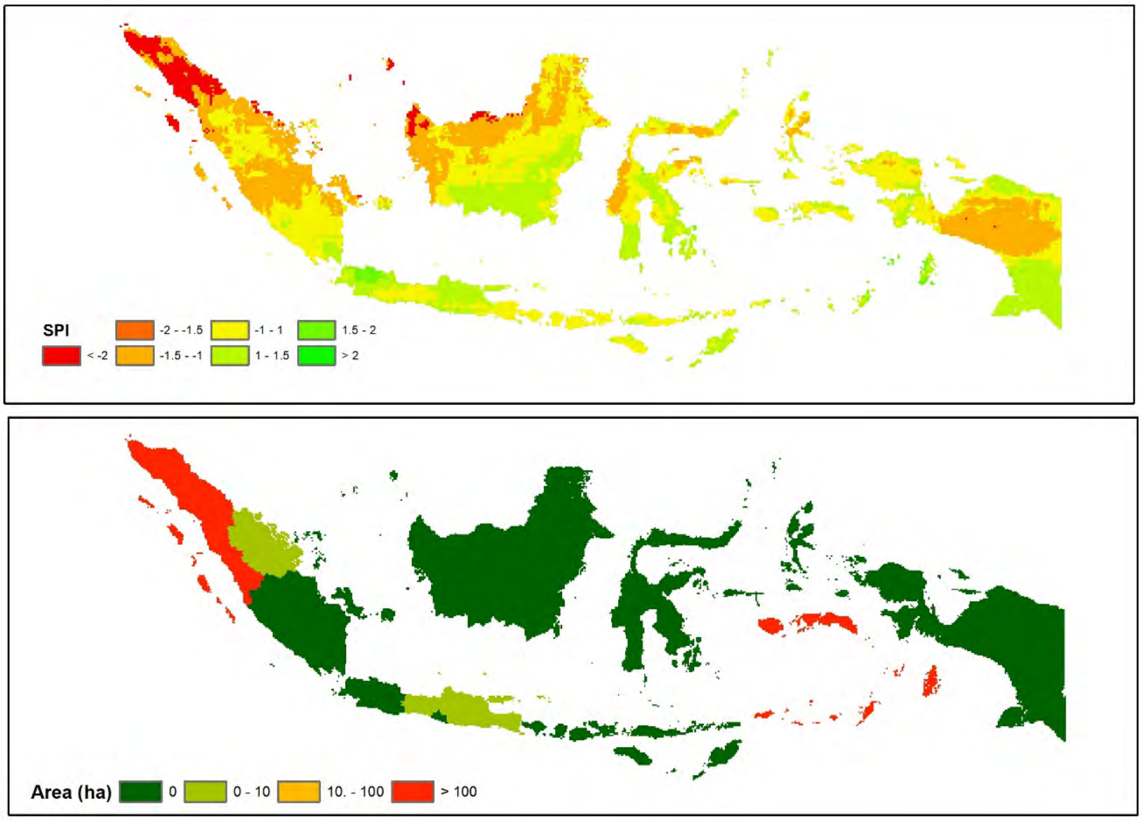


Fig. 1 Comparison area of crop failure to SPI value

## 5. Conclusions

The study aims to compare the SPI values to the drought of agriculture to find the suitable period and threshold of SPI. Based on the results shows the crop failure area of some regions corresponds to the SPI value. However, more observation data with higher resolution could give a better estimation of the threshold value of SPI.

## References

1. Lee, J.; Park, J.; Chung, E.; Woo, N. Assessment of Groundwater Drought in the Mangyeong River Basin, Korea. *Sustainability* **2018**, *10*, 831, doi:10.3390/su10030831.
2. Leelaruban, N.; Padmanabhan, G.; Oduor, P. Examining the Relationship between Drought Indices and Groundwater Levels. *Water* **2017**, *9*, 82, doi:10.3390/w9020082.
3. McKee, T.B.; Doesken, N.J.; Kleist, J. THE RELATIONSHIP OF DROUGHT FREQUENCY AND DURATION TO TIME SCALES.; 1993; p. 6.

# Identifying the Spatiotemporal Variation in Qualitative and Quantitative Characteristics of Groundwater in Attanagalu Oya Basin, Sri Lanka

Vinu I[1*], Danushka U[1], Chaminda S.P[1], Dassanayake A.B.N [1]
[1]Department of Earth Resources Engineering, University of Moratuwa, Sri Lanka

*E-mail: indrakumarvinu94@gmail.com

## Abstract
Attanagalu Oya basin that covers almost the entire Gampaha district of Sri Lanka is an influential hydrologic feature in determining the spatiotemporal variation of the groundwater characteristics. As a consequence of industrialized urbanization, there are seasonally observed variations in the quantitative and qualitative characteristics of the groundwater throughout the basin. This research focuses on the identification and analysis of those characteristic variations in an Engineering approach. A Fortran based algorithm was developed for a time scale of six years to model the surface runoff of the basin and estimate the quantitative subsurface recharge. The changes in the qualitative parameters such as pH, electrical conductivity, turbidity and concentrations of nitrogen, fluoride, ferrous and phosphorous during the pre and post monsoonal seasons were analyzed and compared with water quality standards. The results obtained from the runoff model showed that only 5-10% of the total precipitation gets infiltrated into the subsurface. Also, the downstream region of the basin experienced an outrageous deterioration in the quantitative volume of subsurface recharge throughout the period of study. Qualitatively, there was a considerable fluctuation observed in the parameters typically after the monsoon. In specific, the pH and the phosphorous concentration were well beyond their permissible limits. These results emphasize the immediate significance of developing a sophisticated water management system for the entire basin.

**Keywords:** Fortran, Monsoon, Precipitation, Spatiotemporal, Surface runoff

## 1. Introduction

Groundwater is the primary source of domestic water supply in Sri Lanka. About 80 % of the island's rural drinking water comes from residential open dug wells and tube wells (Panabokke & Perera, 2005). When the country is considered as a single entity, Sri Lanka has little or no water scarcity. But, seasonally varying water scarcity has been observed in many regions of Sri Lanka. Gampaha district has the second-highest population in the country. The Attanagalu Oya basin fulfills the whole water demand of the region for domestic, agricultural and industrial consumptions. According to Falkenmark indicator for water scarcity, from 1991 to 2025, Gampaha is categorized under moderate to severe range of index (Amarasinghe *et al.*, 1999). Spatiotemporal drought and water stress is a critical issue during the dry seasons. In contrast, disastrous floods that occur during the rainy season is another dramatic challenge in the basin.

A runoff model is a set of equations that aid in estimating the amount of rainfall that turns into a runoff as a function of various parameters used to describe the watershed. A runoff model can be developed based on the simple water balance equation (Abdulohom *et al.*, 2018). Precipitation (Rainfall) is the primary mode of water intake to the eco-system, Evapotranspiration, surface runoff, infiltration and extraction are the ways of water discharge. Fortran is a user-friendly platform to develop an algorithmic model that can be used to evaluate those water balance parameters individually.

There are five types of water pollution (Fecal, Industrial, Agrochemicals, Heavy metals and Oil) identified in the Attanagalu Oya basin (Anil Premaratne, 2004). Technical judgement to perceive the degree of pollution level of the entire region has to be made. Hence the qualitative parameters observed from spatiotemporally collected representative samples must be compared with the national and international standards.

## 2. Study Area

The Attanagalu Oya Basin is located in between two major river basins, Kelani and Maha Oya. It has an extent of 727 km$^2$. The dominant portion of the Attanagalu Oya basin falls in the wet zone, with an annual cumulative rainfall of 2000 - 2600 milliliters obtaining from the two primary monsoons. The regional temperature ranges from 23 – 31 $^{O}$C.

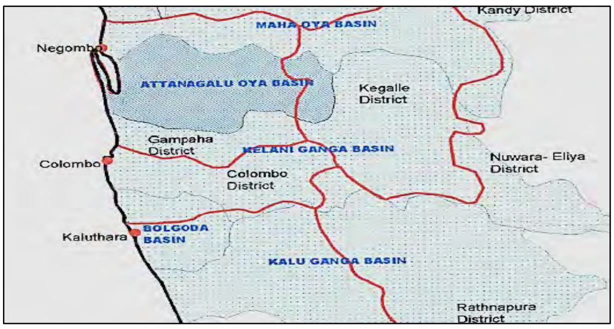


Fig. 1 Geographical location of the Attanagalu Oya Basin

## 3. Methodology

### 3.1 Quantitative Approach (Runoff Model)

Daily rainfall and daily maximum & minimum temperatures were taken as the primary data from 2013 to 2018 to represent the entire basin. Elevation data (DEM), catchment region, streamflow network, soil data and aquifer characteristics were also included in the algorithm. Quantitative estimates of the evapotranspiration, infiltration and surface runoff were obtained from the model process.

### 3.2 Qualitative Approach

Groundwater samples were collected from the study area during the pre-monsoon and post-monsoon periods of 2018 and tested in the laboratory to analyze the water quality parameters. One liter of water sample was collected from each of the 18 locations, representing the entire Attanagalu Oya basin. Sample collection was made within one day as per a criterion basis that on either side of the streamflow and closer to the industries. Special consideration was given to collect the samples from locations that depict the upstream-downstream transition.

## 4. Results and Discussion

The annual variations of rainfall, temperature (maximum and minimum), evapotranspiration (ET), infiltration and surface runoff can be interpreted as follows.

Table 1. Yearly variation of the quantitative parameters

| Year | Temperature | | Rainfall (mm) | ET (mm) | Infiltration (mm) | Surface runoff (mm) |
|---|---|---|---|---|---|---|
| | Max (°C) | Min (°C) | | | | |
| 2013 | 30.98 | 24.45 | 3895.68 | 2142.62 | 194.78 | 1558.27 |
| 2014 | 31.17 | 24.56 | 2874.17 | 1609.54 | 129.34 | 1135.30 |
| 2015 | 31.51 | 24.31 | 3498.37 | 1994.07 | 160.93 | 1343.37 |
| 2016 | 32.04 | 24.85 | 2724.61 | 1580.28 | 106.26 | 1038.08 |
| 2017 | 31.43 | 24.63 | 4272.99 | 2435.61 | 256.38 | 1581.01 |
| 2018 | 32.65 | 24.85 | 2523.74 | 1463.77 | 113.57 | 946.41 |

The simulated model output was calibrated with the observed data of the surface runoff model available in 2015, as depicted in Fig. 2. The degree of closeness was estimated as, Coefficient of determination ($r^2$) = 0.73 and Nash-Sutcliffe efficiency (E) = 0.55. The generalized results of the qualitative analysis with the permissible limits are given in a comparative format as in Fig. 3.

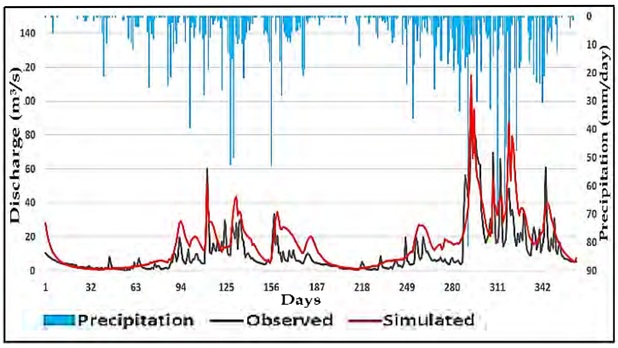


Fig. 2 Calibration of the runoff model

Here the quality standards are based on the regulations made by the Central Environmental Authority (CEA) on Ambient Water Quality, No. 01 of 2019. Most of the quality parameters observed in the pre-monsoon tend to pervert more after the monsoon recharge. Specifically, the pH and the phosphorous concentration exceeded their permissible limits.

## 5. Conclusions

From the runoff model, it can be concluded that out of the total annual rainfall of the basin, almost 50% goes out as evapotranspiration, and 40% goes out as surface runoff. Only 5-10% of the yearly rainfall infiltrates into the ground. The general groundwater quality of the basin in the pre-monsoon period is more suitable and safer for human utilization as per the standards. The downstream region experiences the utmost deterioration in its qualitative and quantitative characteristics. Also, the downstream is almost in an optimum index of pollution risk as it is broadly urbanized and industrialized with an increasing population density. Accurate development of a sophisticated model with advanced simulations is highly recommended to the whole basin to plan, execute and manage the groundwater system appropriately.

## References

1) Athukorala DRM, Danushka U, Kohilan C, Chaminda SP, Dassanayake ABN: Analyzing the Seasonal Variation of Groundwater Characteristics in Attanagalu Oya Basin, Sri Lanka ; ISERME - Sri Lanka, 2019.
2) Chaminda SP, Kazama S, Komori D : Near Future Climatic Impact on Seasonal Runoff in Sri Lanka ; IAHR-APD, 2016.
3) Amarasinghe U, Mutuwatta L, Sakthivadivel R : Water scarcity variations within a country; A case study of Sri Lanka, IWMI Research Report – Sri Lanka, 1999.

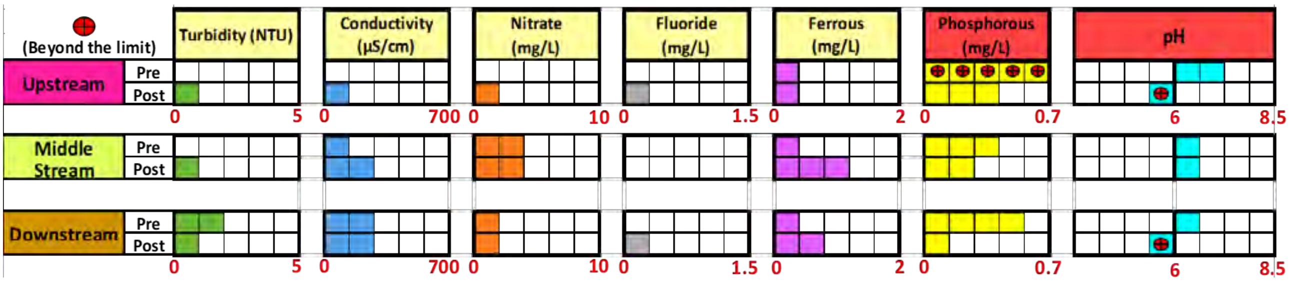


Fig. 3 Results of the qualitative analysis of upstream, middle stream and downstream during the pre and post-monsoons

# Spatiotemporal Variation of Groundwater Quality at Malwathu Oya Basin, Anuradhapura District, Sri Lanka

〇Madhushankha JML, Madhuwan ARB, Menan P, Chaminda SP[1]

[1]Department of Earth Resources Engineering, Faculty of Engineering, University of Moratuwa, Sri Lanka

*E-mail: – chamindaspc@yahoo.com

## Abstract

**Introduction**: Groundwater plays a major role in Dry Zones such as Anuradhapura District as a water resource for drinking purposes. Frequent practices of fertilizers in cultivation deteriorate the quality of surface water and further infiltration into the water table causes contamination of groundwater. **Objective**: This study was conducted to assess spatiotemporal variation in Groundwater quality in terms of Calcium and Magnesium ions since it causes higher degree of hardness in water**. Methodology**: Water samples were collected from wells in September, December 2016 and February 2017 at selected locations. Atomic Absorption Spectroscopy was used to analyzed $Ca^{2+}$ and $Mg^{2+}$ ions concentrations of the samples. Inverse Distance Weighted interpolation and bar chart of each ion concentration for each location as at each day were used to assess spatiotemporal variation of $Ca^{2+}$ and $Mg^{2+}$ ion concentration. **Results and Conclusion**: $Ca^{2+}$ concentration was depleted on December/2016 and February/2017 compared concentration on September 2016 by 27.3% and 26.8%. However, $Mg^{2+}$ concentration was increased on December/2016 and February/2017 compared concentration on September 2016 by 16.2% and 55.5%. Both $Ca^{2+}$ and $Mg^{2+}$ indicate drastic spatial and temporal variation from September to February in Malwathu Oya basin.

**Keywords:** Groundwater, Quality, Spatiotemporal, Hardness

## 1. Introduction

Groundwater is the largest precious liquid phase fresh water resources in the world. Half of the worlds' population used groundwater for the purpose of drinking and agricultural activities (Raghunath, 2007). As a tropical country, Sri Lankan rural communities in dry zone climatic areas consume groundwater as the major source of drinking water and irrigation water (Kurisu *et al.*, 2016). Anuradhapura district belongs to the dry zone and it's a leading kingdom that is commenced the best groundwater management for human consumption. Groundwater plays key role in drinking water and irrigation in Anuradhapura District.

Both natural and human activities cause surface water quality degradation directly cause groundwater quality depletion directly and indirectly. Frequent practice of fertilizer without sufficient knowledge of secure fertilizing method, groundwater has been contaminated and polluted with the time (Gamage, 2021). The taste of the groundwater gets changed because of these contaminations. Because of the issue of water taste, the community people are limiting water consumption which causes indirect health issues. An excess amount of Hardness that mainly presence of $Ca^{2+}$ and $Mg^{2+}$ cause the bad taste of water(Cooray *et al.*, 2019). Since the majority of the rural community used groundwater as the major source of drinking water, there is a necessity to assess spatiotemporal variation of Groundwater quality in terms of $Ca^{2+}$ and $Mg^{2+}$ concentration at Anuradhapura area.

## 2. Study Area

Upstream of Malwathu Oya basin which covers around 2350 km$^2$ area extent lies on Anuradhapura District were selected to carry out this study (Fig.1). According to the classification of aquifer types in Sri Lanka study area is lies on Shallow Regolith Aquifer of the Hard Rock Region (Panabokke and Perera, 2005). Study area is belonging to dry climatic zone and the availability of water resources are very less compared to other two climatic regions in Sri Lanka. Most of the people who lives in this area depend mainly on paddy and other crop cultivation (Perera *et al.*, 2015).

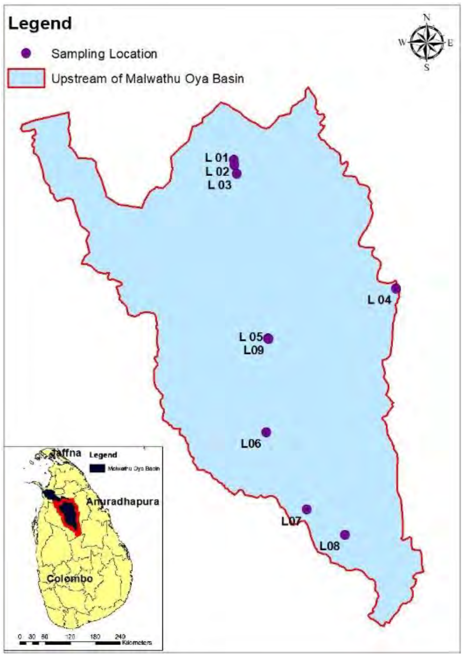


Fig.1 Sample Locations in Upstream of Malwathu Oya Basin at Anuradhapura District, Sri Lanka

## 3. Methodology

### 3.1 Sample Collection and Analysis

Nine sample locations were selected according to accessibility and availability of the water wells. As shown in the Figure 01 sampling locations were spatially distributed on both upstream and downstream. Water sample were collected during three visits on September, December 2016 and February 2017 to assess the temporal variation of the $Ca^{2+}$ and $Mg^{2+}$ ions concentration. Atomic Absorption Spectroscopy (AAS) was used to analyzed the $Ca^{2+}$ and Mg2+ ion concentration in collected samples.

### 3.2 Spatiotemporal Analysis

The measured concentration values for $Ca^{2+}$ and $Mg^{2+}$ were tabulated and plotted bar chart respectively for September 2016, December 2016 and February 2017 in each sampling location. To interpolate spatiotemporal variation of these ions were done using Inverse Distance Weightage (IDW) interpolation method in Arc Map software.

## 4. Results and Discussion

Figure 2 and 3 represent the Ca2+ and Mg2+ spatial and temporal variation in upstream of Malwathu Oya basin. Ca2+ concentration was depleted on December/2016 and February/2017 compared concentration on September 2016 by 27.3% and 26.8%. However, Mg2+ concentration was increased on December/2016 and February/2017 compared concentration on September 2016 by 16.2% and 55.5%.

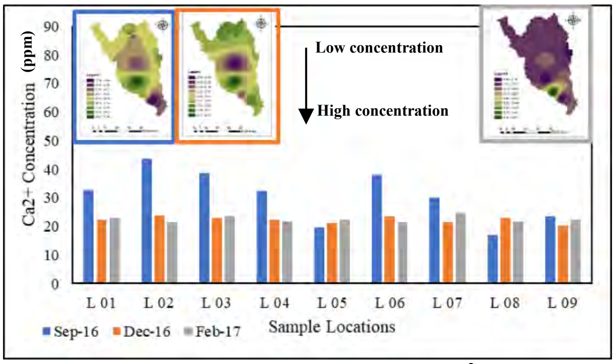


Fig. 2 Spetotemporal distribution of $Ca^{2+}$ ions in Groundwater at Upstream of Malwathu Oya basin

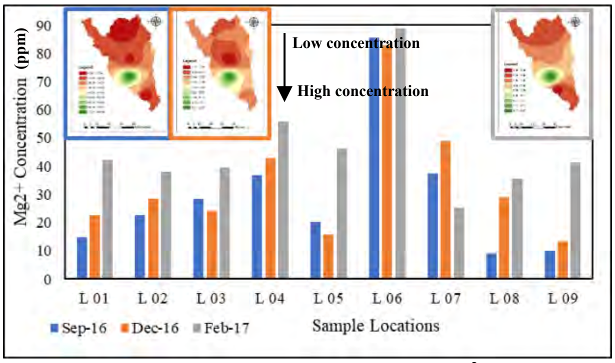


Fig. 3 Septotemporal distribution of $Mg^{2+}$ ions in Groundwater at Upstream of Malwathu Oya basin

The interpolated spatial variability of Ca2+ and Mg2+ in September/2016, December/2016 and February/2017 respectively from right to left in figure 2 and Figure 3. It shown the distinct spatial variation in both Ca2+ and Mg2+ ion concentration in groundwater. It indicates seasonal rainfall pattern affect the particular concertation in groundwater. The scale of the colour indication shown lower concentration to higher concentration from top to bottom. The maximum Ca+ concentration was detected in Location 2 in September/2016 as 43.65 ppm and Mg2+ was detected in Location 6 in February/2017 as 88.9 ppm. Both minimum concentration of Ca2+ and Mg2+ were detected in Location 8 as 17.11 ppm and 9.23 ppm in September/2016 respectively.

## 5. Conclusions

1. The concentration of both Ca2+ and Mg2+ ions is comparatively higher in upstream of Malwathu Oya basin.
2. Hardness of groundwater vary spatiotemporally in Malwathu Oya Basin, Anuradhapura District, Sri Lanka.

## 6. Acknowledgements

I would like to acknowledge Dr. S.P. Chaminda of the Department of Earth Resources Engineering at University of Moratuwa as the Main Supervisor of the Major research of this paper, and I am gratefully indebted to his valuable supervision on this project.

## References

1) Cooray, T. *et al.* (2019) 'Assessment of groundwater quality in CKDu Affected areas of Sri Lanka: Implications for drinking water treatment', *International Journal of Environmental Research and Public Health*, 16(10), pp. 1–16. doi: 10.3390/ijerph16101698.
2) Gamage, K. H. I. (2021) 'Ground Water Quality Assessment in Anuradhapura District for Domestic Purposes', (February).
3) Kurisu, F. *et al.* (2016) 'Trends in Asian water environmental science and technology', *Trends in Asian Water Environmental Science and Technology*, pp. 1–250. doi: 10.1007/978-3-319-39259-2.
4) Panabokke, C. R. and Perera, A. P. G. R. L. (2005) *Groundwater Resources of Sri Lanka*, *Water Resources Borad*.
5) Perera, P. A. C. T. *et al.* (2015) 'Seasonal variation of water quality parameters in different geomorphic Channels of the upper Malwathu Oya in Anuradhapura, Sri Lanka', *Tropical Agricultural Research*, 25(2), p. 158. doi: 10.4038/tar.v25i2.8138.
6) Raghunath, H.M. (2007), *Groud Water*,3rd Edition, New Age International (P) Ltd., New Delhi

# Identifying flash flood potential areas using morphometric characterization of watershed

○Thapthai Chaithong[1*]
[1]Department of Geography, Faculty of Social Science, Kasetsart University, Bangkok, Thailand

*E-mail: thepthai.c@ku.th

**Abstract**
This study aims to identify potential areas of flash floods using drainage morphometric investigations in the Khong watershed, Mae Hong Son, north Thailand. For this study, the Khong watershed was divided into thirteen sub-watersheds using both the ALOS-PALSAR digital elevation model and a geographic information system. Seventeen geomorphometric parameters were used to evaluate the flash-flood-prone areas and categorize areas of potential flash flooding into five classes of susceptibility of vary degrees (very low, low, moderate, high and very high). According to the flash-flood-susceptibility maps produced, two sub-watersheds pertained to the "very high" degree of susceptibility class. The similarities between the geomorphometric parameters of these watersheds indicating this categorization included high relief, stream number and stream length, including large basin areas.

**Keywords:** Flash flood, Morphometric, Watershed, Khong river, Mountainous area

## 1. Introduction

Flash floods are among the most destructive hydrological hazards, causing both infrastructure damage and human fatalities. The general characteristics of flash floods are high-velocity runoff, short lead times and rapidly rising water levels. The severity of the damage depends on the amount of rainwater, the geomorphic features of the watershed and various human factors. Regarding rainwater, flash floods derive from high-intensity, short-duration rainfall. Regarding human factors, land use and changes in land cover enhance the severity of the damage. Land-use changes affect the curve number associated with peak flow. Meanwhile, urbanization may increase the value of the damage caused. In terms of the geomorphic features of the watershed, flash floods mostly occur in watersheds less than 1000 km2 and featuring complex orography. Hence, watershed morphometrics constitute a critical influence on the hazard. (Spitalar *et al.*, 2014, Shehata and Mizunaga, 2018, Abdel-Fattah *et al.*, 2021, Alam *et al.*, 2021)

Geomorphometry describes the science of quantitative land-surface or topographic features analysis (Pike *et al.*, 2009). Numerous research studies have applied morphometric characterizations of watersheds to assess their risk of flash flooding (Perucca and Angilieri, 2011, Adnan *et al.*, 2019, Abdo, 2020). Watershed morphometric analysis involves measuring channel network linear, areal and relief features, which together represent a quantitative description of the drainage system (Alqahtani and Qaddah, 2019). Extracting morphometric parameters utilizes geographic information system (GIS) and remote sensing (RS) data.

Building on this background, this study uses geomorphometry to identify flash-flood-prone areas and produce a flash-flood-susceptibility map for the Khong watershed in Mae Hong Son, northern Thailand.

## 2. Study area

The Khong watershed (No. 0104) is a sub-watershed of the Salawin watershed (No. 01). The Khong watershed is located in the Pang Mapha district of Mae Hong Son province in northern Thailand. The total area of the watershed is approximately 684.22 km$^2$ (Fig. 1). The Khong watershed features mountainous topography, and the major types of land cover are agriculture and forest.

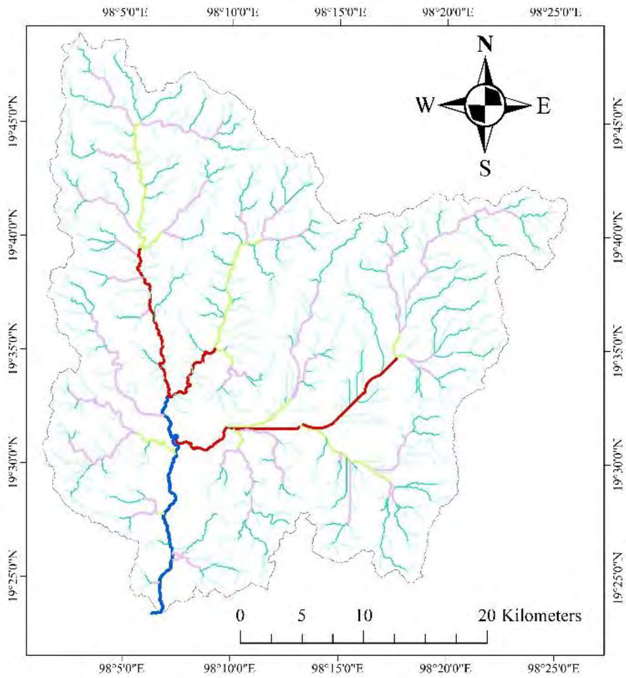


Fig.1 Khong watershed

## 3. Data and Methodology

Digital elevation models were used to capture essential input data. More specifically, an Advanced Land Observing Satellite-Phased Array-Type L-Band Synthetic Aperture Radar (ALOS-PALSAR) digital elevation model with a spatial resolution of 12.5 metres was downloaded and used to extract information about the drainage system's elevation and the sub-watershed boundaries. The steps followed for this study's geomorphometric analysis are presented in Fig. 2, and the elevation map of the Khong watershed is presented in Fig. 3.

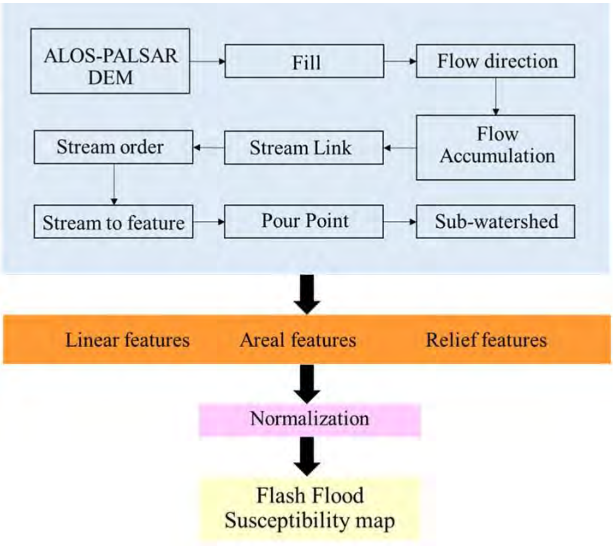


Fig. 2 Steps of geo-morphometric analysis

There are 21 geomorphometric parameters, which can be categorized into the following four main groups: basic, linear, areal and relief features. Table 1 presents the geomorphometric parameters belonging to each group.

Table 1 Geo-morphometric parameters

| | |
|---|---|
| Basic parameters | |
| 1. Watershed area | 5. Basin Length |
| 2. Perimeter | 6. Stream order |
| 3. Maximum elevation | 7. Stream number |
| 4. Minimum elevation | 8. Stream length |
| Linear parameters | |
| 9. Bifurcation ratio | 12. Drainage density |
| 10. Mean bifurcation ratio | 13. Length of overland fow |
| 11. Stream frequency | |
| Areal parameters | |
| 14. Circulatory ratio | 17. Lemniscates ratio |
| 15. Elongation ratio | 18.Compactness coefficient |
| 16. Form factor | |
| Relief parameters | |
| 19. Relief | 21. Ruggedness number |
| 20. Relief ratio | |

Of the parameters shown in Table 1, 17 parameters were selected to guide the development of the flash-flood-susceptibility map. The analysis separated the 17 parameters into two groups. Group I comprised ten parameters, including watershed area, circulatory ratio, relief, relief ratio, drainage density, stream frequency, stream number, stream length, bifurcation ratio and form factor. Group I parameters were assumed to positively correlate with flash flooding (Adnan *et al.*, 2019, Mahood and Rahman, 2019). Conversely, parameters in Group II were assumed to negatively correlate with flash floods. That is, they are inversely proportional to the degree of flash flooding. If the parameters in Group II demonstrate high values, flash-flood-susceptibility is low (Adnan et al., 2019, Mahood and Rahman, 2019). Group II comprises seven parameters, including elongation ratio, compactness coefficient, length of overland flow, ruggedness number, mean bifurcation ratio and lemniscates ratio. Group 1 parameters were normalized using equation 1, and Group II parameters were normalized using equation 2.

$$\text{Ranking score} = 4\left(\frac{x - x_{\min}}{x_{\max} - x_{\min}}\right) + 1 \qquad (1)$$

$$\text{Ranking score} = 4\left(\frac{x - x_{\max}}{x_{\min} - x_{\max}}\right) + 1 \qquad (2)$$

when $x_{\min}$ is the minimum value of each geomorphometric parameters. $x_{\max}$ is maximum value of each geomorphometric parameters.

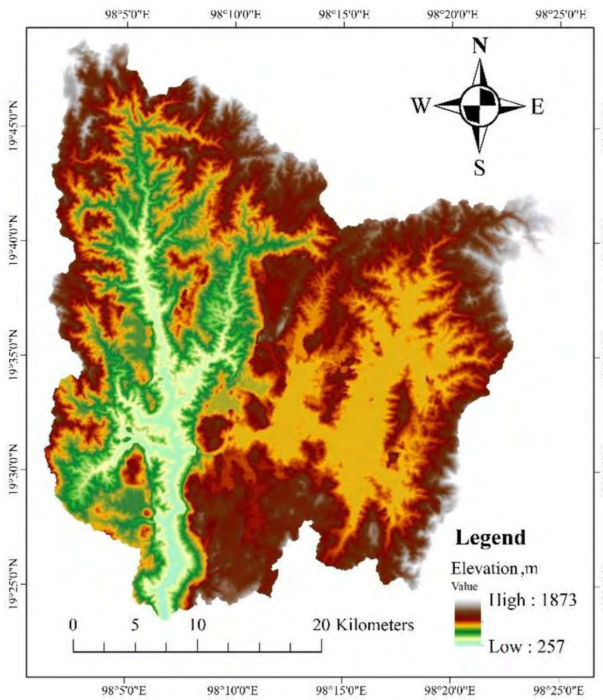


Fig. 3 Elevation map of Khong watershed

## 4. Results and discussion

There are 13 sub-watersheds in the study area, as Fig. 4 shows. The maximum stream order is sixth. The highest elevation within the Khong watershed is 1873 MSL, and the lowest elevation is 257 MSL.

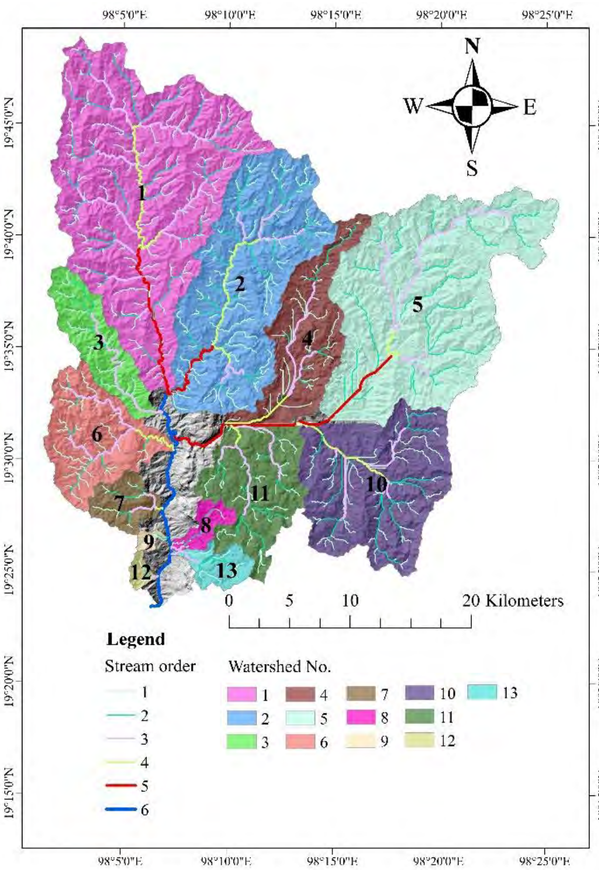


Fig. 4 Sub-watershed in the study

Fig 5 presents the flash-flood susceptibility map. Flash-flood-susceptibility was divided into five classes: very low, low, moderate, high and very high. Watersheds 1 and 5 were considered to be very highly susceptible to flash flooding; meanwhile, watersheds 3 and 8 were considered to feature very low susceptibility. Given their mutually very high susceptibility to flash flooding, there are many similarities between watersheds 1 and 5, such as a high value for the relief parameter (ranking above all other watersheds), high stream numbers, long streams and large watershed areas. Meanwhile, watersheds 3 and 8 shared similarly high elongation ratios and mean bifurcation ratios.

## 5. Conclusions

Flash floods are natural hazards. They often occur in mountainous areas featuring steep terrain or complex orography. Accordingly, the geomorphometric technique is a useful tool for identifying the areas most susceptible to flash floods. In particular, a GIS has been developed over a long period of time to support the geomorphometric technique. However, other factors influence the severity of flash-flood damage. Future studies should consider the impact of land use and rainfall on flash-flood susceptibility.

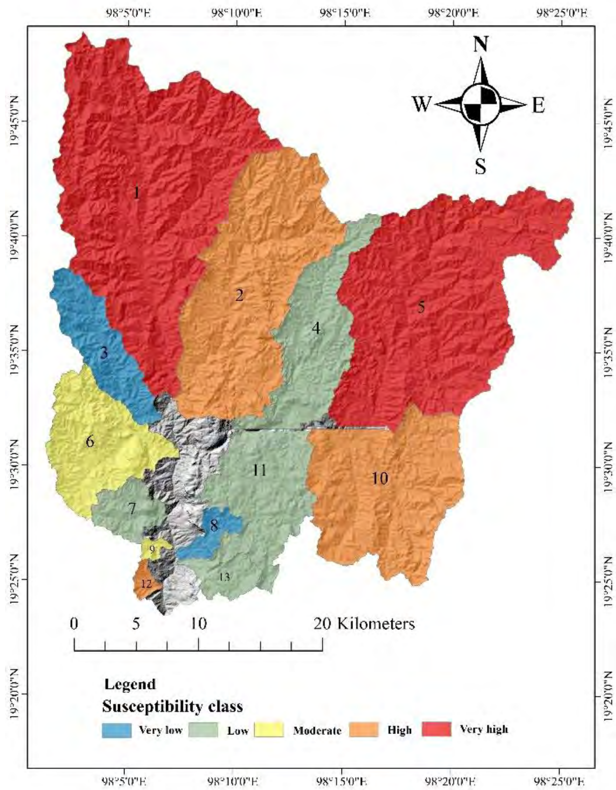


Fig. 5 Flash-flood susceptibility map

## References

1) Abdel-Fattah M, Kantoush SA, Saber M, Sumi T: Evaluation of structural measures for flash flood mitigation in Wadi Abadi region of Egypt. Journal of Hydrologic Engineering 26(2), 2021.
2) Abdo HG: Evolving a total-evaluation map of flash flood hazard for hydro-prioritization based on geohydromorphometric parameters and GIS-RS manner in Al-Hussain river basin, Tartous Syria. Nautal Hazards. 104, 681-703, 2020.
3) Adnan MSG, Dewan A, Zannat KE, Abdullah AYM: The use of watershed geomorphic data in flash flood susceptibility zoning: a case study of the Karnaphuli and Sanga river basins of Bangladesh. Natural Hazards 99, 425-448, 2019
4) Alam A, Ahmed B, Sammonds P: Flash flood susceptibility assessment using the parameters of drainage basin morphometry in SE Bangladesh. Quaternary International 575-579, 295-307, 2021.
5) Alqahtani F, Qaddah AA: GIS digital mapping of flood hazard in Jeddah-Makkah region from morphometric analysis. Arabian Journal of Geosciences 12(199), 2019.
6) Mahmood S, Rahman A: Flash flood susceptibility modeling using geo-morphometric and hydrological approaches in Panjkora Basin, Eastern Hindu Kush, Pakistan, Environmental Earth Sciences 78(43), 2019.
7) Perucca LP, Angilieri YE: Morphometric characterization of del Molle basin applied to the

evaluation of flash floods hazard, Iglesia Department, San Juan, Argentina. Quaternary International 233, 81-86, 2011
8) Pika RJ, Evans IS, Hengl T: Geomorphometry: A brief guide. Geomorphometry Concepts, Software, Application. Elsevier, Amsterdam, The Netherlands. 2009.
9) Shehata M, Mizunaga H: Flash flood risk assessment for Kyushu Island, Japan. Environmental Earth Sciences 77(76), 2018.
10) Spitalar M, Gourley JJ, Lutoff C, Kirstetter PE, Brilly M, Carr N: Analysis of flash flood paramters and huma impacts in the US from 2006 to 2012. Journal of Hydrology 519, 863-870, 2014.

**Employing satellite image derived water surface areas to estimate the small tank capacities in data-scarce regions.**

S. M. A. D. R. M. Sammandapperuma[1]*, N. K. Gunasekara[2] and C. Herath[3]

[1, 2] Deaprtment of Civil Eningineering, Faculty of Engineering, General Sir John Kotelawala Defence University, Ratmalana, Sri Lanka

[3] Project Management Unit, Climate Resilience Improvement Project (CRIP), No 11, Jawatta Road, Colombo 5, Sri Lanka

*E-mail: 35-eng-137@kdu.ac.lk, rmanujith@gmail.com

**Abstract**

Sri Lanka has significant number of minor tanks which are human made reservoirs called "wewa". Some river basins lie on intermediate climate zone in Sri Lanka. Therefore, as a method of reusing water, many tank systems are associated with river basin and used to store and preserve water. The study is targeted in finding an accessible method to acquire minor tank water capacity data when such data is limited or unavailable. The study focuses for formation of a relationship between water spread area and capacity and using GIS methods for acquiring water spread areas with the assistance of satellite images.

Keywords: minor tanks, area-capacity relationship, satellite images, GIS, spatial analyst

**Introduction**

Minor Tanks are small man-made reservoirs to mainly use for agriculture or day to day essentials. In Sri Lanka, minor tanks are mainly used for irrigational applications. Minor tanks relatively small capacities than reservoirs and has a small command area and rarely being used for commercial purposes (Somarathne *et al* 2003). The hydrological data needed for water management is lacking in some areas within the country and does not collect and consumed actively. Since the country has different climate zones, which are also has limited rainfall, tank systems become important to reuse water collected in rainy season to utilize in dry season. Collecting data and using, analyzing them leads to improved water management practices.

**Study Area**

Deduru Oya has the fifth largest in terms of basin area, covering 2616 km$^2$ and has around 3000 minor tanks (Wickramarachchi, 2019) Most of the river basin lies in Intermediate climate zone. The river basin mostly lies on northwestern region of Sri Lanka and has an annual rainfall around 1600mm (Somarathne *et al* 2003). The location of the river basin is shown as in fig 1.

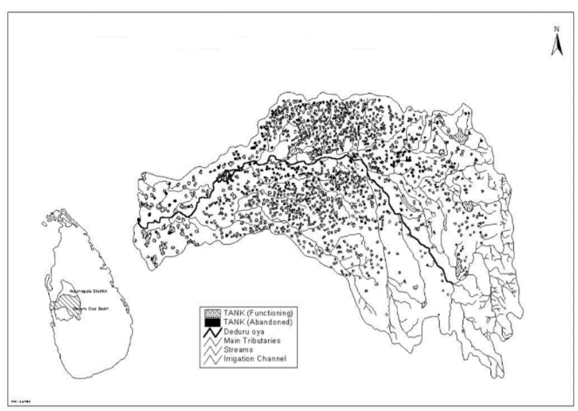


Fig 1 Deduru Oya basin and its irrigation systems(Wickramarachchi, 2019)

## Methodology

### Area – Capacity relationship.

Data gathered from government institutions were utilized to find a relationship between area-capacity for a pre-determined model, which is a power relationship.

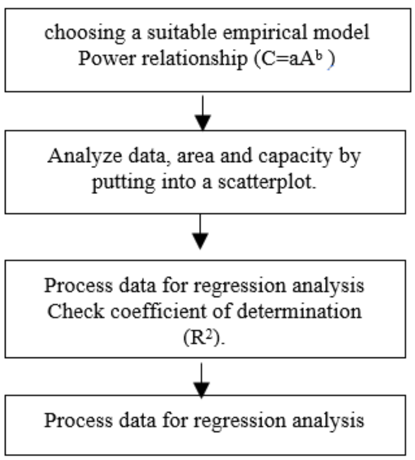


Derived relationship was validated by comparing capacity values calculated with equation to a sample of true value of capacities.

### GIS Application

Usefulness of GIS application to apply the results from a developed area-capacity relationship into scenarios where data is not recorded or missing. Function of the area-capacity relationship in such scenarios combined with GIS application makes it more effective and valuable. Satellite images of Landsat 8, less than 10% of cloud was processed to enhance waterbodies using spectral band combinations. Waterbodies extracted through supervised classification and areas were calculated using the geometry calculator. The deviation of derived areas by spatial analyst should be minimum to actual water spread areas.

### Results and Discussion

The values of surface area received by Agrarian Development department of Sri Lanka is used for developing the area-capacity relationship using the model $C=aA^b$, (Priyadarshana *et al*) where a and b are constant, A is log value of area and C is log value of capacity. A sample of data of areas were used for validation. A scatterplot was used to observe the data.

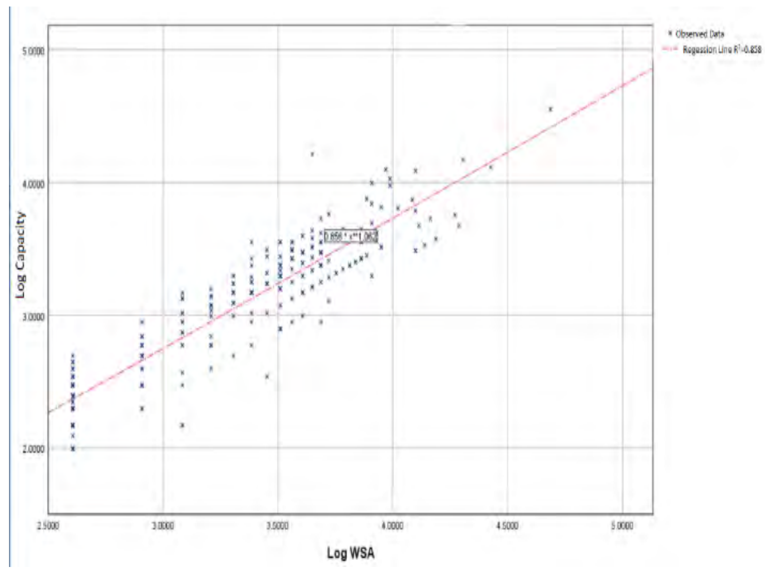


Fig 2 scatterplot between log water spread area and log capacity

The Pearson's correlation and regression analysis was used to observe the relationship is statistically valid. SPSS 25 was used for statistical analysis. Capacity and area are corelated with significant at 0.01 in two tailed test. Coefficient of determination ($R^2$) from regression analysis is $R^2$=0.858 which indicates a strong relationship between capacity and area. The received relationship is $C=0.856A^{1.062}$. The areas extracted from spatial analysis was compared to actual areas, which does not deviate much from the measured by surveys.

### Conclusions

A statistically compared accurate relationship between area and capacity of small tanks can be derived using existing surveyed data. Also, an applicable GIS usage with spatial analyst also can be implemented for receiving hydrological data such as water spread area.

**Acknowledgements**

I thank for data and support given by CRIP and Thank Prof. S. S. Wickramasuriya, who helped in getting data.

**References**

S T. N. Wickramaarachchi, "Preliminary Assessment of Surface Water Resources - a Study From Deduru Oya Basin of Sri Lanka," no. July 2004, 2019.

P.G.Somaratne, J. K, L. R. Perera, B. R. Ariyaratne, D. J. Bandaragoda, and I. W. Makin, Developing effective Institutions for water Resources Management: A Case study in the Deduru Oya Basin, Sri Lanka. Working Paper 58. 2003.

H.L Sanjaya, T.Priyadarshana, and N. Wijayarathna, "Determination of the Potential Water Storage Capacity in Ancient Abandoned Tanks in Walawe River Basin , Sri Lanka," Int. J. Res. Agric. Food Sci., vol. 2, no. 7, pp. 2311–2476, 2014, [Online]. Available: http://www.ijsk.org/ijrafs.html.

# A comparison of the quality of spatial rainfall data products available over Attanagalu Oya catchment, Sri Lanka

N. K. Gunasekara[1*], T.D.S. Rashmika [1]

[1] Department of Civil Engineering, Faculty of Engineering, General Sir John Kotelawala Defence University, Ratmalana 10390, Sri-Lanka

*E-mail: nilupul.gunasekara@kdu.ac.lk

## Abstract

The use of satellite-derived precipitation data products is the next option available for regions where rain gauge data are scarce or unavailable. In this study two satellite-derived precipitation data products, TRMM and GPM were compared against measured precipitation time series of four precipitation gauge stations of Attanagalu Oya basin for data accuracy in two time scales; daily and monthly. The Pearson coefficient, NAS coefficient and Root Mean Square Error were calculated to evaluate the performance of the time series. The study reveals that GPM data perform better than TRMM data while both the data sets show errors. The monthly time series gave higher performance than daily data indicating the possibility of employing GPM monthly precipitation data in hydrological applications in similar catchments.

**Keywords:** TRMM, GPM, time scales, errors

## 1. Introduction

Sri Lanka has an installed rain gauge network in the country, with majority of the rain gauges covering the wet-zone of the island. However, low rain gauge density in most areas inhibit the possibility of better research and applications.

According to some researches, the minimum requirement of gauge density can be as low as 1 station per 575 $km^2$ (Rubyhanusha and Rajapakse, 2019). But previous researchers have found out the minimum number of rain gauges that required to take optimum results as, 24 gauges per 1000 $km^2$ (WMO, 2018) and another research has stated the gauge density as 10 per 605 $km^2$ and 38 stations per 2148 $km^2$ (Jayawardene et. al., 2005). But we only have 487 gauge stations and 38 automatic weather stations (AWS) within the country (Dept. of Meteorology, 2021) and it is less than the half of the minimum requirement for optimum results.

Satellite based rainfall data can be used as an alternative to rain gauge data, where data is scarce. Before using these in further applications, it is required to address the reliability and the accuracy of the data. Here the comparison of spatial rainfall data was done over rain gauge data to find the accuracy of spatial data with respect to the gauge data over Attanagalu Oya catchment. Four stations in Attanagalu Oya river basin were selected with fair distribution of stations over the whole area and TRMM and GPM precipitation data were taken as satellite-derived spatial data.

## 2. Study area

Attanagalu Oya catchment lies in the wet zone of Sri Lanka with coordinates, latitudes extend from 7 to 7° 17' N and longitudes from 79° 50' to 80 15' E and the total catchment is having 2 the area of 727$km^2$ approximately and it covers total of eleven divisional secretariats of Kegalle in Sabaragamuwa and Gampaha in western province.

## 3. Methodology

Two sets of TRMM data were selected since only two coordinates were matched with coordinates of gauge station data and its acceptable range. But due to high spatial resolution of GPM data four sets of GPM data were extracted which compatible with each of the four gauge stations chosen to represent up-stream, mid-stream and down-stream regions of the basin (Table 1).

Qualitative verification of data was adapted in order to find the reliability and accuracy of spatial data and for that series of traditional error indexes were calculated which includes

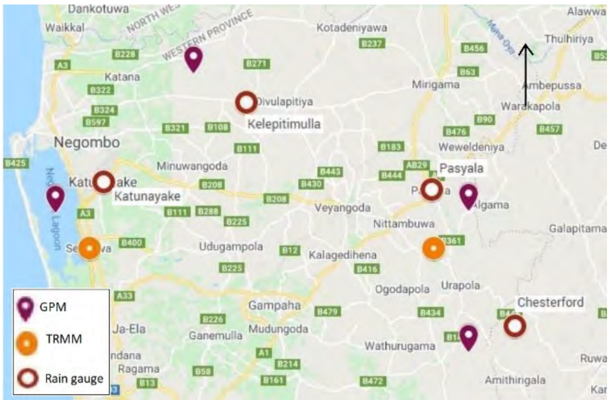


Fig. 1 Study area overlaid with the GPM, TRMM grid centroids and the considered rain gauge locations.

Pearson linear correlation coefficient (R), NASH Sutcliffe Efficiency Coefficient (NSE) and Root Mean Square Error (RMSE).

$$R = \frac{\sum_{i=1}^{n}(G_i-\bar{G})(S_i-\bar{S})}{\sqrt{\sum_{i=1}^{n}(G_i-\bar{G})^2}\sqrt{\sum_{i=1}^{n}(S_i-\bar{S})^2}} \quad (1)$$

$$NSE = \frac{\sum_{i=1}^{n}(OBS_i-SIM_I)^2}{\sum_{i=1}^{n}(OBS_i-\overline{OBS})^2} \quad (2)$$

$$RMSE = \sqrt{\frac{1}{n}\sum_{i=1}^{n}(S_i-G_i)^2} \quad (3)$$

Where $S_i$ is satellite precipitation value and $G_i$ is the gauge station value of ith station where $\bar{S}$ and $\bar{G}$ are the mean satellite and gauge station data and $OBS_i$ means to gauge station data and $SIM_i$ refers to satellite precipitation data and $\overline{OBS}$ is stated for average gauge station value.
First comparison of each spatial data set, TRMM and GPM with respective gauge stations were done in both daily and monthly data basis for each year which started from 1 January 2000 to 31 December 2007 and then comparison between obtained statistical values of TRMM and GPM was done to select the better spatial data set out of two data sets. And finally Root Mean Square Error was calculated for each year in basis of both daily and monthly.

Table 1 basic properties of satellite-derived data used

| Property | TRMM | GPM |
|---|---|---|
| Spatial resolution | 0.25°× 0.25° | 0.1°× 0.1° |
| Temporal resolution | daily | daily |
| Number of grids | 2 | 4 |

## 4. Results and discussion

The calculated performance metrics are compared in Tables 2 and 3 for the daily and monthly data precipitation data respectively, for TRMM and GPM in comparison with the measured precipitation gauge data.
It could be clearly seen that all the three performance metrics show better values (values closer to unity in R and NSE, lower values in RMSE) in GPM, compared to TRMM. One reason for this could be because of the finer resolution of GPM data, giving better proximity to the precipitation gauges. The other observation is that the monthly data show R and NSE values closer to unity than the daily data, indicating higher usefulness of satellite-derived precipitation in monthly time series. Even though the RMSE has increased compared to the daily data (Table 2), the increase has not been cumulative or proportional. It is lower than that.
This analysis suggests that the monthly time series of GPM data will be of better use in hydrological applications rather than TRMM data.

Table 2 Performance evaluation metrics of daily precipitation data (ranges are mentioned in parenthesis)

| | TRMM | GPM |
|---|---|---|
| R | 0.59 (0.40 - 0.72) | 0.83 (0.58 - 0.93) |
| NSE | 0.23 (-0.32 - 0.49) | 0.67 (0.31 - 0.86) |
| RMSE | 13.31 (10.91 - 17.17) | 8.78 (4.93 - 13.41) |

Table 3 Performance evaluation metrics of monthly precipitation data (ranges are mentioned in parenthesis)

| | TRMM | GPM |
|---|---|---|
| R | 0.83 (0.63 - 0.98) | 0.96 (0.84 - 0.99) |
| NSE | 0.68 (-0.07 - 0.96) | 0.88 (0.70 - 0.99) |
| RMSE | 75.42 (39.10 - 178.20) | 46.86 (26.87 - 83.29) |

## 5. Conclusions

All three performance indicators- R, NSE and RMSE indicate improved values for GPM data series, and also shows that the monthly time series of GPM will provide better precipitation time series, where measured gauge data are unavailable or lacking. However, the effect of altitude to the satellite derived precipitation was not explored in the current study.

## 6. Acknowledgements

The Climate Resilience Improvement Project and the Department of Meteorology is acknowledged for the provision of data to this study.

## References

1) P. Rubyhanusha and R. L. H. L. Rajapakse, "Significance of Spatial Variability in Precipitation for Stream Flow Modeling in Maha Oya River Basin, Sri Lanka," MERCon 2019 - Proceedings, 5th Int. Multidiscip. Moratuwa Eng. Res. Conf., pp. 656–661, 2019.
2) WMO, Guide to Meteorological Instruments and Methods of Observation, no. 8, 2018.
3) H. Jayawardene, D. Sonnadara, and D. Jayewardene, "Trends of Rainfall in Sri Lanka over the Last Century," Sri Lankan J. Phys., vol. 6, no. 0, p. 7, 2005.
4) Department of Meteorology, Sri Lanka, 2021. https://www.meteo.gov.lk/index.php?lang=en.

# A comparison of the design peak-flow estimated using simulated and storm-hydrographs

○Faisal Al-Hinai[1*], Luminda Gunawardhana[2]
[1]Department of Civil and Architectural Engineering, Sultan Qaboos University, Al-Khoud 123, Oman

[2]Department of Civil Engineering, University of Moratuwa, Katubedda, Sri Lanka

*E-mail: s116060@student.squ.edu.om

**Abstract**
The design of hydraulic structures requires the estimation of peak-flow corresponding to a given return period. Currently, there are two methods commonly practiced to estimate the peak-flow. In the first method, an appropriate probability distribution function is fitted to the recorded annual maximum (AM) wadi-flow series to determine wadi-flow rate with a certain exceedance probability. In the second method, in the absence of long-term wadi-flow data, peak-flow simulated by rainfall-runoff models are used. In this study, these two methods were used to estimate the differences between the design peak-flows in the Wadi Al-Khoud catchment area. For the use of hydrological modelling, Intensity-Duration-Frequency (IDF) curves were developed by using General Extreme Value Probability Distribution (GEV) function. Kolmogorov-Smirnov test was used for testing the goodness of GEV fit with observed data distribution. Comparison of IDF curves developed for the Wadi Al-Khoud area and the ones presented in the Highway Design Manual in Oman (2010) indicated that the difference between the IDF curves becomes larger as the return period increases. Geospatial Hydrologic Modeling Extension (HEC-GeoHMS) and the rainfall-runoff model (HEC-HMS) were used for delineating the catchment area and simulating rainfall-wadi flow relation. The 10-year peak-flow estimated by the observed wadi-flow records is 503 $m^3/s$, which is much different from the average peak-flows of the simulated 10 scenarios (2878 $m^3/s$). This difference can be attributed to the absence of the long-term rainfall and wadi-flow data for the probability estimations and the inability to capture the spatial distribution of the rainfall over a large catchment area as Wadi Al-Khoud catchment.

**Keywords:** annual maximum wadi-flow, GEV distribution, HEC-HMS, IDF curves, peak-flow, Wadi Al-Khoud

## 1. Introduction

Absence of the frequent rainfall events and long-term data is one of the major barriers to infrastructure development in many countries; including the Sultanate of Oman. In particular, design flood events are necessary for planning, design and operation of hydraulic structures.

Probability distribution functions are generally fitted to the maximum-recorded flood series to determine flood discharges of different probabilities. However, choosing the best-fitted probability distribution function is often controversial. In addition, as parameters are estimated from the sample data, any error in the recorded data will propagate through the results. Furthermore, the short length of observed data, outliers and missing data lead to uncertainty in the extrapolation of floods estimated by the flood frequency method.

Beven (2003) reported that rainfall–runoff modeling can also be considered as one of the approaches for designing flood events. In the absence of long-term wadi-flow data, peak-flow simulated by rainfall-runoff models with the appropriate rainfall inputs can be considered in designs. Rainfall-runoff models can produce results over space, time, and representations of internal flow processes.

The Sultanate of Oman is located in the southeastern part of the Arabian Peninsula, which is covered with different landforms. Oman is characterized by hyper-arid, through the arid and semi-arid environments that are experienced in different parts of the country.

This study will focus on the above two methods to compare the design peak-flow. The first method used the observed wadi-flow data and their probability distribution for developing peak-flow frequency relationships. The second method used the rainfall-runoff model developed using HEC-HMS software and HEC-GeoHMS software.

## 2. Study area

Wadi Al-Khoud locates in Muscat, the capital city of the sultanate of Oman. Wadi Al-Khoud has an area equal to 1660 $km^2$ and the longest wadi-length is 92 km. The catchment area is consists of a mountain range on the upstream side with the highest elevation of 2463 m above the mean sea level. Land area is mainly bare rock with sparse vegetation (Abdel-

Fattah *et al*., 2018). There are 7 rainfall gages and one wadi-flow gage station within Wadi Al-Khoud catchment. Fig. 1 shows the location, delineated of the catchment area and the distribution of the gage stations.

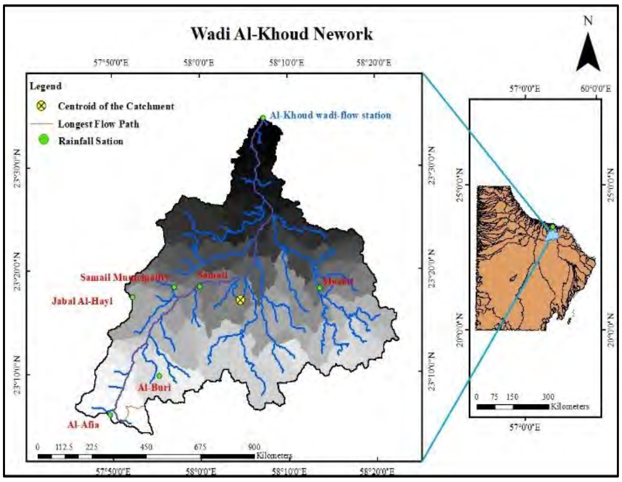


Fig.1 Delineated catchment area and wadi the network of the Wadi Al-Khoud.

## 3. Methodology

### 3.1 Development of IDF curves

The development of the IDF curves is based on the AM rainfall series and the GEV distribution function. The AM hourly rainfall events were identified for 18 years of observation (1996-2013). The developed IDF curves for the Wadi Al-Khoud area was compered with the ones presented in Highway Design Manual in Muscat area (2010).

### 3.2 Peak-flow frequency analysis for wadi-flow data

Hourly wadi-flow rates observed at the catchment outlet were used to calculate the peak-flows in 10-year return period using GEV function and Kolmogorov-Smirnov test.

### 3.3 Rainfall-Runoff Model

HEC-HMS model was used to simulate the wadi-flow hydrographs resulted from hyetographs produced by the IDF. Inverse Distance Weighting method was used for calculating the catchment average rainfall. Soil Conservation Service Curve Number method was used for loss and transformation methods. Curve number (*CN*), initial-abstraction ($I_a$) and lag-time ($T_{lag}$) parameters were calibrated with respect to the observed wadi-flow hydrographs. Percent Error in Peak and Peak-Weighted RMS Error were used as objective functions in the simulation. The Nash-Sutcliffe coefficient method was used to assess the goodness of the simulation.

## 4. Results and discussion

According to the Kolmogorov-Smirnov method test statistics, the GEV distribution fits well with both rainfall and wadi-flow time series. Fig. 2 shows the developed IDF curves for Wadi Al-Khoud. A comparison of results between the developed IDF curves and the IDF curves of the Highway Design Manual (2010) for the Muscat area indicated that the difference between the IDF curves becomes larger as the return period increases. For observed data, the peak-flow for the 10-year return period was found to be equal to 503 $m^3/s$. Two wadi-flow events were used to calibrate the model parameters. One of the biggest wadi-flow events happened on June, 2007 in Oman (Cyclone Gonu) was used for validation the model parameters, Fig. 3. Accordingly, it was found that $CN$=89, $I_a$ =7 mm and $T_{lag}$ =181 minutes. There were 10 hyetographs were developed with respect to the time of concentration and IDF curves. The average peak-flow calculated by these hyetographs was 2877 $m^3/s$, which is much different to the estimation by the first method.

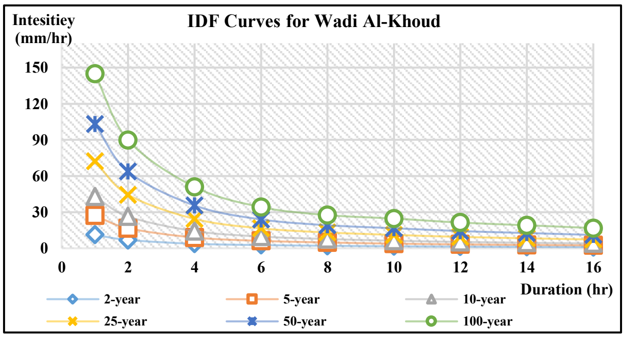


Fig. 2 IDF Curves for Wadi Al-Khoud station.

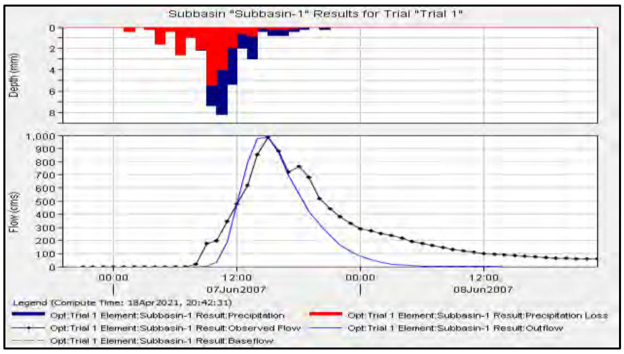


Fig. 3 Comparison between the simulated and observed direct runoff hydrograph and the gross rainfall hyetograph for Gonu Event.

## 5. Conclusions

The comparison of peak-flow between the observed and synthetic data indicated that there is a significant difference between the estimation by two methods. This difference can be attributed to the absence of the long-term rainfall and wadi-flow data for the probability estimations and the inability to capture the spatial distribution of the rainfall over that a large catchment area as Wadi Al-Khoud catchment.

## References

1) Beven, K. (2003). Rainfall-Runoff Modelling Chichester, England: John Wiley & Sons. doi:10.1002/9781119951001

2) Abdel-Fattah, M., Kantoush, S., Saber, M., & Sumi, T. (2018). Rainfall-Runoff Modeling for Extrem Flash Flood in Wadi Samail, Oman. *Journal of Japan Society of Civil Engineers, Ser,* 74, 691-696.

# Evaluation of the surface water-groundwater interaction in estimating water yield from an ephemeral river catchment in Western Australia

Amila Prasad Basnayaka[1*], Ranjan Sarukkalige [1]
[1]School of Civil and Mechanical Engineering, Curtin University, Bentley, Western Australia

*E-mail: a.basnayak@postgrad.curtin.edu.au

**Abstract**
Estimating catchment water yield in arid regions is vital to plan and manage the limited water resources not compromising water dependent ecologies. The catchment water yield estimations in these regions can be very difficult due to the ephemeral nature of their river systems, unexplored geology and aquifer systems, complex surface water-groundwater interaction, and limited data availability. The less complex and high-level water balance models that depends on lessor amount of data for model calibration can be utilised for water yield estimates in arid ephemeral river systems. The ephemeral river systems produce excessive flood peaks as a result of extreme storm events and could flow post storm with a rapid recession. The baseflow contribution is critical to reduce the post storm recession. Therefore, the water balance models should account for the surface water-groundwater interaction for a better accuracy.
This study evaluated the surface water-groundwater interaction in estimating catchment water yield in upper Marillana Creek, an ephemeral tributary of Fortescue River in Pilbara region in Western Australia. The study utilised the Australian Water Balance Model (AWBM), a widely used lump model for the runoff estimation. The baseflow parameters of the AWBM were adopted to match annual average baseflow separated from the observed flow hydrograph. The AWBM was calibrated against the observed annual and monthly flows for a 22-year record. Study provided a range for baseflow parameters that can be used in similar catchment conditions. Results of the study suggested that the AWBM, once the baseflow parameters were refined, can be used to estimate long-term ephemeral river water yields. The calibrated model can be used as an option analysis tool to analyse different climate and anthropogenic conditions, thus assist water resource decision making.

**Keywords:** Surface Water-Groundwater Interaction, AWBM, Catchment Yield

## 1. Introduction
The catchment water yield estimation is vital for water resources planning and management in arid regions with limited water resources. The ephemeral rivers in these regions flow seasonally during intense storm events. They also could flow for days or weeks after storms due to groundwater inflow. Better understanding of surface water-groundwater interaction in ephemeral river systems assists water yield estimating studies.
Estimating water yield from these systems can be challenging due to noncontinuous flow hydrographs, highly variable catchment losses with different rainfall intensities and pre-burst conditions, complex and less understood aquifer systems, thus the surface water-groundwater interaction, and lack of data.
This study evaluated surface water-groundwater interaction during a water yield estimation study for an arid ephemeral river catchment. The study used a less complex but widely accepted water balance model that can be calibrated with limited amount of data. The study still accounted the surface water-groundwater interaction as in baseflow of the model. The baseflow separated from the observed flow hydrograph was used to refine the water balance model baseflow parameters.

## 2. Study area
Fig. 1 shows the upper catchment of Marillana Creek, an ephemeral tributary of Fortescue River in arid/semi-arid Pilbara region in Western Australia. The river catchment was delineated at circa 1369.5 $km^2$ with average annual rainfall and evaporation of about 452 mm and 3082 mm, respectively. The daily river flow series in Fig. 2 (top) shows the ephemeral nature of the river with excessive peaks and zero flows during storms and dry periods, respectively. Several mining activities can be found downstream of the creek.

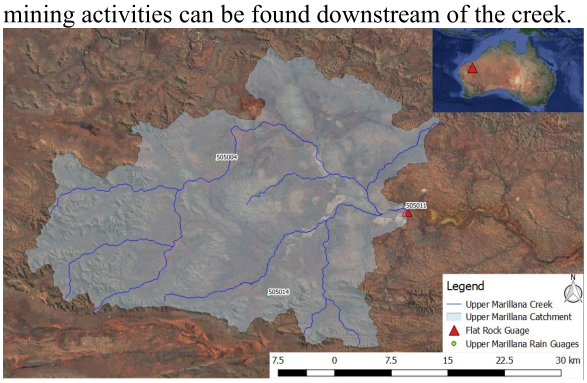


*Fig.1 Upper Marillana Creek catchment*

## 3. Methodology
### 3.1 Data analysis
We analysed the daily series of rainfall and river flow data sourced from DWER (2021) and grided meteorological data sourced from DES (2021).
Comparison of rainfall data from three rain gauges (Fig.1) shows a high variability of daily rainfall across the catchment up to maximum of 164 mm between gauges. This is about 71% from the maximum observed daily rainfall of 229 mm. The study averaged the rainfall data between three gauges

and compared with the grided data by plotting against the observed river flow hydrograph. The average gauged data series showed a better correlation to the river flow than the grided data, thus adopted for the study. An aerial reduction factor (ARF) was adopted during the calibration process (Section 3.4) considering the spatial variation of rainfall. Gridded daily evaporation data was adopted as the daily evapotranspiration data series.

### 3.2 Baseflow separation

Based on the analysis of rainfall and river flow series, the baseflow that occurs with a storm event seems to rapidly recede within a short duration (varies from a couple of days to about two months). Two sample plots of baseflow occurs during two different storm events are shown in Fig. 2 (bottom). The power function of the recession curves varies with the event intensity, pre-burst conditions and the subsequent minor rainfalls, thus no general formula that matches the recession curve would be applicable. We estimated the average annual baseflow component at about 6% from the total river flow. This estimate was later used to define a range to the baseflow parameters for the water balance model (Section 3.3).

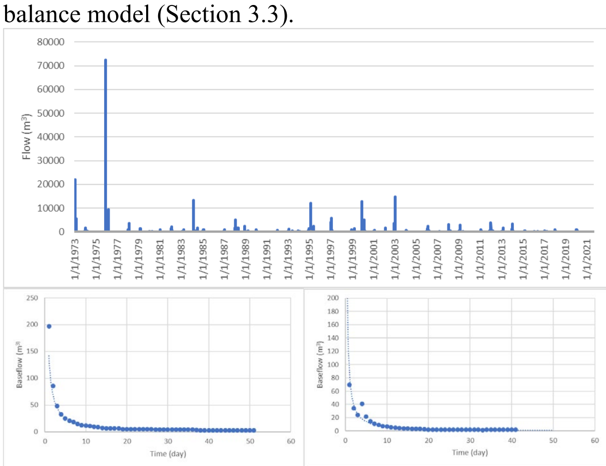


*Fig. 2 Daily river flow (top) and sample baseflow recession series (bottom)*

### 3.3 Water balance modelling

We utilised the Australian Water Balance Model (AWBM), a simple but widely accepted model developed by Boughton (1999 and 2004) to estimate catchment runoff yield. The AWBM consists some parameters to define surface and baseflow storages, excess, and recession constants.
Boughton (2003, 2006, 2007, 2009) provide AWBM parameters and parameter selection methods for some regions in Australia, but not for Pilbara. They also recommend the AWBM to be used in other catchments once calibrated.

### 3.4 Model calibration

We selected 22-year long observed hydrograph from 1980 to 2002 for AWBM calibration. The calibration process was:
Step 1 – Adopted the model parameters and selection methods recommended for the other regions: The attempt was unsuccessful as the parameters did not represent the ephemeral nature of the Marillana creek.
Step 2 – Randomly adjusted the model parameters by trial-and-error: We managed to calibrate to a reasonable accuracy. It is noted that there were multiple parameter combinations that provided similar results.
Step 3 – Adopted an ARF of 0.85 by trial-and-error for rainfall considering the spatial variation of rainfall (Section 3.1) and re-adjusted the other parameter combinations. It was noted that the model was better calibrated with this the ARF than without it, thus results agree with Boughton (2009).
Step 4 – Adjusted the baseflow index and baseflow recession constant so that the modelled average annual baseflow agrees with the estimates in Section3.2. i.e. average annual baseflow about 6% from the river flow. Then, we re-adjusted the other parameter combinations and calibrated the model.
Fig. 3 and Fig. 4 summarise the annual and monthly modelled vs observed flow series. The root mean squared error (RMSE), $R^2$ for the average annual and monthly series are about 0.8 and 0.5 respectively.

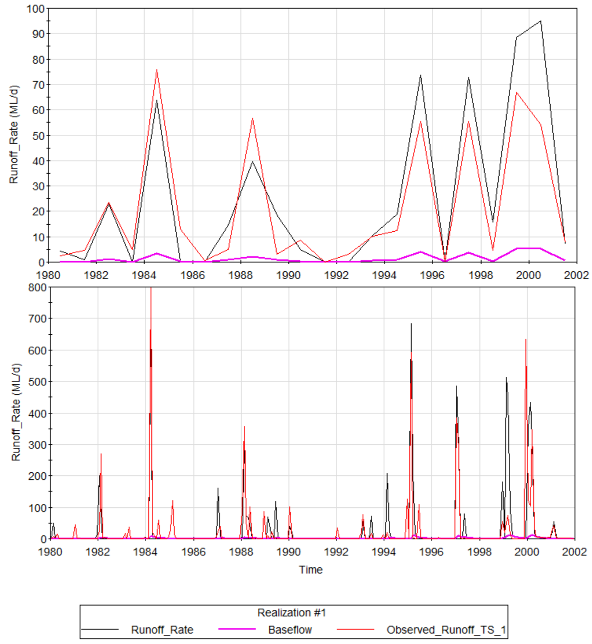


***Fig.3 a. annual (top) and b. monthly (bottom) modelled vs observed flow hydrographs***

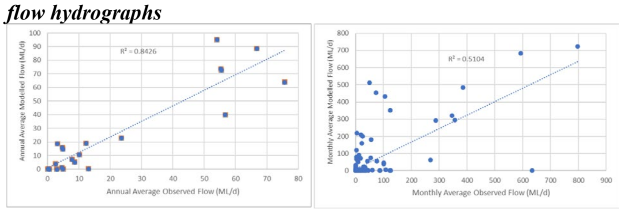

***Fig.4 a. annual (left) and b. monthly (right) modelled vs observed flow hydrographs***

## 4. Results and discussion

Based on the observed hydrograph for 48-years, the average annual baseflow for Upper Marillana Creek is about 6% of the total river flow. This increases during storm events but recedes rapidly post storm. The recession time and the rate varies with pre-burst conditions, storm intensity, and the subsequent rainfall. However, study results show the long term average of the ephemeral river baseflow would provide enough accuracy to be used in water yield studies.
Based on the study, the AWBM parameter and the parameter selection methods recommended for other regions, were not successful to the Marillana Creek. This is due to the ephemeral nature of the river. The study calibrated the AWBM the Marillana Creek and found multiple parameter

combinations would provide the same results. The adopted ARF for daily rainfall series considering the spatial variability across the catchment provided a better calibration. The study further adjusted the baseflow index and the baseflow recession constant so that the modelled annual average baseflow agrees the observed. Based on the modelling results, the baseflow index for Upper Marillana Creek can be range from 0.03 to 0.1. The potential rang for baseflow recession constant was estimated from 0.9 to 0.99. The study calibrated the model based on 22-year period of long-term data for annual and monthly RMSE at 0.8 and 0.5, respectively. The adopted baseflow index and baseflow recession constant was 0.055 and 0.99 respectively.

The study results suggest that the AWBM can be used to estimate water yield from ephemeral rivers in arid regions. The understanding of surface water-groundwater interaction, thus the baseflow contribution is useful to further refine modelling parameters.

The developed water yield model for Marillana Creek can be used as an option analysis tool to assess water resources against scenarios such as climate change, prolonged extreme weather conditions, mine water abstraction etc. The model also can be used together with stochastic climate data for probability analyses.

## 5. References


Boughton, W. (2004). *The Australian water balance model*. Environmental Modelling & Software, 19(10), 943-956.

Boughton, W. (2006). *Calibrations of a daily rainfall-runoff model with poor quality data*. Environmental Modelling & Software, 21(8), 1114-1128.

Boughton, W. (2009). *Selecting Parameter Values for the AWBM Daily Rainfall-Runoff Model for Use on Ungauged Catchments*. Journal of Hydrologic Engineering, 14(12), 1343-1350.

Boughton, W., & Chiew, F. (2003). *Calibrations of the AWBM for use on Ungauged Catchments*.

Boughton, W., & Chiew, F. (2007). *Estimating Runoff in Ungauged Catchments from Rainfall, PET and the AWBM Model*. Environmental Modelling & Software, 22(4), 476-487.

Boughton, W. C. (1999). *A Daily Rainfall Generating Model for Water Yield and Flood Studies*. Retrieved from

DES. (2021). Scientific Information for Land Owners (SILO) Data Drill. https://www.longpaddock.qld.gov.au/silo/

DWER. (2021). River Monitoring Stations. Retrieved from https://kumina.water.wa.gov.au/waterinformation/telem/stage.cfm

International Conference on Sustainable Water Resources Management
- Global Challenges & Opportunities - (September 10th, 2021)
Committee on Global Environment
JSCE

# Assessing the risk of river bank erosion under the context of climate change for Ho Chi Minh City, Vietnam

○Ngoc Pham [1*], Hoa Thi Pham [2], Angeli Doliente Cabaltica [1]
[1]Department of Civil Engineering, International University, Viet Nam National University Ho Chi Minh City, Vietnam
[2]School of Biotechnology, International University, Viet Nam National University Ho Chi Minh City, Vietnam

*E-mail: pngoc@hcmiu.edu.vn

**Abstract**
Supporting for natural disaster management in Ho Chi Minh City (HCMC), the risk of river bank erosion under the context of climate change (CC/SLR) was simulated by using fuzzy logic approach in ArcGIS environment and Mike 21 hydrodynamic model. As the result, bank erosion risk maps have been developed for the main rivers in HCMC corresponding to 8 scenarios: current situation; 5 CC/SLR scenarios legally published; and 2 upstream flood discharge scenarios with the frequency of 5% and 1%, respectively. The simulated results also indicated that CC/SLR more or less increases the risk of riverbank erosion but not to a serious extent. However, when two upstream reservoirs discharge flood happened, it would make river bank erosion much worse situation; therefore we need to have solutions to minimize the risk from these scenarios.

**Keywords:** Fuzzy Logic, river bank erosion, climate change risk assessment, Ho Chi Minh City

## 1. Introduction

Ho Chi Minh City (HCMC) is the biggest city of Vietnam with the area of 2.061 $km^2$. Located in lower Dong Nai River Basin, the city is characterized as a lowland area, having a dense river network and highly tidal impacted (figure 1). The rivers bring many benefits for socio-economic development of the city. On the other hand, river bank erosion (RBE) also causes serious damage to property and infrastructure of the City. The total damage caused by RBE in the city approximately was 24.6 billion VND reported from 1997 to 2007. Therefore, researching on RBE assessment becomes more important.

Previuosly, there are number of publications with the topic related to RBE assessment (e.g., Hoang Van Huan, 2008). However, the methods used in these studies are deterministic approaches such as hydro-dynamic models or geological models or emperical models; which are not accurate enough for evaluating the RBE phenomena resulting from a complex set of interacting processes of internal and external factors. Alternatively, the risk-based approach is applying in this study, widely adopted for disater risk management in many countries.

In additional, climate change (CC/SLR) have been indicated as one of the most serious factor recently impacting to the natural condition of the city (Chau Nguyen Xuan Quang, 2015; Nguyen Ky Phung and Nguyen Thi Thu An, 2012; Ministry of Natural Recourses and Environment, MONRE, 2016), but mainly considered to hydrological regime or rainfall pattern or urban inundation situation in the HCMC. There is lack of research on qualifying the potential effect of CC/SLR on RBE of the city. Consequently, supporting for nataral disater risk management of the city, the ojective of this research is to quatitatively predict the spatial - temporal risk of RBE in the city under the context of CC/SLR. Moreover, with aid of ArcGIS software, the risk maps also are conducted.

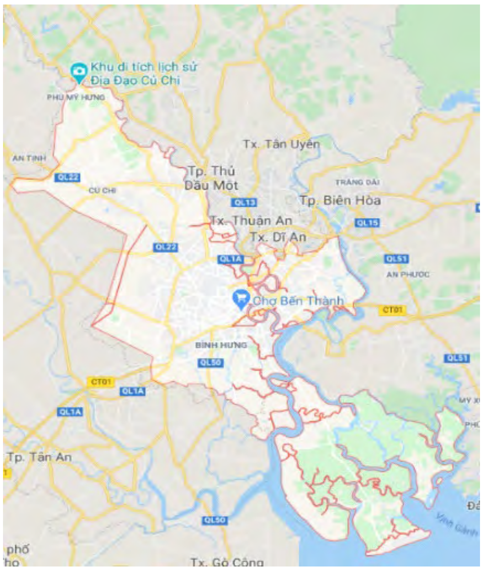


Fig.1 The administrative map of Ho Chi Minh City

## 2. Methodology

### 2.1 Data collection

Both secondary and primary types of data were collected. The climatic and hydrological time-series data observed at official gauging stations, topographic data on terrain and river cross sections, and current situation of RBE were collected from governmental agencies. Moreover, additional field survey data on location and magnitude of erosion area along main rivers were investigated. Furthermore, hourly mean water levels at some cross-sections in Sai Gon and Dong Nai rivers were measured at the site.

### 2.2 Risk assessment process using fuzzy logic

Fuzzy logic approach implemented in the ArcGIS environment has been used for modeling riverbank erosion vulnerability or risk. Firstly, the input parameters, consisting of many internal and external factors, were grouped into three different modules. Bank erodibility was first modeled based on the physical characteristics of the bank including: bank protection depending on existing protected structures; bank material or soil types; bank slope, and bank vegetation. The second module considered climatic factors as well as human activities as erosion intensifiers, which are rainfall pattern, land use and navigation. The results from the two modules were combined with hydrodynamic factors – velocity and water level fluctuations simulated from Mike 21 model to compute the final index of bank erosion risk.

Secondly, formulation of membership functions and fuzzy rules has been set up. The rules were if-then statements that relate the combination of parameters to riverbank erosion. These functions and rules are formulated based on literature gathered on the subject, "expert knowledge", and calibrating process using actual data on existing erosion areas.

Finally, for processing of the data, 50 m on either side of the water's edge were considered as active bank zones. Then, the river bank was longitudinally rasterized into 5 m x 5 m cells. The final output were the risk maps showing the spatial distribution of the calculated riverbank erosion index. Five risk levels were defined with relevant colors for the HCMC such as: low in blue, medium in yellow, high in orange, very high in red, and extreme in purple.

## 3. Results and discussion

As the result, bank erosion risk maps have been developed for the main rivers in HCMC corresponding to 8 scenarios: current situation; 5 CC/SLR scenarios legally published by MONRE; and 2 upstream flood discharge scenarios with the frequency of 5% and 1%, respectively; in which hydraulic parameters (velocity and water level fluctuations) are calculated from Mike 21 model, the remaining parameters are calculated the same as the current status. For example, the figure 2 shows the simulated results of bank erosion risk zoning for main river network in HCMC, corresponding to CC/SLR scenario to 2050.

The simulated results between the CC/SLR scenarios and the current situation show only a small change because it is assumed that climate change affects only hydrodynamic parameters. Moreover, the research used Hjulstrom curve to build the velocity correlation function; in which velocity values greater than 1 m/s are considered in high risk level. Furthermore, it is predicted that there is a large change in the higher risk level when comparing the flood discharge scenarios with the current scenario due to large fluctuations in hydraulic parameters, leading to an increase in the area of extreme risk zones.

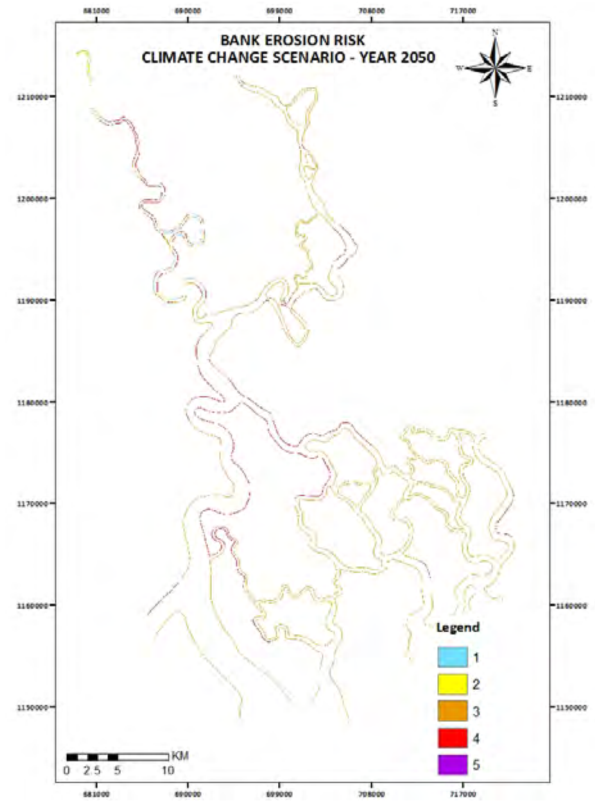


Fig.2 Predicted river bank erosion risk map to 2050

## 4. Conclusions

By using fuzzy logic approach in ArcGIS environment and Mike 21 hydrodynamic model, this study predicted that CC/SLR more or less increases the risk of riverbank erosion but not to a serious extent. However, when two upstream reservoirs discharge flood happened, it would make river bank erosion much worse situation; therefore we need to have solutions to minimize the risk from these scenarios.

## 5. Acknowledgements

The authors would like to thank the Department of Science and Technology of HCMC for their funding.

## References

1) Chau Nguyen Xuan Quang: Analysing tendency of yearly maximum water levels in lower Dong Nai -Sai Gon river Basin. Journal of Agriculture and Rural development (2), 65–71, 2015. (In Vietnamese)
2) Hoang Van Huan: River bed deformation of river system in lower Dong Nai -Sai Gon river Basin and recommendation of prevention solutions. Journal of Water Resources and Enveronmetal Engineering (23), 167-178, 2008. (In Vietnamese)
3) Ministry of Natural Recourses and Environment: Scanerios of Climate change and Sea level rising for Vietnam. Vietnam Natural resourses Environment and Map Publisher, 2016. (In Vietnamese)
4) Nguyen Ky Phung and Nguyen Thi Thu An: Application of SWAT model to evaluate impact of climate change to flow in Dong Nai river Basin. Journal of Water Resources and Enveronmetal Engineering (12), 96-101, 2012. (In Vietnamese)

# Spatial changes of Urban Heat Island formation and its effect on the Ecology: A case study of Colombo City, Sri Lanka.

○K A K M Kurugama[1*], S P Chaminda [1], D M D O K Dissanayake[1]
[1]Department of Earth Resources Engineering, University of Moratuwa, Katubedda 10400, Sri Lanka

*E-mail: kmadhawa94@gmail.com

## Abstract

Colombo is one of the main commercial metropolitan towns of South Asia that has the most infrastructure and population densities in Sri Lanka, leading the city as an ideal destination to form Urban Heat Islands (UHI). This research is intended to examine the UHI effect in the Colombo area and treat its adverse effects on the ecology using Landsat 8 satellite images. The temperature inequality of the city was obtained by deriving Land Surface Temperature (LST), using Radiative Transfer Method. Main Land use classes were identified by supervised classification. Ecological criticality was evaluated using Urban Thermal Field Variance Index (UTFVI), a quantitative indicator of the ecological quality of urban life with based on UHI effect. The verification of the model has been obtained by visual interpretations and theoretical relations between the LST, the vegetation index by normalized difference (NDVI) and the normalized construction index (NDBI). LST variations in Colombo city uncovered that, majority of the environmentally alarming areas were situated along the coastal belt, central business area along the main transport system and around the harbor. As claimed by UTFVI, the city of Colombo experiences two contraries as areas with favorable micro-climate and areas with critical heat stresses alarming that the necessity of strong UHI reduction steps in future landscape urban planning and development of the city.

**Keywords:** UHI, LST, NDVI, NDBI, UTFVI

## 1. Introduction

Accompanied by globalization, the recent increase in the population in urban areas and the Industrial Revolution led to urbanization, which provoked severe changes of land use patterns to cling to the needs of the economy. During the years between 2015-2020, 2020-2025 & 2025-2030, Urban population is expected to grow approximately 1.84%, 1.63% & 1.44% per year respectively all over the world (WHO, 2020). These urban areas generally have high thermal capacity, Major absorption of solar radiation, and although the municipality of infrastructure with darker surfaces such as roads, vehicle parking lots, bridges, pavements, roof tops and buildings are made up from lower albedo materials with low solar reflectivity (Jiang *et al*, 2006). Debugging in this way, the densely packed areas tend to experience relatively higher temperatures compared to the country areas in the surrounding. This phenomenon leads to a land effect called "Urban Heat Island" (Oke, 1982).

The elimination of large vegetation-cover and replacement by artificial surfaces is one of the main reasons behind the formation of UHI. The release of residual heat from factories, urban houses, air conditioners, and motor vehicles are some of other major causes (Senanayake et al, 2013). The impact on the water quality and the aquatic ecosystem, the clumps and the climatic patrons and the problems with the human health are some of the adverse effects. Integration of Remote sensing (RS) & Geographic information system (GIS) plays a major role in detection of thermal energy released from earth surface (Streutker, 2002). In this study, environmental criticality due to UHI effect was analyzed using Urban Thermal Field Variance Index (UTFVI) In a GIS environment.

## 2. Study area

Colombo, located in the western province of Sri Lanka, is the commercial capital of the island and hosts over one million people. It is one of the most competitive metropolitan areas in Asia. The city is the administrative and economic core of the country. Colombo is located between Northern latitudes 6° 55'-6059' and Eastern longitudes 79° 51'-79° 53' extending over 37km$^2$. The city of Colombo experiences a typical good weather climate and is located in a lowland region with an average annual rainfall of 2300 mm and average annual temperature is approximately 29 °C.

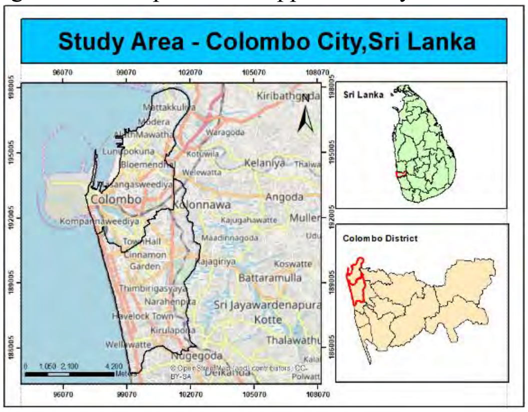


Fig.1 Study Area Map

## 3. Methodology

### 3.1 Data Sources

Landsat 8 OLI & TIRS satellite image in 2019, was selected based on the quality, cloud cover etc. in this study. Supervised classification method was used for the Land Use classification.

### 3.2 Retrieving Land Surface Temperature (LST)

The LST was derived using the radiation transfer method, using the thermal band (band 10) of the Landsat 8 satellite image, as described in the Landsat 8 Scientific User Manual (NASA, 2020). Then, the parameters NDVI, NDBI, Albeo were derived to study the relationship with respect to LST. Finally, the ecology of the study area was assessed using the UTFVI index map using the above parameters.

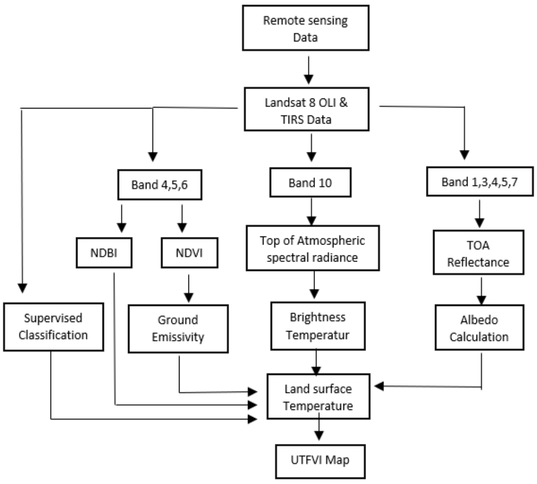


Fig.2 Work Flow chart

## 4. Results and discussion

### 4.1 Land Use Distribution

Land use in the area is mainly divided into 4 categories: water bodies, vegetation, barren land and built-up areas. According to Figure 3, 87.08% of the area was occupied by a built-up area, while water bodies, vegetation and barren areas covered 3.21%, 4.5% and 5.21%, respectively.

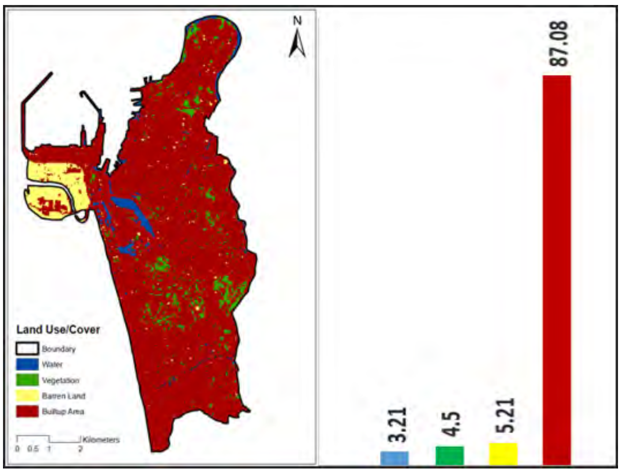


Fig. 3 Land Use Classification

### 4.2 LST Distribution

The LST distribution was divided into 5 categories based on histogram values and red and green respectively indicate the highest and lowest temperature categories and the red area is considered as UHIs. The avarage LST was 35.26 ° C, the maximum and minimum LST were 40.33 ° C & 28.71 °C, respectively. The highest LST (> 35.50 C) was concentrated near the port city and the port of Colombo, the central part where government services and other public and private buildings are located), strongly following the urban spatial development and multi-story construction while the southeastern and southern regions with greater green coverage found sub-moderate temperatures. Overall, 39.16%, 57.6% and 3.16% of the area showed high, moderate and low temperatures.

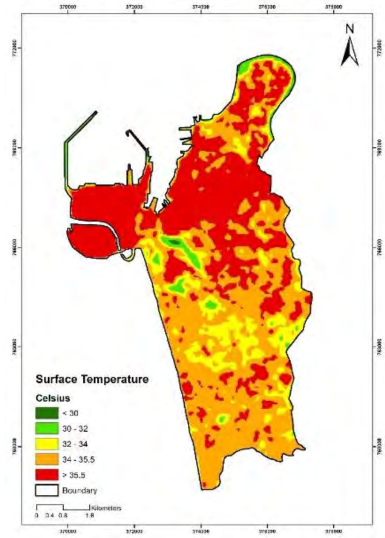


Fig. 3 LST Distribution

The theoretical relationships between the variables LST, NDVI and NDBI were qualitatively verified by visual interpretations of these variables and quantified by correlation analysis based on comparison of pixel-based images comparison.

Table.1 Correlation Matrix

| | LST | NDVI | NDBI |
|---|---|---|---|
| **LST** | 1.00 | -0.4513 | **0.5935** |
| **NDVI** | **-0.4513** | 1.00 | -0.6800 |
| **NDBI** | 0.5935 | -0.6800 | 1.00 |

According to Table.1, positive and negative correlations obtained between LST & NDBI and LST & NDVI respectively.

### 4.3 Albedo Distribution

The albedo distribution is classified into 5 categories based on histogram values and according to Figures 3 and 4, most UHIs are formed where the low and fair albedo surface albedo types such as asphalt, tar, gravel, corrugated roof and concrete etc. Most roofs are covered with concrete slabs or asbestos, which fall into the category of low albedo materials. The pier and parking lots at Colombo . The Colombo harbor jetty and parking lots are constructed with dark albedo materials like asphalt which is a major contributor of UHI formation

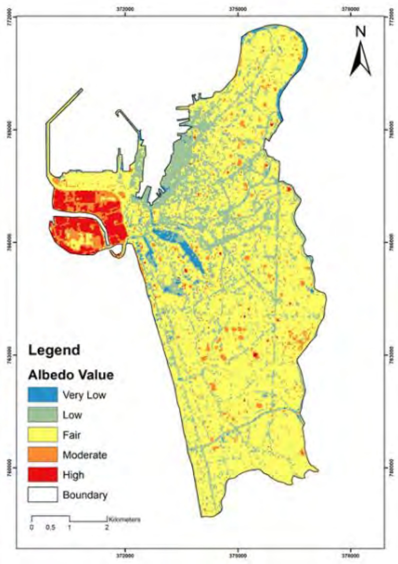


Fig. 4 Albedo Distribution

### 4.4 Ecological Evaluation of UHI

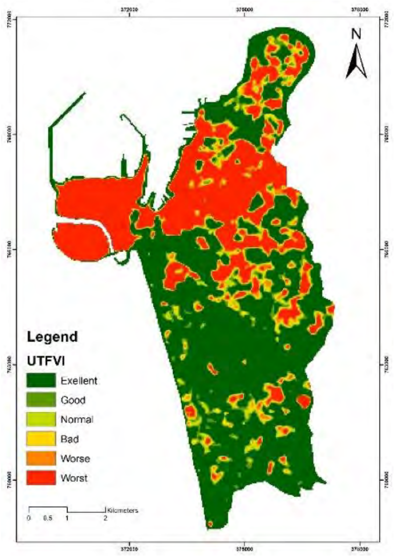


Fig. 5 UTFVI Map

Urban The variation index is an indicator of the urban ecological quality with respect to the UHI phenomenon. Based on a comprehensive literature review, UTFVI values were divided into 6 categories ranging from excellent to worse ecological conditions. According to Figure 6, 53.85% experience optimal thermal conditions and 27.50% of the area is affected by the worst thermal conditions around commercialized and urbanized areas.

## 5. Conclusions

According to Land use distribution in Colombo city, 87% and 4.5% of area was occupied by the built-up area and vegetation indicated the urbanization level of the city. UHIs directly followed spatial pattern of urban development and high building density and it was confirmed by the results of correlation analysis between LST, NDVI and NDBI such that built-up area can strengthen UHI effect while vegetation cover can reduce the effect of UHIs. Moreover, Low albedo materials can accelerate UHI phenomenon. Finally, as claimed by UTFVI map, Colombo city experiences both extreme ecological conditions and 27.50% of those experiences worst conditions indicating that the need of well-designed urban planning system and UHI mitigation strategies.

## 6. Acknowledgements

We would like to thank the academic staff of the Department of Earth Resources Engineering at the University of Moratuwa for the financial support given to the success of this research study.

## References

1) Jiang. G, Li. Z and Nerry. F, "Land surface emissivity retrieval from combined mid-infrared and thermal infrared data of MSG-SEVIRI", Remote Sensing of Environment, vol. 105, no. 4, pp. 326-340, 2006.
2) "Landsat 8 Data Users Handbook Now Available « Landsat Science", *Landsat.gsfc.nasa.gov*, 2020. [Online]. Available: https://landsat.gsfc.nasa.gov/landsat-8-data-users-handbook-now-available/. [Accessed: 02- Feb- 2020].
3) Oke.T, "The energetic basis of the urban heat island", Quarterly Journal of the Royal Meteorological Society, vol. 108, no. 455, pp. 124, 1982.
4) Senanayake. I, Welivitiya . W, and Nadeeka. P, "Remote sensing based analysis of urban heat islands with vegetation cover in Colombo city, Sri Lanka using Landsat-7 ETM+ data", Urban Climate, vol. 5, pp. 19-35, 2013.
5) Streutker. D, "A remote sensing study of the urban heat island of Houston, Texas", *International Journal of Remote Sensing*, vol. 23, no. 13, pp. 2595-2608, 2002.
6) "World Health Statistics", *World Health Organization*, 2020. [Online].Available:https://www.who.int/gho/publications/world_health_statistics/en/. [Accessed: 12- Feb- 2020].

# Local action on climate change: Opportunities and constraints in the lower Yom and Nan River basins, Thailand

○Weerayuth Pratoomchai[1*], Naphol Yoobanpot [1]
[1]Department of Civil Engineering, Faculty of Engineering, King Mongkut's University of Technology North Bangkok, Bangkok, Thailand

*E-mail: weerayuth.p@eng.kmutnb.ac.th

## Abstract

Flooding is the second severe impact on socio-economic losses in Thailand after the COVID-19 Pandemic. The 2011 flood event was recorded as the extremely national flood disaster. Lower Yom and Nan River basins (LYN) and Chao Phraya basin (CPB) including northern part of Bangkok were inundated for almost 4 months. Changing of climate is blame as the catalysis of the event. Based upon the climate change model projections using multiple models and scenarios over the period 2021-2040, surface air temperature shows increasing trend while amount of rainfall does not clearly change relative to the past observed data (1981-2000). However, proactive action called "Bangrakum Model" or flood retarding scheme is implemented in the LYN since 2017 for securing local people production (rice) and storing water budget for off-seasoning. Shifting the rice growing time (2 months earlier), retarding about 400 million $m^3$ of flood volume for almost 3 months after harvesting, and draining flood surplus downstream at the end of rainy season are 3 major stages of the measure. Over 3 years of Bangrakum operating plan, seasonal rice production in the LYN has been saved from flood damage. Huge amount of water volume is expected to fulfill groundwater during the second stage, but the observed data shows decline trend. Overuse of groundwater and lacking of facility inducing recharge are the main problem and what should implement next for enhancing this scheme as a sustainable and long-run project. However, there are some bad feed backs from farmers who allow their fields as the flood retention areas on unjustified compensation.

**Keywords:** Bangrakum model, Climate change, Flood management, Groundwater depletion

## 1. Introduction

Among several disasters, flood is the most severe natural disaster affecting on multi-sectors in both direct and indirect impacts. The historical record of 2011 mega-flood event in Thailand plunged for approximately USD 46.5 billion in economic loss, which was the biggest amount due to disaster. However, this event awakes people to realize on causes and effects of flooding and called for mitigation measures. Under climate change conditions, a severe flood magnitude like the 2011-flood event is projected to repeat (Gopalan et al., 2020). Therefore, countermeasures against floods are needed for alleviating and protecting potential damages. Flood retarding scheme in the LYN called Bangrakum model has been implemented in 2017. The project is not benefit only to the LYN but also extends to central region including the capital city, Bangkok.

## 2. Study area

Fig. 1 shows the topographical setting of the LYN and 2011 flood extended area. There are two main streams, i.e., the Yom, and Nan Rivers; both rivers flow from the north to the south and finally merge to each other at Nakhon Sawan province. Since the upper part of the basin is a mountainous area; therefore, a huge water volume from heavy rainfall rapidly flows to the low land area. This low land area now is called LYN's flood prone area which is designed for retarding flood water under the Bangrakum Model.

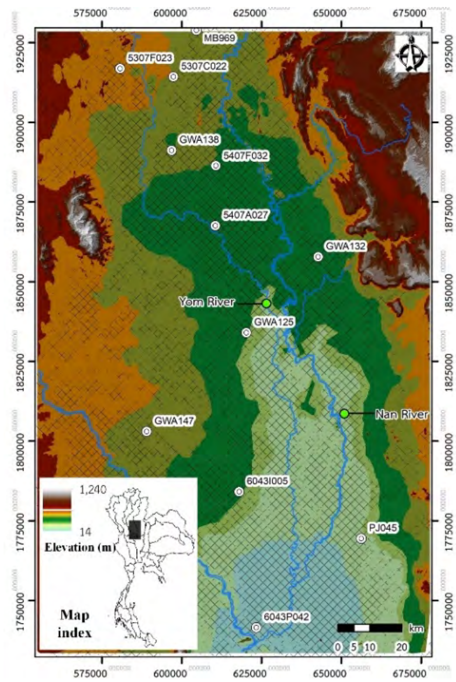


Fig.1 Topographic setting of lower Yom and Nan basins and observation wells

## 3. Methodology

### 3.1 Projection of climate change

In this paper, 3 GCMs were selected, namely, 1) MIROC, 2) HadGEM, and 3) GFDL models. These 3 GCMs from different climate research institutes were selected to reflect uncertainties within the models. Three scenarios (i.e., representative concentration pathways, or RCPs), including low (RCP2.6), intermediate (RCP4.5), and high (RCP8.5) levels of emissions, were used to project the future climate for the period 2021-2040, and shifting and scaling technique was applied for bias correction (Hanasaki and Mateo, 2012).

### 3.2 Bangrakum model

Bangrakum model or flood retarding scheme covers an area approximately 424 $km^2$. The operation scheme consists of 3 stages: shifting the rice growing period (2 months earlier), retarding about 400 million $m^3$ of flood volume for almost 3 months after harvesting, and draining flood surplus downstream at the end of rainy season. Sirikit-reservoir operation and enhancing use of groundwater during irrigation water shortage are also component of the flood management and adaptation to handle such an extreme event (RID, 2018).

## 4. Results and discussion

The projection of average surface air temperature and annual rainfall over the period 2021-2040 using multiple GCMs and scenarios is shown in Fig. 2. Rising air temperature between 1.4-2.3 °C relative to the based period (1981-2000) is clearly seen from the result. There is a consensus from all GCMs on increasing temperature. For annual rainfall, only the MIROC model showed more rainfall in the future while less amount is found under the Hedge and GFDL models. Climate change does not impact much on annual rainfall, on average.

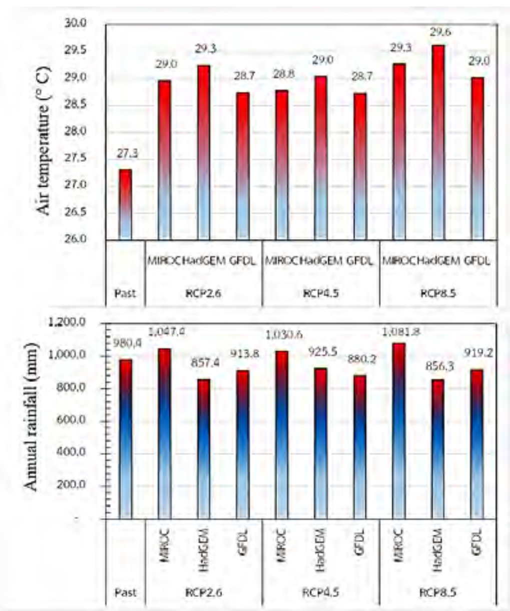


Fig. 2 Projection of air temperature and annual rainfall in the lower Yom and Nan River basins

LYN is the severe flood damage area because of topographic condition and no big reservoir in the Yom basin. Since 2017, the operation of Bang akum model showed substantial change in terms of flood loss. Almost a hundred percent of people production has been harvested before a coming of seasonal flood. The successful of the scheme is reflected by an increase of a number of local people supporting the project and willing to give a cooperation. However, there are some bad feed backs from farmers who allow their fields as the flood retention areas on unjustified compensation.

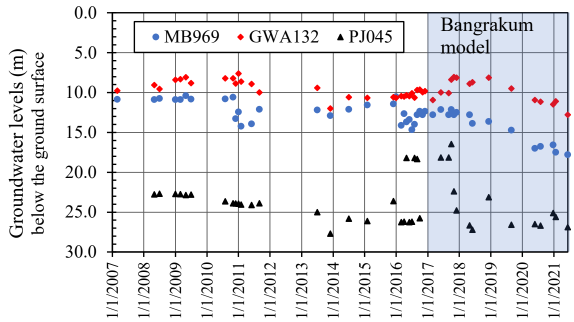


Fig. 3 Observation of groundwater levels

Start planting seasonal rice at April do need huge amount of water for field preparation and irrigation water. Famers living far away from a service of irrigation canal have to subtract groundwater for this activity. As shown in Fig.3, it can be concluded that groundwater has been exploited too much. Depletion of groundwater levels may be a drawback of the project and constraint for long-term operation.

## 5. Conclusions

Flood is a commonly natural disaster in Thailand especially in the LYN. Because of mega-flood in 2011, the bang akum model has been implemented as the proactive action against flood damage. Based on 3 years project operation, there is no major loss induced by flooding implying the success of the action in short-term. For the long-run operation, without the strong cooperation from local people, the scheme might not be a sustainable solution. Overuse of groundwater needs to be addressed.

## 6. Acknowledgements

The authors appreciate the supporting data from Department of Groundwater Resources, Thailand.

## References

1) Gopalan SP, Hanasaki N, Champathong A, Tebakari, T: Impact Assessment of Reservoir Operation in the Context of Climate Change Adaptation in the Chao Phraya River Basin. Hydrol. Process, 2020.
2) Hanasaki N, Mateo CM: H08 regional application: Case study of the Chao Phraya River. H08 supplemental documentation 1.2012.
3) Royal Irrigation Department: Bangrakum Model (in Thai), 2018.

International Conference on Sustainable Water Resources Management
- Global Challenges & Opportunities - (September 10th, 2021)
Committee on Global Environment
JSCE

# Evaluation of altered flow regimes by dams and climate change in the Omaru River network using a distributed hydrological model

○Haruki Mineda[1*], Kei Nukazawa [1], Yuto Tanimura[1], Yoshihiro Suzuki[1]
[1]Department of Civil and Environmental Engineering, Miyazaki University, Miyazaki 889-2192, Japan

*E-mail: hh17046@student.miyazaki-u.ac.jp

**Abstract**
Hydrological alterations could decline aquatic biodiversity through disrupting natural flow regimes that characterize life cycles of organisms. However, past studies have faced difficulty in quantifying the impacts of dams and climate change, major drivers of hydrological alterations. Here, we aimed to evaluate and compare the flow regime alterations by dams and climate change throughout the Omaru River catchment, Japan, using a distributed hydrological model. We found dams altered flow regimes greatly (moderate to large alterations) than climate changes that projected marginal flow alterations specifically under RCP2.6 and RCP4.5 scenarios. However, in a catchment-scale standpoint, climate change projected wider ranges of flow alterations along the tributaries and uppermost main stem. Our approach that uses a distributed hydrological model demonstrated that an overall picture of flow alterations by dams and climate change were better understood.

**Keywords:** Flood protection, indicators of hydrologic alteration, regulation, runoff analysis, watershed-scale

## 1. Introduction

Natural flow regimes in rivers worldwide have been altered through flood control, water resource development and climate change. Researchers pointed out that changes in the flow regimes could decline riverine biodiversity through disruption of the life history and habitat degradations (Poff et al., 1997). Dams greatly modify riverine natural flow regime with different alteration patterns according to its type. For example, water withdrawal by large dams often creates a section where the river flow dramatically decreases. On the other hand, changing climates triggered unexpected magnitude of floods, and led to changes in river flow regimes. Therefore, quantifying to what extents dams and climate change alter flow regime is a central challenge for safeguarding riverine environments by river managers.

Using distributed hydrological models (DHMs) to obtain longitudinal profiles of river flow data, we are able to infer spatial patterns of flow regimes and their alterations caused by dams/weirs and climate change. So far, DHMs have been used to evaluate changes in the flow regimes by dams/weirs but in a severely limited research case (Ryo et al., 2015). In addition, to the best of our knowledge, no studies have separated the impacts of dams and climate change and compared the extents of flow regime changes.

The present study aimed to evaluate and compare the flow regime alterations caused by dams and climate change throughout the Omaru River catchment, Japan.

## 2. Methodology

### 2.1 Meteorological data and study area


Fig.1 The Omaru River catchment. The main stem and tributaries are depicted by white and blue colors, respectively. Arrows indicate water conveyance from the dams to the hydropower stations.

We used observed data such as air temperature and precipitation as input over the study catchment shown in Fig. 1. For future climate data, we acquired monthly surface temperature and precipitation data from each of the eight general circulation models (GCMs) targeting the two future periods, the near future (2031-2050) and the far future (2081-2100). Future emissions and radiative forcing were considered using the three Representative Concentration Pathways (RCP2.6, RCP4.5 and RCP8.5).

### 2.2 Distributed hydrological model

We developed a DHM in the studied catchment by modifying slightly to the one originally developed in the Natori River catchment (Kazama et al., 2007). The Nash-Sutcliffe efficiency (NSE) were used to evaluate the model performance for 10-years study period (2010 to 2019).

### 2.3 Evaluation of flow alterations

To assess the impacts of dam and climate change independently, we performed runoff analyses either using dam discharge or future climatic data (2 future periods × 3 RCPs). Subsequently, we derived Indicators of Hydrologic Alterations (IHA), composing of the ecologically relevant 33 indicators, to quantify percent changes in flow alterations by comparing those to IHA under a natural condition (i.e., without dam or climate change data). If the absolute value of percent change shows greater than 20 (%/day), IHA is considered significantly altered. Furthermore, we counted the number of significantly altered IHA (# altered IHA) to evaluate the extents of the flow regime alterations; no flow alteration occurs where the number of significantly altered IHA is 0, while small, moderate, and large alterations occur where the number of significantly altered IHA is 1 to 10, 11 to 20, and 21 or more, respectively. The percent changes of each IHA and The number of significantly altered IHA were derived at all river channel meshes (n = 555) and visualized throughout the catchment.

## 3. Results and discussion

### 3.1 Model validation

The model predicted the discharges with high accuracy along up- to down-streams for 10 years (NSE=0.921-0.964).

### 3.2 Flow alteration by dams and weir

We found moderate to large alterations (# altered IHA ranged from 12 to 21) in a river section from the downstream of the Kijino Weir to the mesh upstream of the Do River confluence and moderate to large alterations (13 to 27) in river sections between the downstream of the Matsuo Dam and the river mouth (Fig. 2).

### 3.3 Flow alteration by climate change

Under all climate change scenarios (2 future periods × 3 RCPs), limited number of IHA was projected to be altered (0 to 10 IHA). Under RCP2.6 and RCP4.5, fractional alteration was projected in partial river meshes. Larger number of significantly altered IHA were projected at most river meshes under RCP8.5 than RCP2.6 and RCP4.5 (Fig. 2).

### 3.4 Comparison of the impacts of dams and climate change

In the Omaru River and a major tributary (the Do River), the percent changes of the most IHA were greater under the Dam scenario than the Climate change scenario, and in turn, the greater number of IHA was significantly altered. On the other hand, in a catchment-scale standpoint, wide spreading flow alterations were projected in the tributaries and uppermost main stem where unaffected by the dams under

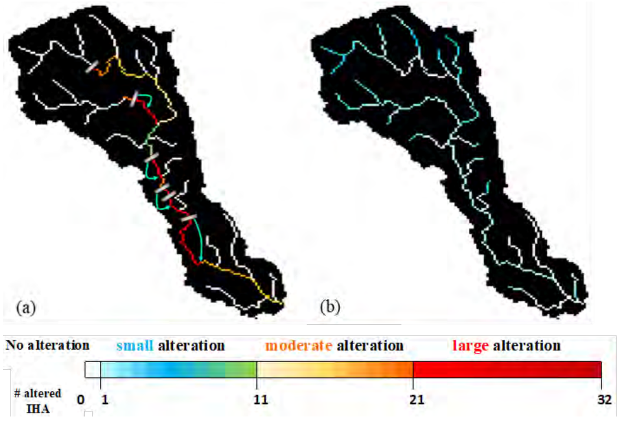


Fig.2 The spatial distributions for the number of significantly altered IHA (# altered IHA) under the (a) Dam scenario and (b) RCP8.5 in the far future.

the Climate change scenario. Even a small alteration triggers potentially population losses for species that are vulnerable to such changes (e.g., rheophilic species), resulting in the loss of biodiversity. Therefore, adequate environmental countermeasures for climate change should be implemented to safeguard biodiversity in tributaries since such marginal corridors account for most of the total streamflow length in a river system.

## 4. Conclusions

In the Omaru River and the Do River, the greater number of the IHA were significantly altered by dams than climate change. In a catchment-scale standpoint, climate change was projected to alter flow regimes widely in the tributaries and uppermost main stem. Our approach that uses a distributed hydrological model demonstrated that an overall picture of flow alterations by dams and climate change were better understood.

## 5. Acknowledgements

We gratefully acknowledge Kyusyu Electric Power Co. and Miyazaki prefecture, which provided all the data for hourly outflow discharge from the dams. This study also received financial support from the Japan Society for the Promotion of Science (19K15101).

## References

1) Poff, NL., Allan, DJ., Bain, BB., Karr, JJR., Prestegaard, KL., Richter, BD., Sparks, RE. and Stromberg, JC. : The Natural Flow Regime, Biosciences, Vol..47, pp.769-784, 1997.
2) Ryo, M., Iwasaki, Y., Yoshimura, C. and Saavedra VOC.: Evaluation of Spatial Pattern of Altered Flow Regimes on a River Network Using a Distributed Hydrological Model, PLoS One, Vol..10(7), e0133833, 2015.
3) Kazama, S., Matsumotob, S., S. Priyantha Ranjana, Hamamotoa, H., Sawamoto M. Characterization of firefly habitat using a geographicalinformation system with hydrological simulation, Ecological Modelling, Vol. 209, pp.392-400, 2007

# Effects of Climate Change on Surface Water and Groundwater Recharge in the Yom and Nan River basin, Thailand

○Chanchai Petpongpan[1*], Chaiwat Ekkawatpanit[1], Duangrudee Kositgittiwong[1]
[1] Department of Civil Engineering, King Mongkut's University of Technology Thonburi,
126 Prachautit Rd. Bangkok 10140, Thailand

*E-mail: Chanchai_Petchpongpan@outlook.co.th

## Abstract

In Northern Thailand, flood and drought have always occurred because of the climate change impact and non-systematic management in the conjunctive use of both sources of water. Therefore, this study aims to assess the climate change impact on surface water and groundwater of the Yom and Nan River basins, located in the upper part of Thailand. The future climate scenarios are considered from the Representative Concentration Pathways (RCPs) 2.6 and 8.5, presented by the Coupled Model Intercomparison Project Phase 5 (CMIP5), in order to mainly focus on the minimum and maximum Green House Gas (GHG) emission scenarios during the near future (2021–2045) period. The results show that the surface water (water yield) and groundwater recharge (water percolation) in the Yom River basin seem to be decreased by 443.98x$10^6$ and 316.77x$10^6$ $m^3$/year under RCP 2.6 and RCP 8.5, respectively. While, in the Nan River basin, it is projected to be increased by 355x$10^6$ $m^3$/year under RCP 2.6 but decreased by 20.79x$10^6$ $m^3$/year under RCP 8.5.

**Keywords:** climate change impact, surface water, groundwater recharge, SWAT-MODFLOW, Thailand

## 1. Introduction

Over the past few decades, the increase in global air temperature has caused several impacts, especially on climatic conditions. The number of extreme weather events has surged and there have been many natural disasters (Supharatid, 2015; Wang *et al.*, 2013) because of the elevated CO2 concentration and uncertainty in weather circulation, influencing changes in the hydrologic cycle. As reported, the water cycle around the world has been changing and seems to be more severe in the future due to the climate change (Dong *et al.*, 2020; Pereira *et al.*, 2019).

One of the primary factors producing flood and drought phenomena is the amount of surface water and groundwater. Flood events can occur easily when the surface water cannot be drained immediately due to a large amount of groundwater in the wet season and limitation of capacity in the drainage system. In contrast, drought and water shortage can occur easily when there are less surface water and groundwater during the dry season. It can be seen that the change in climate conditions has a direct impact on the amount of surface water and groundwater, affecting the possibility of floods and droughts (Wang *et al.*, 2013).

Thus, this study aims to assess the climate change impact on surface water and groundwater recharge (percolation) of the Yom and Nan River basins in Thailand. The trends of both sources of water under the future scenarios can be applied to anticipate the intensity of drought disasters that may occur in the future and could also be an approach for the development of the water management plan in the near future period.

## 2. Study area

Yom and Nan River basins are important and vulnerable regions located in Northern Thailand between 14°50′ N and 99°16′ E, and 18°37′ N and 101°21′ E (Fig. 1). This area covers approximately 58,782.93 km$^2$ or 37% of the Chao Phraya River basin. The flood and drought disasters have occurred in both basins several times due to a different river capacity between upstream and downstream areas, lack of rainfall, and unsystematic water management, even though there is the Sirikit Dam in the Nan River basin.

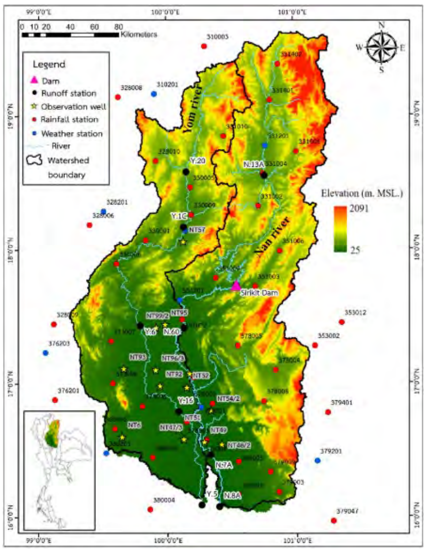


Fig.1 Study area in the Yom and Nan River basins

## 3. Methodology

The bias-corrected GCM data were inputted into the calibrated SWAT-MODFLOW model for future scenarios simulation of surface water and groundwater. Results of the reference period (1981–2005) and projected period (2021–2045) were compared to assess the changes in surface water and groundwater. The future scenarios would be depended on global annual Green House Gas (GHG) emission scenarios, presented as the Representative Concentration Pathways (RCPs) 2.6 and 8.5 in order to consider the minimum and maximum GHG emission issues. Climate change impacts on surface water and groundwater was analyzed by comparing the air temperatures and rainfall with variations in both water resources. Moreover, the amount of surface water and groundwater from each scenario was correlated with an expected water demand to assess water availability under divergent climate scenarios.

## 4. Results and discussion

The annual water yield and percolation during 1981–2005 (reference period) and 2021–2045 (near future period) are illustrated in Fig.2-4 by comparing to the amount of water demand, reported by the Department of Water Resources.

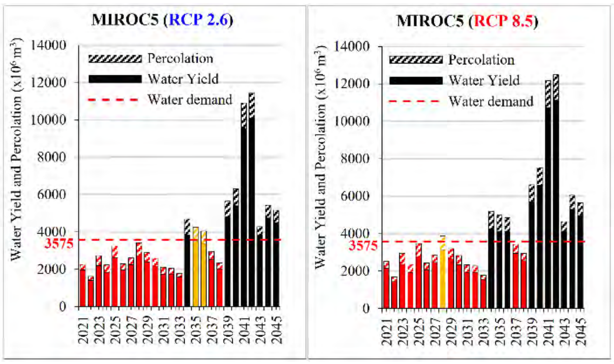


Fig.3 Annual water yield and percolation in the Yom River basin during the near future period under RCP 2.6 and 8.5

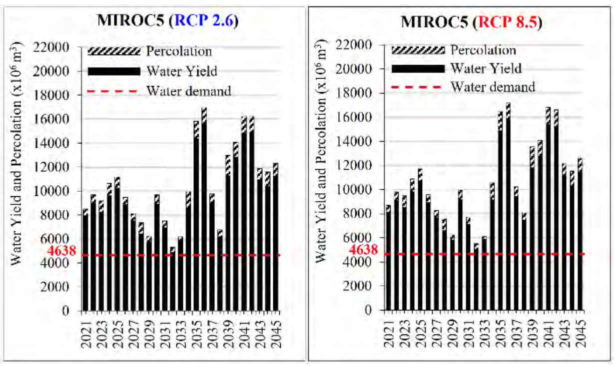


Fig.4 Annual water yield and percolation in the Nan River basin during the near future period under RCP 2.6 and 8.5

The simulation of future scenarios directly using the single GCM runs as input is quite a preliminary approach. This would be a source of uncertainty influencing the climate condition evaluated. The intensity of air temperature and precipitation might be underestimated when compared with a projection on a global scale. Usually, hydrologists make use of RCM outputs and even these are sometimes too coarse for hydrologic predictions. However, in this study, future simulations of surface water and groundwater regimes are implemented during the near future period (2021–2040) in order to avoid the effect of land use change. Hence, these analyzed results can be used as the approach for future study related to this area, and also in planning for an elementary water management plan.

## 5. Conclusions

The amount of water yield and percolation under scenario RCP 8.5 became lower than that received from the reference period and scenario RCP 2.6 because of the higher air temperature. In the Yom River basin, the years with percolated water needed are almost constant compared to the reference period under scenario RCP 2.6. While under the scenario RCP 8.5, it was found to be a water shortage year due to a greater lack of water availability. However, the water shortage year significantly increased during the near future under both GHG emission scenarios. Moreover, there is a possibility that the water shortage year during the near future period can become more severe than any that occurred in the reference period. Whereas, the water shortage and water percolation needed years of the Nan River basin remains constant from the reference period.

## 6. Acknowledgements

This research was supported by King Mongkut's University of Technology Thonburi's Post-doctoral Fellowship. The authors also thank the Department of Civil and Environmental Engineering, Colorado State University, for hosting Mr. Petpongpan during the research project.

## References

1) Dong Q, Wang W, Shao Q, Xing W, Ding Y, Fu J: The Response of Reference Evapotranspiration to Climate Change in Xinjiang, China: Historical Changes, Driving Forces, and Future Projections. Int. J. Climatol. 40, 235–254, 2020.
2) Harpa GV, Croitoru AE, Djurdjevic V, Horvath C: Future Changes in Five Extreme Precipitation Indices in the Lowlands of Romania. Int. J. Climatol. 39, 5720–5740, 2019.
3) Pereira SC, Marta-Almeida M, Carvalho AC, Rocha A: Extreme precipitation events under climate change in the Iberian Peninsula. Int. J. Climatol. 39, 1–24, 2019.
4) Supharatid S: Skill of Precipitation Projection in the Chao Phraya River Basinby Multi-Model Ensemble CMIP3-CMIP5. Weather Clim. Extrem. 12, 1–14, 2015.
5) Wang Z, Luo Y, Zhu X: Watershed Modeling of Surface Water-Groundwater Interaction under Projected Climate Change and Water Management in the Haihe River Basin, China. Br. J. Environ. Clim. Chang. 3, 421–443, 2013.

International Conference on Sustainable Water Resources Management
- Global Challenges & Opportunities - (September 10th, 2021)
Committee on Global Environment
JSCE

# Forest fire severity estimation for the 2017 Kamaishi forest fire

○Sengphrachanh Phrakonkham[1*], Sisouvanh Kittavong [1], So Kazama[2]

[1]Department of Environmental Engineering, Faculty of Engineering National University of Laos, Laos

[2]Graduate School of Engineering, Tohoku University, Sendai 980-8579, Japan

*E-mail: bphrakonkham@gmailcom

## Abstract

The object of this study was conduct to simulate climage change impact to flood hazard areas in Xedon catchment area, Salavan and Champasak province. Using GIS and HEC RAC. 100-year rainfall period was used in this study to analysis climate change of RCP 2.6, 4.5 and 8.5 impact to flood hazard areas for two time period near future (2020 – 2050) and far future (2051-2099). The results of the analysis provide the conclusion, the flood area increased from 126.30 km$^2$ RCP 2.6 near future scenario to 483.90 km$^2$ RCP 8.5 far future scenario. In addition, we use 22 historical events for our flood hazard maps validation.

**Keywords:** Flood, Hazard, Climate change, HEC RAS

## 1. Introduction

Floods are among the most dangerous natural hazards. Flooding can happen anywhere, and sometimes, it is unavoidable. The economy, people's livelihood and the infrastructure of many countries around the world have been affected by flooding [1]. Lao People's Democratic Republic (or Lao PDR) suffers from flooding every year. Lao PDR is a developing country located in Southeast Asia. The country's people depend heavily on agriculture and natural resources for their livelihood. Currently, the water supply system in the country is not well distributed, particularly in rural areas. Therefore, most people living in rural areas are resettled downstream of dams and irrigation areas [2].

Climate change increases the intensity of rainfall and more rainfall events happen, it is means for the risk of flooding. However, it is varied widely from location to location depend on the studied hydrological climatic area. In this study, we focus on the hydrological system in Laos. many of researchers believe that increasing in a number of hydrological extreme events such as flood, landslide and so on are happened because of climate change [3], [4].

In recent years, many researchers have conducted global studies on the impact of climate change on the water cycle and its effect on people's livelihood [5]–[7]. According to the Intergovernmental Panel on Climate Change (IPCC) report, Southeast Asia will suffer from increasing flood frequency in the future [4]. General Circulation Models (GCMs) have been developed to study future climate scenarios and the associated impacts, and they help support strategies and mitigation plans to address the effect of climate change

The main objective of this study was to analyse flood hazard area in Xedon catchment area by using Arc GIS and HEC RAS.

## 2. Study area and data

Xedon catchment (Figure 1) is located in Salavanh and Champasak province. The Xedon catchment is significant to farmer in both Province area due to the riverbank soil is very rich nutrients. For this study, we used hydrological and meteorological dataset from Mekong River Commission. Daily rainfall dataset range from 1970 to 2000 (30 years) from 40 stations. Land use type is use as one of factor in infiltration. Soil data were based on the Harmonized World Soil Database (HWSD). For the climate change, we use average rainfall from 7 GCMs [8].

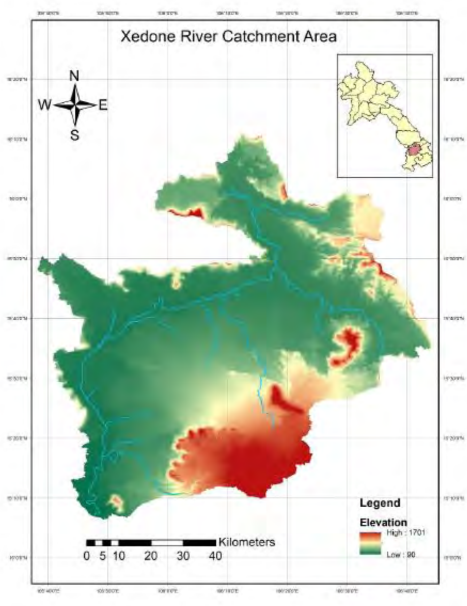


Fig.1 Xedon catchment area

## 3. Methodology

HEC RAS is a hydraulic model by US Corporation Engineers Hydraulic Engineering Centre to manage the rivers and model river flow. HEC RAS can simulate either 1- and 2-dimensional modeling of river flow. The rainfall data, 30*30-meter DEM, Land use/cover and soil data were used for developing flood hazard maps. The future projection daily rainfall data were obtained from the study of Phrakonkham et al 2021.

## 4. Results and discussion

. The results are shown in Figure 2, where we can see the potential flood hazard area from scenario of RCP 2.6-8.5 far future. The results reveal that low hazard areas cover 89.64% of the total area, medium hazard areas cover 8.4 %, and high and very high hazard areas respectively cover 2.95% and 6.55%. Even though the high and very high hazard percentages are low, we still must pay attention to land use types in those areas.

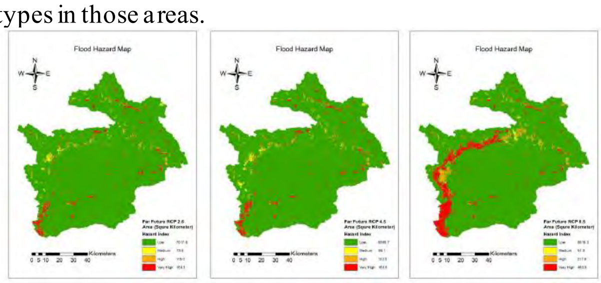


(1) (2) (3)

Fig. 2 Flood hazard map (1) RCP 2.6, (2) 4.5 and (3) 8.5

To validate the performance of the map, flood historical events were compared to the flood hazard maps (figure 3). The majority flood historical events were located in high and very high hazard areas. Hence, the reliability of the integrated hazard map was confirmed.

.

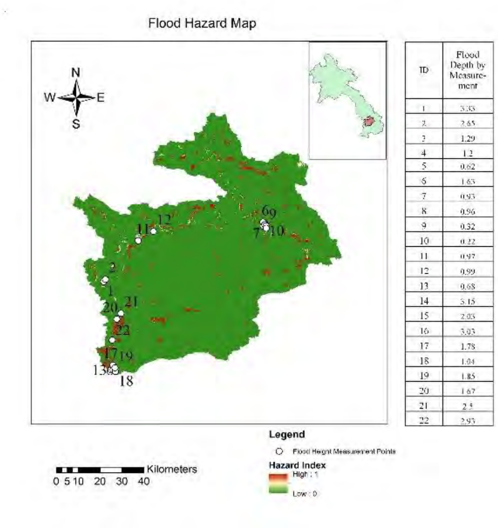


Fig 2. Flood hazard map and historical events

## 5. Conclusions

The main propose of this study is to evaluate applicable of HEC RAS and analyze climate change impact to flood hazard area through validation with evidence from GPS coordinate point that specify historical events as well as information from local people and the local authorities.


## 6. Acknowledgements

This research was partially supported by the Grants-in-Aid for Scientific Research (B), 2015-2017 (15H05218, So Kazama) from the Ministry of Education, Science, Sports and Culture. The authors thank the Environmental Research and Technology Development Fund (s-14) from the Ministry of the Environment, Japan.


## References


1) S. Golian, B. Saghafian, and R. Maknoon, "Derivation of Probabilistic Thresholds of Spatially Distributed Rainfall for Flood Forecasting," *Water Resour. Manag.*, vol. 24, no. 13, pp. 3547–3559, Oct. 2010, doi: 10.1007/s11269-010-9619-7.
2) I. G. Baird and B. Shoemaker, "Unsettling Experiences: Internal Resettlement and International Aid Agencies in Laos," *Dev. Change*, vol. 38, no. 5, pp. 865–888, Sep. 2007, doi: 10.1111/j.1467-7660.2007.00437.x.
3) Y. Hirabayashi, S. Kanae, S. Emori, T. Oki, and M. Kimoto, "Global projections of changing risks of floods and droughts in a changing climate," *Hydrol. Sci. J.*, vol. 53, no. 4, pp. 754–772, Aug. 2008, doi: 10.1623/hysj.53.4.754.
4) IPCC, *IPCC: Climate change 2007 : mitigation of climate change : contribution of Working Group III to the Fourth Assessment 455 Report of the Intergovernmental Panel on Climate Change.* Cambridge University Press, 2007.
5) A. Adeloye, N. R. Nawaz, and T. J. Bellerby, "Modelling the impact of climate change on water systems and implications for decision-makers," 2013, pp. 299–326.
6) C. Parmesan and G. Yohe, "A globally coherent fingerprint of climate change impacts across natural systems," *Nature*, vol. 421, no. 6918, pp. 37–42, Jan. 2003, doi: 10.1038/nature01286.
7) S. Westra *et al.*, "Future changes to the intensity and frequency of short-duration extreme rainfall," *Rev. Geophys.*, vol. 52, no. 3, pp. 522–555, Sep. 2014, doi: 10.1002/2014RG000464
8) Phrakonkham S, Kazama S, Komori D, " Integrated mapping of water-related disasters using the analytical hierarchy process under land use change and climate change issues in Laos," *Nat. Hazards Earth Syst. Sci.*, 21, 1551–1567, 2021, https://doi.org/10.5194/nhess-21-1551-2021.

# BIAS CORRECTION OF WRF-ROMS FOR RAINFALL FORECASTING IN UPPER PING RIVER BASIN, THAILAND

○Prem Rangsiwanichpong[1*], Phakawat Lamchuan [1], Thienchart Suwawong[1]
[1]Department of Water Resources Engineering, Faculty of Engineering, Kasetsart University, Bangkok 10900, Thailand

*E-mail: Prem.r@ku.th

**Abstract**
Accurate gridded rainfall forecasting is an essential tool in hydrological research for flood prediction. Thus, in this study, we applied the short-range rainfall forecast product at 1-day lead-times to forecast the precipitation in the upper Ping river basin (P1 catchment) 1 days in advance. The product was developed by Hydro Informatics Institute using the WRF (Weather Research and Forecasting) and ROMS (Regional Ocean Modeling System) model. The rainfall data of 2016, 2017 were used for the investigation. However, we compared our forecasted rainfall with the observed data. The performance of the bias-corrected WRF-ROMS 1-day lead time gave the performance indices better than the original one.
**Keywords:** WRF-ROMS Model, Short-Range Rainfall Forecast, Rainfall-Runoff Model

## 1. Introduction

The Weather Research and Forecasting (WRF) is a numerical weather prediction software to simulate and predict the atmospheric characteristics. Rainfall forecast is one of its products and applied to many hydrological problems. Givati (2011) investigated the operational streamflow forecast system for the Jordan River using WRF and found that the results from WRF showed good agreement with the actual measurements. Coupling with Regional Ocean Modeling System (ROMS), WRF-ROMS improves rainfall forecast. For example, Samala et al. (2013) used WRF-ROMS to study the influence of air-sea interactions on the simulation of the Indian summer monsoon. The results, both seasonal rainfall and intra-seasonal oscillations of the rainfall, are satisfactory. Recently, Luiz do Vale Silva (2018) applied WRF and WRF-ROMS to simulate extreme rainfall events from 10 to 25 June 2010 in eastern Northeast Brazil and found that the coupling greatly improved the predictions. Two institutes, Thai Meteorological Department (TMD) and Hydro Informatics Institute (HII), Thailand have developed WRF and WRF-ROMS for Thailand. Generally, the performance of microphysics schemes of WRF model gave a good rainfall and good heavy rainfall area prediction, compared with observation data over the Southern part of Thailand (Kaewmesri et.al. (2017)). Deeprasertkul and Praikan (2016) studied the daily rainfall for 3-days forecast using the HII WRF-ROMS model. As a result, this study aims to extend the application of the WRF-ROMS rainfall forecasting data by HII to forecast streamflow in a small mountainous catchment in Thailand. We evaluated the accuracies of both rainfall and streamflow forecasts using the original and bias-corrected WRF-ROMS at 1-day lead times.

## 2. Study area

Our study area is the catchment area upstream of the P1 streamflow station (P1 catchment) in the Upper Ping River Basin as shown in Fig. 1. The P1 catchment is located in the northern part of Thailand. It has an area of approximately 6,350 km2. Rainfall from 13 rainfall gauge stations in the P1 catchment were collected in this study. The average annual runoff and rainfall are approximately 6,815 million m3 and 1,170 mm, respectively.

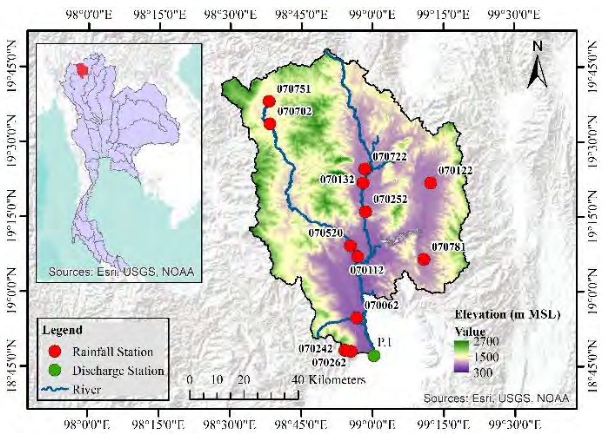


Fig.1 The study area (P1 catchment)

## 3. Methodology

### 3.1 Data Collection

3.1.1 Meteorological and hydrological data

Daily meteorological data was collected from 2001 to 2017. The precipitation data from 13 stations in the P1 catchment were collected and examined by the double mass curve method to discard unreliable data.

3.1.2 WRF-ROMS data

Hydro Informatics Institute (HII), Thailand has developed WRF-ROMS with hourly forecasting products. The resolution of WRF-ROMS is 3 km, which domain including Thailand, Laos, Myanmar, Vietnam, and Cambodia.

### 3.2 Bias Correction using Gamma Distribution

The accuracy of observed rainfall was investigated and interpolated into pixel-based with a resolution of 0.03x0.03 degrees (Approx. 3 km) across P.1 catchment by using a common method which is Inverse Distance Weight (IDW)

$$W_i = \frac{(1/D_i^2)}{\sum_{i=1}^{n}\frac{1}{D_i^2}} \qquad (1)$$

where $D_i$ is the distance from each rainfall stations to the centroid of the pixel, and $n$ is the number of rainfall stations.

The WRF-ROMS were corrected on a daily scale. The parameters of gamma distribution were estimated using the Maximum Likelihood Method (MLE), zero values of input dataset were replaced by 0.0001 to avoid the limitation of MLE estimation and it can be calculated as Eq.2 to Eq.3.

$$F(x|\alpha,\beta) = x^{\alpha-1}.\frac{\Gamma_\beta(\alpha)}{\beta^\alpha.\Gamma(\alpha)}.e^{\frac{-x}{\beta}}\,; x \geq 0;\ \alpha,\beta > 0 \qquad (2)$$

$$R_{corrected} = F^{-1}\left[F\left(R_j|\alpha_j,\beta_j\right)|\alpha_{obs},\beta_{obs}\right] \qquad (3)$$

## 4. Results and discussion

The rainfall product by WRF-ROMS is corrected on a daily scale using the Gamma Distribution (GD) for years 2016 and 2017. Table 1 shows the comparison of the annual rainfalls for P.1 catchment from the observation, original WRF-ROMS and corrected WRF-ROMS. It is found that the original WRF-ROMS annual rainfalls are almost twice as high as the observed and corrected. Thus, it is necessary to correct the original WRF-ROMS rainfall before applying in our study. Table 2 shows the correlation coefficient (R) and the root means square error (RMSE) of the original and bias-corrected WRF-ROMS products. The R values between the original and corrected WRF-ROMS do not vary significantly because the GD method does not reconstruct the variation of time series. However, the RMSE values by the corrected WRF-ROMS are lower than those by the original one.

## 5. Conclusions

A lot of research focuses on the application of WRF-ROMS to forecast rainfall on a large scale. Thus, we performed to use the bias-corrected WRF-ROMS forecast rainfall in small catchment of the tropical zone. Forecasting rainfall by WRF-ROMs generally gave an overestimate of the observed rainfall. Thus, we corrected it using the bias correction. It was found that the values of the RMSE reduce obviously.

## 6. Acknowledgements

This research was supported by the Agricultural Research Development Agency (Public Organization), ARDA, Thailand. The authors would like to thank the Royal Irrigation Department (RID) and Hydro-Informatics Institute (HII) for providing all the required data for this research. The authors would also like to thank Jiramate Changklom, Ruetaitip Mama, and Wachira Surin for their valuable and constructive suggestions during the planning of this research work

Table 1. Comparison of annual rainfalls from the observation, the original WRF-ROMS, and the corrected WRF-ROMS during 2016-2017 for P.1 Catchment.

| Observation (mm) | Original WRF-ROMS (mm) | Corrected WRF-ROMS (mm) |
|---|---|---|
| | 1 day | 1 day |
| 2296.11 | 3941.77 | 2281.03 |

Table 2. Statistical assessment between WRF-ROMS and observed rainfalls during 2016-2017 for P.1 Catchment.

| | Lead Time | Original WRF-ROMS | Corrected WRF-ROMS |
|---|---|---|---|
| Correlation (R) | 1 | 0.53 | 0.52 |
| RMSE (mm) | 1 | 7.96 | 5.11 |

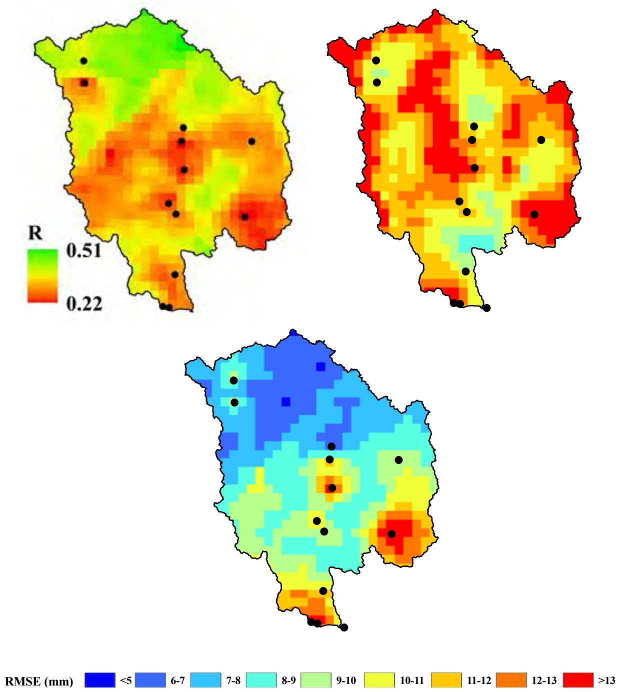


Figure 4. The Spatial RMSE between WRF and observed rainfall during 2016-2017 for P.1 Catchment, the black spot is rainfall station.

## References

1. Deeprasertkul, P. and Praikan, W., 2016, October. A rainfall forecasting estimation using image processing technology. In 2016 International Conference on Information and Communication

Technology Convergence (ICTC) (pp. 371-376). IEEE.

2. Givati, A., Lynn, B., Liu, Y. and Rimmer, A. (2012). Using the WRF model in an operational streamflow forecast system for the Jordan River. Journal of applied meteorology and climatology, 51(2), pp.285-299.
3. Kaewmesri,P., Humphries, U., and Sooktawee, S. (2017). Simulation of high-resolution WRF model for an extreme rainfall event over the southern part of Thailand. International Journal of Advance and Applied Sciences, 4(9), pp. 26-34.
4. Luiz do Vale Silva, T., Veleda, D., Araujo, M. and Tyaquiçã, P. (2018). Ocean-Atmosphere Feedback during Extreme Rainfall Events in Eastern Northeast Brazil. Journal of Applied Meteorology and Climatology, 57(5), pp.1211-1229.
5. Samala, B.K., Banerjee, S., Kaginalkar, A. and Dalvi, M. (2013). Study of the Indian summer monsoon using WRF–ROMS regional coupled model simulations. Atmospheric Science Letters, 14(1), pp.20-27.

# Assessment of Landslide Risk using Hydrological Model in the Upper Yom River basin, Thailand

○Chaiwat Ekkawatpanit [1*], Chanchai Petpongpan [1]

[1] Civil Engineering Department, King Mongkut's University of Technology Thonburi, Bangkok 10140, Thailand

*E-mail: chaiwat.ekk@kmutt.ac.th

**Abstract**

This study applies the Block wise application of TOPMODEL, with the Muskingum-Cunge routing method (BTOPMC) for a river runoff simulation and landslide risk assessment in the Upper Yom River basin. The hydrological data used for simulation and model performance investigation consist of hourly rainfall intensity and river discharge during the heavy rainfall periods. The slope failure is analyzed by using the slope-instability analysis method with the groundwater level and soil topography index obtained from simulation. The landslide vulnerable areas are spatially indicated as the area having a Factor of Safety (FS) less than one. The results show that BTOPMC provides high potential for the hourly simulation of the hydrological regime in the Upper Yom River basin during high rainfall intensity. Therefore, this is trustworthy for using in the landslide warnings policy to mitigate the loss of lives and assets.

**Keywords:** Hydrological Model, BTOPMC, Landslide, Yom River basin

## 1. Introduction

A landslide is a natural occurrence of mass movement that occurs when the shear stress of soil materials in the slope region exceeds the shear strength ratio. For landslide risk assessment, a variety of approaches combining a physically-based hydrological model with a statistical analysis method are constantly considered. This is because the occurrence of a landslide is strongly linked to the hydrological process.The BTOPMC model, which combines block-wise TOPMODEL with the Muskingum-Cunge routing algorithm, is a semi-distributed model frequently used for this problem. Surface runoff and groundwater systems may be distributed spatially as a grid cell, which is useful for watershed and groundwater estimates at a large scale.

The aim of this research is to use the BTOPMC model to simulate the hydrological regime in the Upper Yom River basin, as well as to identify landslide-prone regions. Various model parameters are manually stated, and the model's performance is compared to the measured hourly river flow from the observed runoff station, both graphically and statistically. The Safety Factor of a landslide at that moment is assessed using the Slope-instability analysis technique and spatially displayed as a risk map based on the results of a simulation that provides peak discharge.

## 2. Study area

The Upper Yom River basin (Figure 1A) is a vulnerable area in northern Thailand, comprising 7,464 $km^2$ and encompassing four provinces: Phayao, Nan, Lampang, and Phrae. In terms of landslide effect, the Upper Yom River watershed has lately seen an increase in the likelihood of slope collapses due to an increased trend in rainfall intensity and mountain cultivation. Several sub-districts are at danger of landslide occurrences, according to the Department of Mineral Resources (DMR) (2017), based on satellite image, aerial photograph, terrain, climate, community settlement information, and field geological survey data. Over half of the communities in these areas would be badly harmed, particularly in the districts of Pong, Ngaw, Song, Ban Luang, and Rong Kwang (Figure 1B).

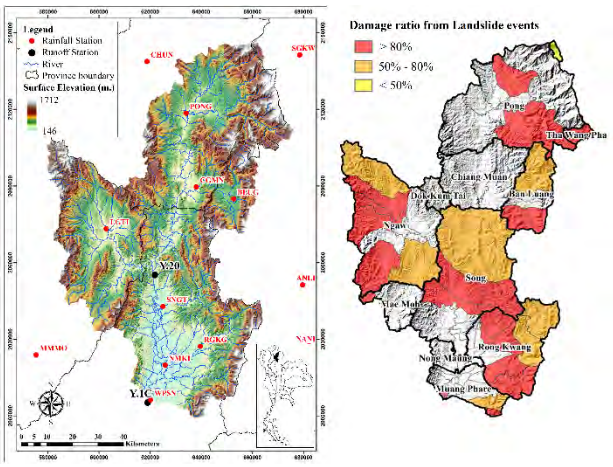


(A) DEM and river network (B) Landslide vulnerable area
Fig.1 The Upper Yom River basin

## 3. Methodology

### 3.1 BTOPMC

The BTOPMC model is a semi-distributed conceptual rainfall-runoff model for hydrological modeling in large watersheds. The whole watershed is divided into numerous sub-basins, each with a significant number of grid cells, in this model. When it comes to river routing, the Muskingum-Cunge technique is used to determine the flow direction of the water as it flows through the channel. Groundwater flow across grid cells is based on an exponential of a soil saturation deficiency. Furthermore, the BTOPMC model's characterization of watershed features is based on soil and land use type attributes. The saturated transmissivity of soil ($T_0$), the decay factor of saturated transmissivity of soil (m), the capability of root zone storage ($S_{rmax}$), the initial saturation deficit of soil ($Sbar_0$), and the manning roughness coefficient (n) are five factors that must be included in the BTOPMC model.

3.2 Landslide Risk Assessment

The simulated results (groundwater level and soil topographical index) were combined with ISRIC World Soil Information soil characteristics data (cohesion, friction angle, and bulk density) to estimate the risk of landslide in the Upper Yom River basin. The slope-instability analysis technique (Lee, 2009), which was derived as equation (1), was used to establish the landslide's safety factor in this study.

$$FS = \frac{C + (D\rho_s - h_w\rho_w) g \cos^2 \beta \tan\phi}{\rho_s g D \sin\beta \cos\beta} \qquad (1)$$

where $FS$ is the safety factor of a landslide, $C$ is a cohesion of soil (kPa), $D$ is soil thickness (m.), $g$ is the gravitational acceleration (m/s2), $\rho_s$ is soil bulk density (kg/m$^3$), $\rho_w$ is water density (kg/m$^3$), $h_w$ is groundwater level (m.), $\beta$ is the local topographic slope (rad.) and $\phi$ is friction angle of soil (rad).

4. Results and discussion

Fig. 2 shows the landslide's Safety Factor (FS), as determined by the slope-instability analysis approach. The vulnerable area for landslide occurrences is classified as a Red zone, with FS values less than 1.00. The results indicate that the level of groundwater estimated during the study's highest rainfall intensity period (30 August - 6 September 2014) is insufficient to trigger slope collapse in the Upper Yom River watershed. However, some sites have FS values of 1.01-3.00 (Purple zone), indicating that they are extremely vulnerable to landslide occurrences caused by significantly increased rainfall. The landslide-prone regions produced by combining the BTOPMC model with the slope-instability analysis approach are compared to historical landslide events and landslide susceptible communities to verify the proposed model (Fig. 2B).

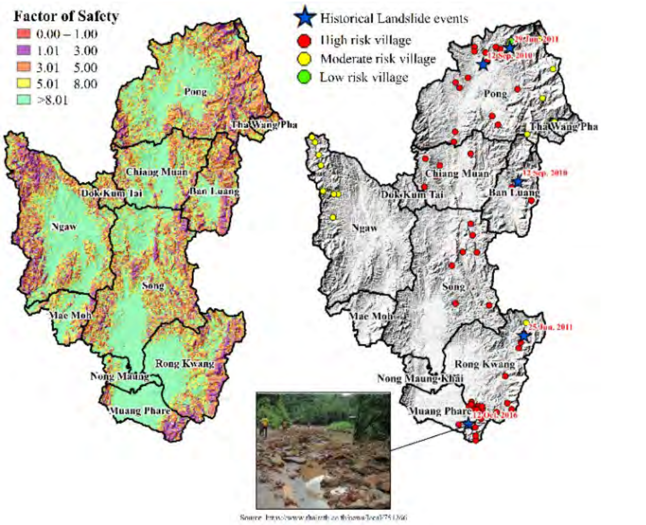


Fig. 2 (A) Safety Factor of the landslide in the Upper Yom River basin analyzed by the Slope-instability analysis method and (B) Recorded landslide events and vulnerable villages

### 5. Conclusions

In terms of landslide assessment, a spatial estimate of the Factor of Safety shows that Ngao district in Lampang province, Pong district in Phayao province, Ban Luang district in Nan province, including Song district and Rong Kwang district in Phrae province, are vulnerable areas with a high probability of experiencing a landslide event during a heavy rainfall storm. The risk map examined by the Land Development Department is compatible with the spatial distribution of landslide risk calculated using the BTOPMC model and the slope instability analysis technique. These findings can help to improve information that is used in the design of landslide protection and mitigation.

### 6. Acknowledgements

We wish to thank Department of Civil Engineering, King Mongkut's University of Technology Thonburi for financial support.

### References

1) Ekkawatpanit, C., Kazama, S., Sawamoto, M., Ranjan, P., 2009. Assessment of water conflict in Mae Chaem River Basin, Northern Thailand. Water International 34(2), 242-263.
2) Lee, K.T., Ho, J.Y., 2009. Prediction of landslide occurrence based on slope-instability analysis and hydrological model simulation. J. Hydrol. 375, 489–497.
3) Land develop Department Thailand, 2003. Land slide and flood hazard map of Thailand. http://oss101.ldd.go.th /web_dat&map/soilerosion.html (accessed 28 December 2016).
4) Wang, G., Zhou, M., Takeuchi, K., Ishidaira, H., 2007. Improved version of BTOPMC model and its application in event-based hydrologic simulations. J. Geogr. Sci. 17, 73–84.